Bacteriophage SPP1 entry into the host cell

Lina Jakutyte

UNIVERSITÉ PARIS-SUD 11 et UNIVERSITÉ VILNIUS

ECOLE DOCTORALE :
INNOVATION THÉRAPEUTIQUE : DU FONDAMENTAL A L'APPLIQUÉ
PÔLE : INGENIERIE DES PROTEINES ET CIBLES THERAPEUTIQUES

DISCIPLINE : Structure, fonction et ingénierie des protéines

ANNÉE 2011 - 2012 SÉRIE DOCTORAT N° 1156

THÈSE DE DOCTORAT
soutenue le 15/12/2011

par

Lina JAKUTYTE

BACTERIOPHAGE SPP1 ENTRY INTO THE HOST CELL

Directeur de thèse :	Paulo TAVARES	Docteur (VMS, CNRS, Gif sur Yvette)
Directeur de thèse :	Rimantas DAUGELAVICIUS	Professeur (Vytautas Magnus University,Lituanie)

Composition du jury :

Président du jury :	Herman VAN TILBEURGH	Professeur (IBBMC, Université Paris-Sud, Orsay)
Rapporteurs :	David PRANGISHVILI	Docteur (Institut Pasteur, Paris)
	Jaunius URBONAVICIUS	Docteur (Université Libre de Bruxelles, Belgique)
Examinateur :	Lucienne LETELLIER	Docteur émérite (IBBMC, Université Paris-Sud, Orsay)

“Far and away the best prize that life has to offer is the chance to work hard at work worth doing.”

-Theodore Roosevelt

To my family

ACKNOWLEDGMENTS

I would like to thank deeply to my supervisors Dr. Paulo Tavares and Prof. Rimantas Daugelavicius for being the excellent supervisors and for this amazing opportunity to prepare my thesis under joint supervision between France and Lithuania. Thank you for generously sharing your knowledge and experience and for your care and support throughout these years.

I am deeply grateful to all the co-workers, especially Dr. Rut Carballido-Lopez, Carlos São-José and Dr. Catarina Baptista, for their valuable and rewarding contributions to this thesis work. Dr. Rut Carballido-Lopez is warmly acknowledged for opportunity to work in her group, for sharing her experience in microscopy of *B. subtilis* and for her kind support and fruitful discussions during these years. Warm thanks to Dr. Carlos São-José and Dr. Catarina Baptista for their support and advice on my work, for helpful discussions and valuable experiments. I thank Dr. Rudi Lurz for fantastic electron microscopy photos. I thank François-Xavier Barre for plasmid pFX276 and the primers 124-2 and 125-2. Alan D. Grossman and Cathy Lee are acknowledged for strain MMB357 and Prof. Shelley Grimes for strain 12A. I thank Adriano O. Henriques and Gonçalo Real for sharing initial microscopy observations of YueB-GFP and the gift of pEA18. I thank Neal C. Brown for kindly provided HPUra. I am indebted to Prof. Mário A Santos for communication of unpublished results.

I warmly thank reviewer Dr. Elena Bakiene for the careful reading of this thesis and for providing valuable suggestions that helped improving the manuscript. Elena, thanks especially for everyday care of the homely atmosphere and lab supplies in Vilnius.

I thank Dr. Lucienne Lettelier, Dr. David Prangishvili, Dr. Jaunius Urbonavicius and Pr. Herman van Tilbeurgh for acceptance to be members of my thesis defence jury.

I acknowledge the financial support of University of Vilnius, the Université Paris-Sud, the French embassy in Lithuania, the program Egide Gilibert between France and Lithuania, the European Union Erasmus Program, and the Région Ile-de-France (SETCI) which made this work possible.

I thank Mme Agnès Vannereau from Paris-Sud *Relations Internationales* for her help with administration procedures for fellowships and accommodation. I thank the *Residence les Rives sur Yvette* for allowing me to meet so many nice people and homely atmosphere.

I acknowledge Prof. Vida Kirveliene and Stase Vaskeviciene from Vilnius University for flexibility and possibility to prepare and defend my thesis. Colleagues at the Department of Biochemistry and Biophysics, Ausra, Silvija and Arturas are acknowledged for their help during my thesis preparation. I am grateful to Martas, Virga, Birute, Andrius, Ana, Sandra, Justina, Simona, Daiva, Ausra for the great time we had together.

I acknowledge all the people in the VMS laboratory that so nicely welcomed me. I thank present and former members of Dr. Tavares group Ana, Sandrine, Leonor, Isabelle(s), Odile, Valérie, Laetitia, Charlène, Mohamed, Anait, Noureddine, Karima, Eileen for creating a homely atmosphere in the lab. I am very grateful for all the moments we shared together.

I also thank all the team of Philippe Noirot at INRA, Jouy en Josas that hosted me for a months. I acknowledge Anne-Stephanie, Arnaud, Calum, Celia, Michal, Maria-Victoria, Johan, Eric, Elena, Yoni, Sandrine, Emilie, Sean for their friendship and help.

I thank my friends Neringa, Egle, Edita, Akvile, Jolita, Zita, Ruta, Kristina, Abla, Wissam, Abdessalem for their unconditional friendship.

I wish to express my deepest gratitude to my parents, grandparents, sister and her family for their love, care and believe on me. Finally, my very special thanks are reserved for Antanas, for his love, support and patience during these years.

ABBREVIATIONS

CFP	cyan fluorescent protein
cfu	colony forming unit(s)
CM	cytoplasmic membrane
e.o.p.	efficiency of plating
EM	electron microscopy
GD	gramicidin D
Glc*N*Ac	*N*-acetylglucosamine
i.m.	input multiplicity
IFM	immunofluorescence microscopy
IgG	immunoglobulin G
LPS	lipopolysaccharide
LTA	lipoteichoic acids
MAD	membrane-anchoring domain
Mur*N*Ac	*N*-acetylmuramic acid
OM	outer membrane
OMP	outer membrane protein
p.i.	post-infection
pfu	plaque forming unit(s)
PG	peptidoglycan
RBP	receptor binding protein
SP	signal peptide
T6SS	Type VI secretion system
T7SS	Type VII secretion system
TMD	transmembrane segments
TPP^+	tetraphenylphosphonium cation
WTA	wall teichoic acids
Δp	protonmotive force
$\Delta\Psi$	transmembrane difference of electrical potential (membrane voltage)

RÉSUMÉ

Les quatre étapes principales d'infection des bactéries par leurs virus sont (i) la reconnaissance spécifique de la cellule hôte et l'entrée du génome dans le cytoplasme, (ii) la réplication du génome viral, (iii) l'assemblage des particules virales, et (iv) leur relâchement, menant dans la plupart des cas à la lyse de la cellule. Bien que la description des étapes individuelles du cycle viral a été relativement bien établie, les détails de comment d'ADN viral chemine du virion jusqu'au cytoplasme de la bactérie hôte et de comment l'environnement cellulaire participe au processus restent mal compris.

La première étape de l'infection est la reconnaissance d'un récepteur à la surface de la bactérie hôte par la machinerie d'adsorption du phage. Les barrières que l'agent infectieux doit franchir par la suite sont la membrane externe de la bactérie Gram-negative, la paroi cellulaire et la membrane cytoplasmique. Ceci implique une dégradation localisée de la paroi et le cheminement de l'ADN à travers un pore dans la membrane. L'ADN linéaire se circularise normalement dans le cytoplasme et il est répliqué par la suite. On a utilisé le bactériophage SPP1 qui infecte la bactérie Gram-positive *Bacillus subtilis* comme modèle d'étude pour disséquer ces différentes étapes clés pour le démarrage de l'infection virale.

Dans ce travail de thèse les conditions d'infection et d'acquisition de données pour suivre en temps réel la dépolarisation de la membrane cellulaire de *B. subtilis* lors de l'infection par SPP1 ont été mis au point. Il est montré que le démarrage de l'infection déclenche une dépolarisation très rapide de la membrane cytoplasmique. Le potentiel de membrane n'est plus rétablit pendant toute la durée du cycle d'infection. Ce changement du potentiel de membrane au début de l'infection dépend de la présence du récepteur YueB. L'amplitude de la dépolarisation dépend du nombre de particules virales infectieuses présentes et de la concentration du récepteur YueB à la surface de la bactérie hôte. L'interaction du phage avec le récepteur YueB

conduit à l'interaction irréversible et à l'éjection de l'ADN de SPP1. Pour établir si c'est l'interaction avec YueB ou le début de l'entrée de l'ADN qui conduit à la dépolarisation de la membrane on a utilisé des phages SPP1 éclates par EDTA qui adsorbent normalement à *B. subtilis* mais qui n'avaient plus leur ADN. Les résultats obtenus ont montré que la dépolarisation requiert l'interaction du virus intacte avec le récepteur YueB. Des concentrations sous-millimolaire de Ca^{2+} sont nécessaires et suffisantes pour SPP1 liaison réversible à l'enveloppe d'hôte et donc de déclencher la dépolarisation.

La cinétique d'entrée de l'ADN du bactériophage SPP1 dans la bactérie *Bacillus subtilis* a été suivie en temps réel par microscopie de fluorescence. On a mis au point une méthode de microscopie pour visualiser des particules virales marquées avec des «quantum dots» ce qui permit de démontrer que ces particules se fixent préférentiellement aux pôles des bacilli. L'immuno-marquage du récepteur de SPP1, la protéine YueB, a montré que celle-ci a une organisation ponctuée à la surface de *B. subtilis* et se concentre particulièrement aux extrémités de la bactérie. Cette localisation particulière du phage sur la surface de la cellule hôte corrèle avec l'observation que l'ADN viral rentre dans le cytoplasme (<2 min) et se réplique dans des foci situés dans la plupart des cas à proximité des pôles de *B. subtilis*. L'étude spatio-temporelle de l'interaction de SPP1 avec son hôte Gram-positive montre que le virus cible des régions spécifiques de la bactérie pour son entrée et pour sa réplication. Transfert d'ADN dans le cytoplasme dépend des concentrations millimolaires de Ca^{2+}.

Un modèle décrivant les événements précoces de l'infection bactériophage SPP1 est présenté.

Mots-clés: bactériophage SPP1, entrée du virus; ions Ca^{2+}; potentiel de membrane; bactérie Gram-positif; YueB.

ABSTRACT

The four main steps of bacterial viruses (bacteriophages) lytic infection are (i) specific recognition and genome entry into the host bacterium, (ii) replication of the viral genome, (iii) assembly of viral particles, and (iv) their release, leading in most cases to cell lysis. Although the course of individual steps of the viral infection cycle has been relatively well established, the details of how viral DNA transits from the virion to the host cytoplasm and of how the cellular environment catalyzes and possibly organizes the entire process remain poorly understood.

Tailed bacteriophages are by far the most abundant viruses that infect Eubacteria. The first event in their infection is recognition of a receptor on the surface of host bacterium by the phage adsorption machinery. The barriers that the infectious particle overcomes subsequently are the cell wall and the cytoplasmic membrane of bacteria. This implies a localized degradation of the wall and the flow of its double-stranded DNA (dsDNA) through a hydrophilic pore in the membrane. The linear dsDNA molecule is most frequently circularized in the cytoplasm followed by its replication. In this study we used bacteriophage SPP1 that infects the Gram-positive bacterium *Bacillus subtilis* as a model system to dissect the different steps leading to transfer of the phage genome from the viral capsid to the host cell cytoplasm.

The conditions of infection for monitoring the depolarization of *B. subtilis* membrane during SPP1 infection in real-time were developed. It was shown that during entry SPP1 induces a very fast depolarization of the cytoplasmic membrane (CM) of the infected cell. Membrane voltage ($\Delta\Psi$) is not recovered during the infection cycle. Depolarization requires interaction of the SPP1 infective virion with its receptor protein YueB. The amplitude of depolarization depends on the amount of phage particles interacting with the cell and on the concentration of YueB at the cell surface. This interaction is required for phage SPP1 irreversible binding to *B. subtilis* and for triggering DNA ejection from the virion. SPP1 particles that lost their DNA due to disruption of the capsid structure following treatment with EDTA bind

normally to *B. subtilis* but do not trigger depolarization of the CM. Attachment of intact SPP1 particles is thus required for phage-induced depolarization.

The beginning of *B. subtilis* infection by bacteriophage SPP1 was followed in space and time. The position of SPP1 binding at the cell surface was imaged by fluorescence microscopy using virus particles labeled with "quantum dots". We found that SPP1 reversible adsorption occurs preferentially at the cell poles. This initial binding facilitates irreversible adsorption to the SPP1 phage receptor protein YueB, which is encoded by a putative type VII secretion system gene cluster. Immunostaining and YueB – GFP fusion showed that the phage receptor protein YueB is found over the entire cell surface. It concentrates at the bacterial poles too, and displays a punctate distribution over the sidewalls. The dynamics of SPP1 DNA entry and replication was visualised in real time by assaying specific binding of a fluorescent protein to tandem sequences present in the SPP1 genome. During infection, most of the infecting phages DNA entered and replicated near the bacterial poles in a defined focus. Therefore, SPP1 assembles a replication factory at a specific location in the host cell cytoplasm. DNA delivery to the cytoplasm depends on millimolar concentrations of Ca^{2+} allowing uncoupling it from the precedent steps of SPP1 adsorption to the cell envelope and CM depolarization that require only micromolar amounts of this divalent cation.

A model describing the early events of bacteriophage SPP1 infection is presented.

Key-words: bacteriophage SPP1, virus entry; Ca^{2+} ions; membrane voltage; Gram-positive bacterium; YueB.

SANTRAUKA

Pagrindiniai bakterijas infekuojančių virusų (bakteriofagų) litinės infekcijos etapai yra (i) specifinis atpažinimas ir genomo pernaša į ląstelę šeimininkę, (ii) viruso genomo replikacija ir baltymų sintezė, (iii) virusinių dalelių susirinkimas, ir (iv) jų išlaisvinimas, dažniausiai sukeliantis ląstelės lizę. Atskiri virusinės infekcijos etapai yra gana gerai ištirti, tačiau kaip viruso DNR patenka į ląstelės citoplazmą, bei kaip šis procesas yra katalizuojamas ir, galbūt, organizuojamas ląstelės aplinkos žinoma mažai.

Uodeguotieji bakteriofagai yra labiausiai paplitę Eubakterijas infekuojantys virusai. Šie virusai inicijuoja infekciją prisitvirtinimo aparato pagalba atpažindami receptorių ląstelės šeimininkės paviršiuje. Tada infekuojanti viruso dalelė turi įveikti ląstelės sienelės bei citoplazminės membranos (CM) barjerus. Tam tikslui lokaliai suardoma ląstelės sienelė, ir dvigrandininė DNR (dgDNR) į citoplazmą patenka pro hidrofilinę porą membranoje. Patekusi į citoplazmą linijinė dgDNR molekulė dažniausiai tampa žiedine ir yra replikuojama. Siekiant išanalizuoti fago genomo pernešimo iš viruso kapsidės į ląstelės šeimininkės citoplazmą etapus, šiame darbe buvo pasirinkta bakteriofago SPP1, infekuojančio gramteigiamąsias *Bacillus subtilis* ląsteles, modelinė sistema.

Buvo parinktos sąlygos realiame laike tirti fago infekcijos indukuojamus *B. subtilis* membranos laidumo pokyčius. Pademonstravome, jog patekimo metu SPP1 labai greitai depoliarizuoja infekuojamos ląstelės CM ir membranos įtampa ($\Delta\Psi$) infekcinio ciklo metu nėra atkuriama. Depoliarizacijai vykti reikalinga infektyvių SPP1 dalelių sąveika su receptoriniu baltymu YueB. Depoliarizacijos amplitudė priklauso nuo su ląstele sąveikaujančių faginių dalelių kiekio bei ląstelės paviršiuje esančio YueB baltymo koncentracijos. Ši sąveika reikalinga negrįžtamam fago prikibimui prie *B. subtilis* bei DNR ištekėjimui iš viriono kapsidės indukuoti. DNR nebeturinčios SPP1 dalelės, kurių kapsidės suardytos EDTA pagalba, normaliai

prikimba prie *B. subtilis* paviršiaus, tačiau nedepoliarizuoja jų CM. Šie rezultatai parodo, kad fago indukuojamai depoliarizacijai sukelti reikalingos sveikos SPP1 dalelės .

B. subtilis infekcijos bakteriofagu SPP1 pradžia buvo detaliai tiriama nagrinėjant infekcinės sistemos pokyčius erdvėje ir laike. SPP1 prikibimo prie ląstelės paviršiaus vieta buvo nustatoma fluorescentinės mikroskopijos pagalba naudojant virusines daleles pažymėtas kvantiniais taškais. Mūsų rezultatai parodė, kad grįžtamo prikibimo metu SPP1 virionai susitelkia prie ląstelės polių. Šis pradinis prikibimas palengvina negrįžtamą sąveiką su SPP1 receptoriniu baltymu YueB, kuris yra koduojamas numanomos sekrecijos sistemos VI genų sankaupoje. YueB žymėjimas fluorescuojančiais antikūnais bei YueB ir žaliojo fluorescuojančio baltymo genų suliejimas parodė, jog receptorinis baltymas YueB yra randamas visame ląstelės paviršiuje. Jo išsidėstymas yra taškinis ląstelės šonuose ir labiau sutelktas ląstelės poliuose. SPP1 DNR patekimo kinetika ir replikacija buvo vaizdinama realiu laiku stebint atrankų fluorescuojančio baltymo prisijungimą prie pasikartojančių sekų SPP1 genome. Mūsų tyrimų rezultatai parodė, kad SPP1 DNR replikuojama tam tikrame taške netoli nuo patekimo vietos bakterijos poliuose. Mes taip pat nustatėme, kad DNR patekimui į citoplazmą būtina milimolinė Ca^{2+} koncentracija terpėje, nors anksčiau vykstančiam prikibimui bei CM depoliarizacijai pakanka mikromolinių šio dvivalenčio jono koncentracijų. Disertacijoje pateikiamas modelis, aprašantis ankstyvus SPP1 infekcijos įvykius.

Raktiniai žodžiai: bakteriofagas SPP1; virusų patekimas; Ca^{2+} jonai; membranos įtampa; gramteigiamosios bakterijos; baltymas YueB.

OVERVIEW

Bacterial viruses (phages or bacteriophages) are the most abundant biological entities in the Biosphere (Hendrix et al., 1999). Phages are of interest to scientists as tools to understand fundamental molecular biology, as vectors of horizontal gene transfers and drivers of bacterial evolution, as sources of diagnostic and genetic tools, and as novel therapeutic agents. Bacteriophages are a problem in industrial bioprocesses that rely on bacterial fermentation (Callanan and Klaenhammer, 2008; Brüssow, 2001). Studies of the biology of phages and the interactions with their hosts is the key to understand microbial systems and their exploitation.

The life cycle of a bacteriophage encompasses the specific recognition of the host by the viral particle, passage through the bacterial envelope, viral gene expression, viral genome replication, assembly of viral particles and their release from the cell. Molecular details of these processes are biochemically and structurally well established by 50 years of intensive research on several model systems. A significant number of phage multiplication steps were dissected to individual molecular interactions in the assay tube but their cell biology remains largely uncharacterized. Entry into the host bacterial cell is one of the least understood steps in the life cycle of bacteriophages. The different envelopes of Gram-negative and Gram-positive bacteria, with a fluid outer membrane (OM) and exposing a thick peptidoglycan wall exposed to the environment, respectively, impose distinct challenges for bacteriophages binding and (re-)distribution on the bacterial surface and further entry into the host cell cytoplasm.

The goal of this study was to define requirements for entry of the tailed bacteriophage SPP1 in the Gram-positive rod-shaped bacterium *B. subtilis* and to study the initial steps of infection in space and time.

The specific aims of the present study were:

- ✓ to define sequential steps in SPP1 DNA entry in the cell;
- ✓ to define changes in cytoplasmic membrane (CM) permeability during the initial steps of bacteriophage SPP1 infection;
- ✓ to define the role of Ca^{2+} ions in the process of entry;
- ✓ to determine the localization of the SPP1 receptor protein YueB on the surface of *B. subtilis* cells;
- ✓ to determine the spatial-temporal program of bacteriophage SPP1 attachment, DNA penetration and replication inside the host cytoplasm.

Scientific novelty.

In order to deliver its genome to the host cytoplasm SPP1 has to cross the Gram-positive cell envelope. Although the structure, molecular biology and multiplication steps of some phages that infect Gram-positive bacteria is known rather well (Alonso et al., 2006; Brøndsted and Hammer, 2006; Salas, 2006), the mechanism of phage genome transport across the Gram-positive cell envelope is poorly understood. The entry of tailed phages, as well as filamentous phages, infecting Gram-negative hosts, was studied more extensively (for reviews see Letellier et al., 2004; Vinga et al., 2006a). There are only a few examples of detailed studies on phages infecting Gram-positive hosts. The membrane-containing bacteriophage Bam35 (*Tectiviridae* family) uses the lipid membrane of the virion for genome delivery into the Gram-positive host *Bacillus thuringiensis* cytoplasm (Gaidelyte et al., 2006). The short-tailed phage ϕ29 (*Podoviridae* family) infects Gram-positive *B. subtilis* cells and ejects its DNA in a two-step process by an energy-requiring mechanism (González-Huici et al., 2004). Very little is known about delivery to the cell of DNA from bacteriophages with a long non-contractile tail (*Siphoviridae* family). The well studied siphophage SPP1 and its Gram-positive host *B. subtilis* provide an excellent system to study virus-host cell interactions.

In the past 10 years optical imaging technologies suitable to investigate bacterial cell ultrastructure were developed. Discovery of the asymmetric distribution of numerous cell components, their dynamic spatial and temporal re-distribution within the bacterium (Barák et al., 2008; Carlsson et al., 2009; Lemon and Grossman, 1998; Wang et al., 2004; Yamamoto et al., 2003), and the presence of cytoskeletal elements (Cabeen and Jacobs-Wagner, 2010; Carballido-López and Errington, 2003; Carballido-López, 2006) demonstrated a complex organization in bacterial cells. These findings and presently available technology created the momentum to investigate cell biology of bacteriophage infection. Understanding how viruses take advantage of the bacterial cell organization to optimize their multiplication is a novel theme of significant importance to understand infection and to investigate cellular processes. This type of observations is novel for prokaryotic cells infections and provides relevant information to understand the poorly known mechanism of viral DNA entry into bacteria.

Thesis output:

- ✓ Bacteriophage SPP1 irreversible adsorption to YueB protein is associated with fast depolarization of the *B. subtilis* CM;
- ✓ *B. subtilis* CM depolarization and SPP1 DNA entry are two sequential steps that can be distinguished by the requirement for different concentrations of Ca^{2+};
- ✓ The bacteriophage SPP1 receptor protein YueB concentrates at the cell poles and displays a punctate peripheral distribution along the sidewalls of *B. subtilis* cells;
- ✓ The topology of SPP1 receptors on the surface of the host cell determines the site of phage binding, DNA entry and subsequent
- ✓ replication, which occurs in discrete foci.

The present thesis was the result of joint supervision and close collaboration between the laboratories headed by Doctor Paulo Tavares (Unité de Virologie Moléculaire et Structurale, CNRS UPR3296 and IFR 115, Bâtiment 14B, CNRS, 91198 Gif-sur-Yvette, France) and Professor Rimantas Daugelavičius (Department of Biochemistry and Biophysics, Vilnius University, Čiurlionio 21, LT-03101 Vilnius, Lithuania).

Thesis is formed by four main chapters: Introduction, Materials and Methods, Results, and Discussion. Parts of the text used in each chapter were transcribed from published material:

Jakutyte, L., Baptista, C., São-José, C., Daugelavicius, R., Carballido-López, R., Tavares, P., 2011. Bacteriophage infection in rod-shaped gram-positive bacteria: evidence for a preferential polar route for phage SPP1 entry in *Bacillus subtilis*. J. Bacteriol. 193, 4893-4903.

Jakutytė, L., Lurz, R., Baptista, C., Carballido-Lopez, R., São-José, C., Tavares, P., Daugelavičius, R., 2011. First Steps of Bacteriophage SPP1 Entry into *Bacillus subtilis*. Virology, doi: 10.1016/j.virol.2011.11.010.

CONTENTS

I. INTRODUCTION

I.1. General properties of phages

Bacterial viruses (phages or bacteriophages) are the most abundant biological entities in the Biosphere (Hendrix at al., 1999). Phages are ubiquitous and can be found in all reservoirs populated by bacterial hosts, such as soil, sea water or the intestines of animals. Bacteriophages were formally discovered twice in a short time by Frederick Twort (1915) and Félix d'Hérelle (1917). Since that time their ecological impact (Abedon, 2006), their molecular sophistication (Calendar, 2006), their laboratory and medical significance (Waldor et al., 2005), and their ability to kill bacterial pathogens (d'Hérelle, 1917; Kutter and Sulakvelidze, 2005; Weinbauer, 2004) were intensively studied.

Phages may be defined as obligate intracellular parasites of the domain Bacteria which, as viruses, have an extracellular state (virion or viral particle) in their life cycles (Abedon, 2009). A phage can persist but it cannot replicate outside a bacterial cell. For survival, the virion must protect its nucleic acid from environmental aggressions and deliver it into a bacterium. The ability of a particular phage to infect a bacterium is normally limited to a single bacterial species and often to a few strains of that species. Contrary to eukaryotic viruses, the multiplication cycle of most phages is measured not in hours, but in minutes (Ackermann, 1998). Phages are virulent (lytic) or temperate (lysogenic). Infection process involves a number of tightly programmed steps (Guttman et al., 2005):

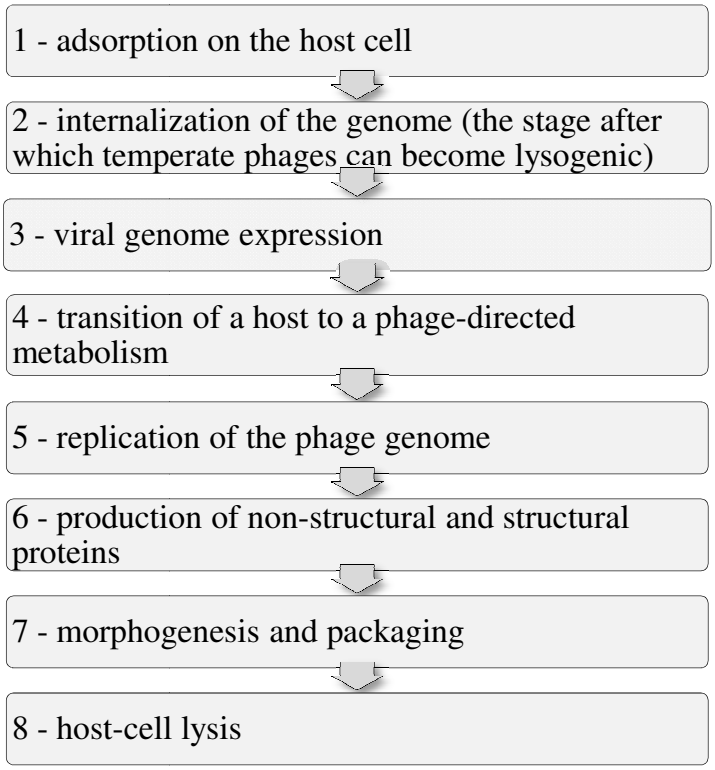

Virulent phages usually kill the cells they infect, while the genomes of temperate phages can persist silent within their hosts as integrated prophages or as plasmids. Under certain circumstances, as the exposure of the host cell to stress conditions, there is a genetic switch in the expression of viral genes of the phage lysogen genome leading to entry into the lytic cycle resulting in phage multiplication and cell death.

I.2. Bacteriophage properties and diversity

A viral particle consists of nucleic acid protected by a protein lattice. Some phages carry also a lipid membrane (Abedon, 2009). Phages include virions with double-stranded DNA (dsDNA, the vast majority), single-stranded DNA (ssDNA), single-stranded RNA (ssRNA), and double-stranded RNA (dsRNA; very rare). Most

virions (96%) have a dsDNA genome and are tailed (Ackermann, 2009). In contrast, most plant viruses have RNA genomes, while viruses of animals have RNA or DNA genomes and are not tailed (Domingo and Holland, 1994). Other bacteriophages are polyhedral, filamentous, or pleomorphic (Ackermann, 2009) (Fig. I.1, table I.1). Based on the type of nucleic acid and virion morphology bacteriophages are classified by the ICTV (International Committee on Taxonomy of Viruses) into ten families (Fauquet et al., 2005). The characteristics of bacterial virus families are summarized in Table I.1.

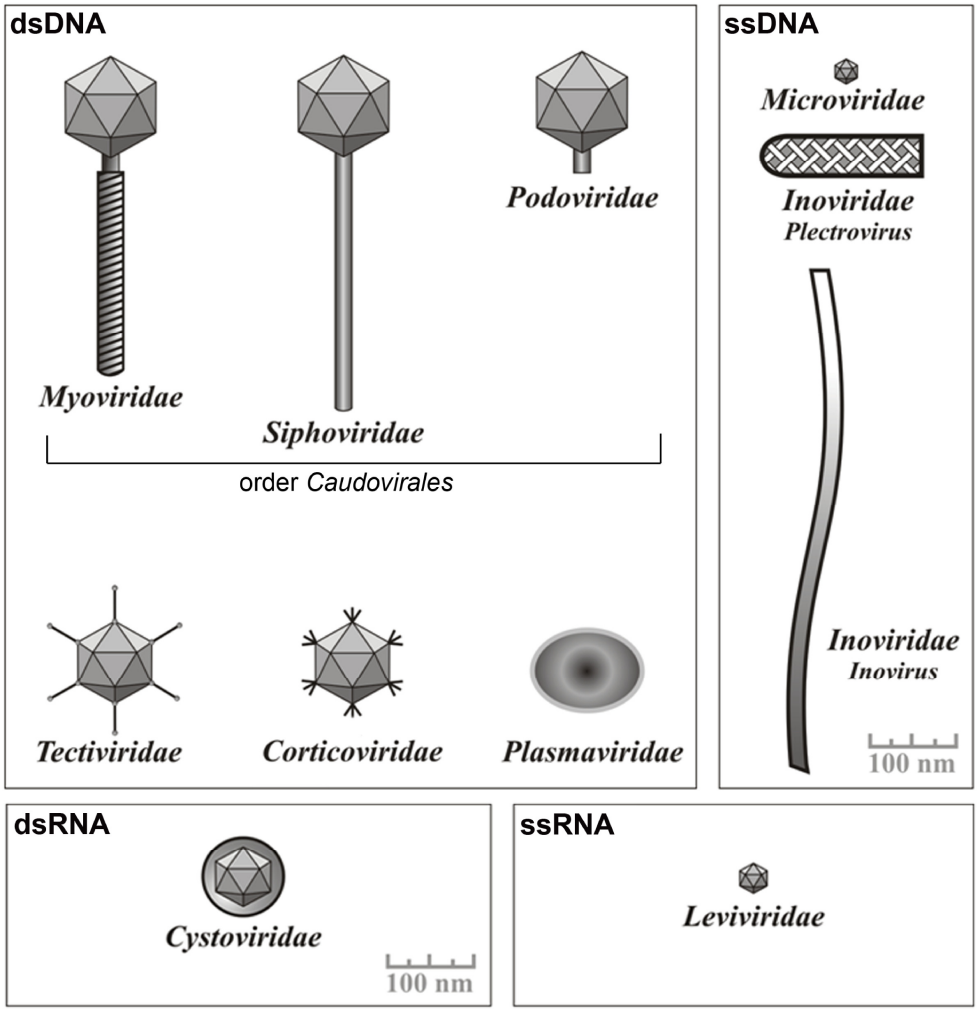

Fig. I.1. Schematic representation of bacteriophage morphotypes (Modified from Virus Taxonomy: Eighth Report of the International Committee on Taxonomy of Viruses (ICTV), 2005).

Table I.1. Overview of bacteriophage families. Adapted from Ackermann, 2009.

Shape	Nucleic acid	Family	Genera	Particulars	Example	Members*
Tailed	dsDNA (L)	*Myoviridae*	6	Long contractile tail	T4, SP01	1,320
Tailed	dsDNA (L)	*Siphoviridae*	8	Long, noncontractile tail	λ, SPP1, T5	3,229
Tailed	dsDNA (L)	*Podoviridae*	4	Short tail	T7, ϕ29, P22	771
Polyhedral	ssDNA (C)	*Microviridae*	4	Nonenveloped	ϕX174	40
Polyhedral	dsDNA (C, S)	*Corticoviridae*	1	Internal membrane	PM2	3**
Polyhedral	dsDNA (L)	*Tectiviridae*	1	Internal membrane, pseudo-tail	PRD1, Bam35	19
Polyhedral	ssRNA (L)	*Leviviridae*	2	Nonenveloped	MS2	39
Polyhedral	dsRNA (L, M)	*Cystoviridae*	1	Envelope, lipids	ϕ6	3
Filamentous	ssDNA (C)	*Inoviridae*	2	Long filaments, short rods	M13, fd, f1	67
Pleomorphic	dsDNA (C, S)	*Plasmaviridae*	1	Envelope, no capsid, lipids	L2	5

C, circular; L, linear; M, multipartite (segmented); S, supercoiled. *Members indicate numbers of phages examined by electron microscopy, excluding phage-like bacteriocins and known defective phages (based on observations reported until January 2006; from reference Ackermann, 2007). **Probably three members.

I.3. Tailed viruses, order *Caudovirales*

Tailed viruses infect Eubacteria and Archaea and are probably very ancient, dating back at least to the last universal common ancestor (LUCA) of the cells (Ackermann, 2009; Krupovic and Bamford, 2010). The order *Caudovirales* (from the Latin *cauda*, "tail") consist of three families of tailed viruses (Fig. I.2).

Myoviridae (from the Greek *my, myos,* "muscle", referring to the contractile tail): Tails consist of a neck, a contractile sheath, a central tube and an adsorption apparatus. Myoviruses tend to be larger than members of other groups and include some of the largest and most complex tailed phages (25% of tailed viruses) (Fig. I.3).

Siphoviridae (from Greek *siphon,* "tube", referring to the long tail): Tails are simple, noncontractile, flexible or rigid tubes. Siphoviruses are the most abundant tailed phages (61% of tailed viruses).

Podoviridae (from Greek *pous, podos,* "foot", referring to the short tail): Tails are short and noncontractile (14 % of tailed viruses) (Ackermann, 2009; Fauquet, 2005).

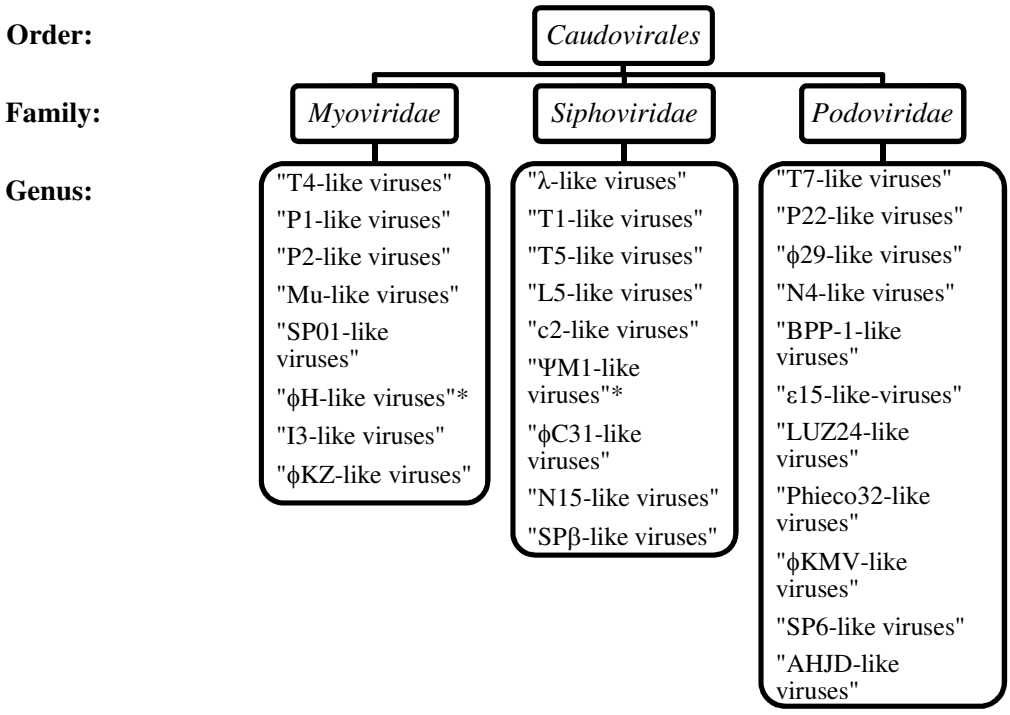

Fig. I.2. Taxonomic structure of the order *Caudovirales.* (adapted from ICTV Master Species List 2009 - Version 10: http://talk.ictvonline.org/files/ictv_documents/m/msl/1231.aspx). Each family has a large number of unclassified viruses. *Archaeal viruses.

Tailed bacterial viruses are an extremely large group with diverse virion, genome, and replication properties (Fauquet, 2005). Virions have isometric or prolate heads (Fig. I.3). Tails can be short or long assemblies that feature structures used for fixation to the host cell (baseplates, spikes, fibers). Tailed phage dsDNA genomes can range up to over 500 kb (Seaman and Day, 2007; Serwer et al., 2007). In contrast, the genomes of tailless phages are less than 15 kb (Abedon, 2009; Fauquet et al., 2005). Figure I.3. shows different morphological types of tailed bacteriophages.

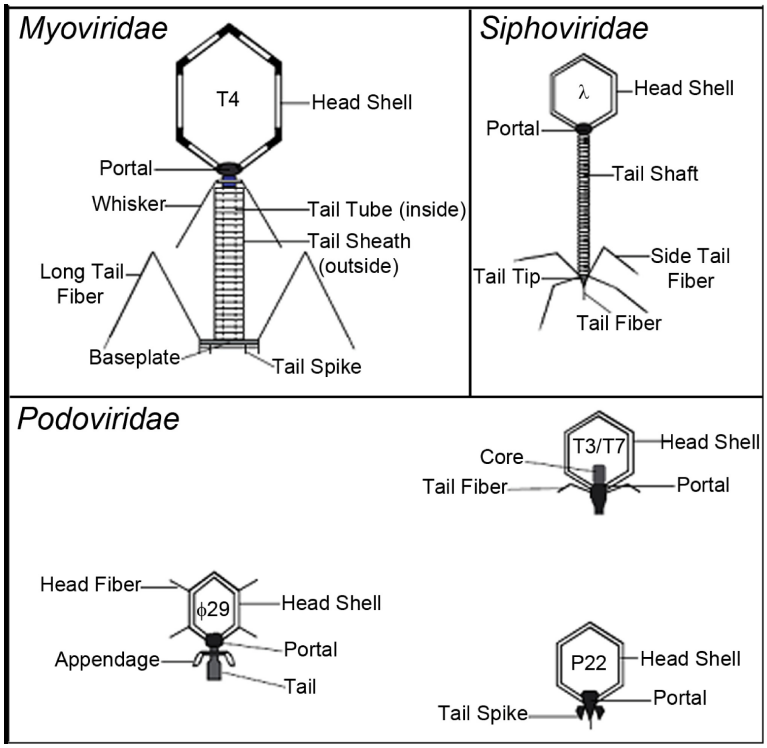

Fig. I.3. Schematic representation of tailed bacteriophage virions from *Myoviridae* (long contractile tail: T4), *Siphoviridae* (long non-contractile tail: λ) and *Podoviridae* (short-tail: ϕ29, T3/T7, P22) families. Phages with prolate (elongated) heads (T4, ϕ29) and phages with isometric heads (λ, T3/T7, P22). The phage adsorption apparatus found at the tail end distal from the head can be a baseplate, a tail spike structure or a tail fiber. The tail binds to a specialized vertex of the capsid structure, the portal vertex. Phage components are indicated. Adapted from Casjens and Hendrix (1988) and Xu, (2001).

Tailed phages adsorb to bacteria through their tail adsorption apparatus, digest the cell wall using specialized enzymes and deliver their DNA through the cytoplasmic membrane (CM). The phage dsDNA enters the cell and the empty capsid remains outside (Hershey and Chase, 1952). This behavior contrasts with that of viral particles of multicellular organisms that enter host cells. Following ejection from the virion and entry in the cytoplasm the genome is either integrated into the host genome, or stays as an independent replication unit in the cytoplasm. In lytic infections gene expression and genome replication ensue followed by assembly of viral particles. The progeny phages are assembled via complex pathways, with phage DNA entering preformed capsids through a specialized portal vertex of these

structures powered by the ATPase activity of the terminase complex (Catalano, 2005). Cell lysis is accomplished by a dual lysis system consisting of peptidoglycan (PG) hydrolases (endolysins), which attack the cell wall, and holins, which damage the CM and allow the endolysin to access the PG (Young and Wang, 2006). Tailed viruses resemble viruses belonging to the family *Herpesviridae* in replication strategy, morphogenesis, and in some cases latency (Fauquet et al., 2005).

Phage SPP1, that is studied in this thesis, infects the Gram-positive bacterium *B. subtilis*. It belongs to λ-like genera, *Siphoviridae* family of the order *Caudovirales*.

I.4. Bacterial cell envelope: the barrier to host cell infection

The barriers encountered by viruses of Eubacteria to reach the cytoplasm are the bacterial cell wall and the CM.

The bacterial cell envelope is a complex multilayered structure that serves to protect the cells against lysis by osmotic forces from within and from chemical or biological aggression from their environment (Silhavy et al., 2010; Young, 2010). Cell envelopes fall into two major categories: Gram-positive and Gram-negative (Fig. I.4). This is based on different Gram-staining properties that reflect major structural differences between the two groups. Gram-negative bacteria are surrounded by a thin PG cell wall, which itself is surrounded by an outer membrane (OM) containing lipopolysaccharides (LPS) (Fig. I.4A). Gram-positive bacteria lack an OM but are surrounded by layers of cross-linked PG many fold thicker than in Gram-negative envelopes. Long anionic polymers of wall teichoic acids (WTA) are anchored in the PG meshwork (Fig. I.4B).

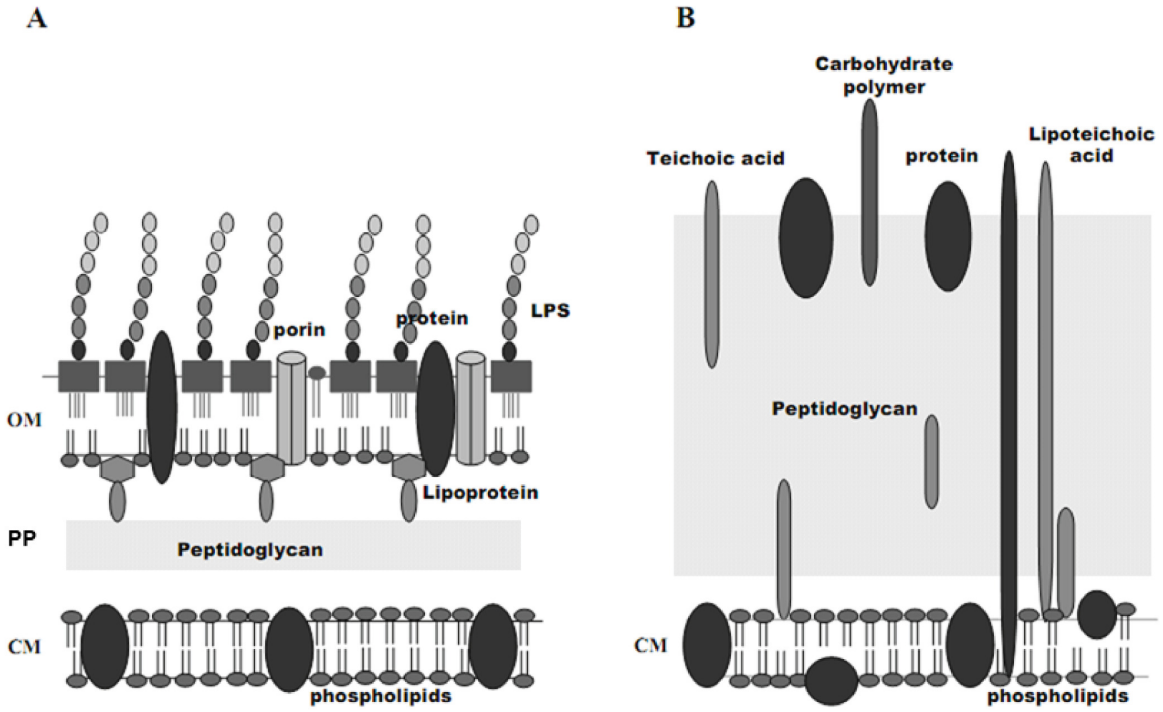

Fig. I.4. Schematic representation of the Gram-negative (A) and Gram-positive (B) cell envelope. CM: cytoplasmic membrane; PP: periplasm; OM: outer membrane; LPS: lipopolysaccharide. The scheme is not in scale. Adapted from Vinga et al., 2006a.

Corynebacterineae is a group of bacteria that includes important pathogens as *Mycobacterium tuberculosis*. Their cell envelope has characteristics of both Gram-positive and Gram-negative bacteria (Fig. I.5). These bacteria are generally classified as high G+C Gram-positives, but unlike other Gram-positive bacteria *Corynebacterineae* have an OM. The original and complex organization of the *Corynebacterineae* envelope plays a major role on their virulence. The PG layer that surrounds a standard CM contains covalently attached arabinogalactan that is covalently attached to mycolic acids (Minnikin, 1982). Recently, cryo-electron microscopy showed that mycobacterial cell wall lipids form an unusual OM. Unlike the OM of Gram-negative bacteria, the mycobacterial OM appears to be symmetrical (Fig. I.4A and I.5; Hoffmann et al., 2008; Zuber et al., 2008).

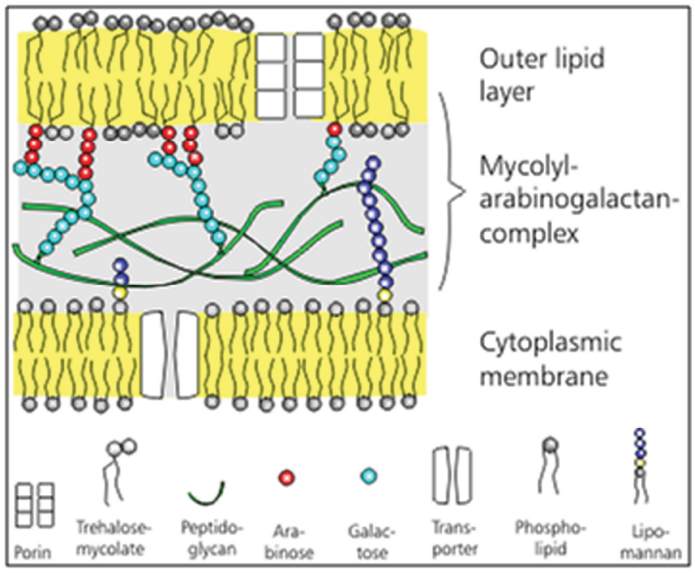

Fig. I.5. Schematic representation of the *cell envelope structure of Corynebacterianeae.* Adapted from: http://www.fz-juelich.de/ibt/amino/cell-wall.

Mycoplasmas are phylogenetically related to Gram-positive bacteria but have no cell wall. They resist to osmotic lysis due to their unusually tough CM (given by sterols) or because they live in osmotically protected environment, such as the animal body (Madigan et al., 1997).

I.4.1. Cell wall

PG (murein) is an essential and specific component of the bacterial cell wall found on the outside of the CM of almost all bacteria (Vollmer et al., 2008). Its main function is to preserve cell integrity by withstanding the cytoplasmic turgor. The PG also contributes to the maintenance of a defined cell shape and serves as a scaffold for anchoring other cell envelope components such as proteins (Dramsi et al., 2008) and WTA (Neuhaus and Baddiley, 2003). It is intimately involved in the processes of cell growth and cell division (Hayhurst et al., 2008; Vollmer et al., 2008).

The main structural features of PG are linear glycan strands cross-linked by short peptides (Rogers et al., 1980). The glycan strands are made up of alternating *N*-acetylglucosamine (Glc*N*Ac) and *N*-acetylmuramic acid (Mur*N*Ac) residues linked by β-1 → 4 bonds and cross-linked by pentapeptide side chains (Fig. I.6). The D-lactoyl group of each Mur*N*Ac residue is substituted by a peptide stem whose composition is most often L-Ala-γ-D-Glu-*meso*-A_2pm (or L-Lys)-D-Ala-D-Ala (A_2pm, 2,6-diaminopimelic acid) in nascent PG, the last D-Ala residue being lost in the mature macromolecule. Cross-linking of the glycan strands generally occurs between the carboxyl group of D-Ala at position 4 and the amino group of the diamino acid at position 3, either directly or through a short peptide bridge. There is a high diversity in the composition and sequence of the peptides in the PG from different species (Vollmer et al., 2008).

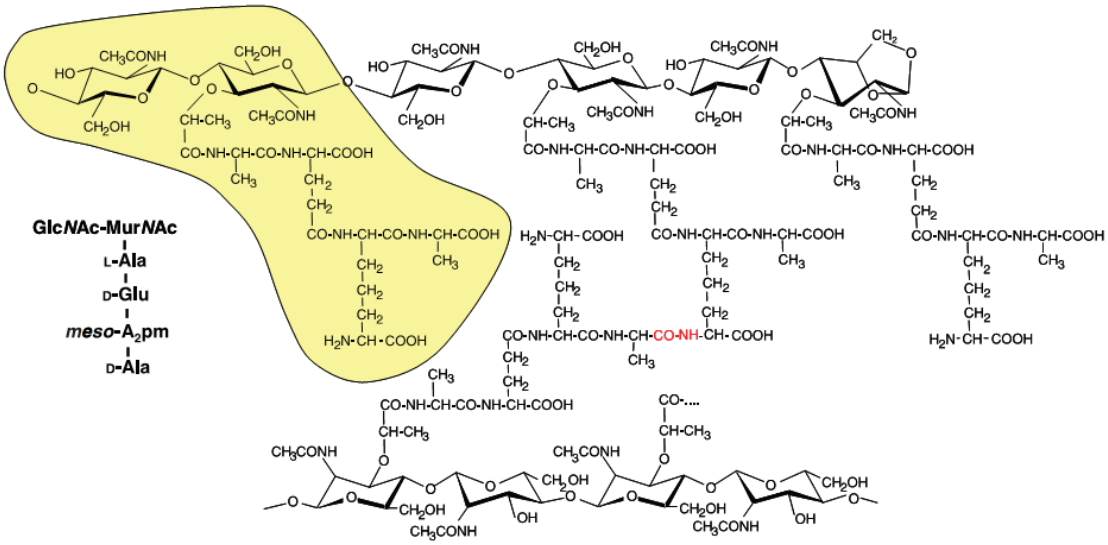

Fig. I.6. Structure of the PG of *Escherichia coli* and *B. subtilis*. The glycan strands consist of alternating, β-1 → 4-linked Glc*N*Ac and Mur*N*Ac residues, and are terminated by a 1,6-anhydroMur*N*Ac residue. The yellowish labeled part represents the basic disaccharide tetrapeptide subunit (monomer), which is also written with the conventional amino acid and hexosamine abbreviations on the left-hand side. The middle part shows a cross-linked peptide, with the amide group connecting both peptide stems drawn in red. Adapted from Vollmer et al., 2008.

Glycan chains run perpendicular to the long axis of a rod shaped cell, i.e., hoops of glycan chains around the short axis of the cell (Gan et al., 2008; Hayhurst et al., 2008). The mesh of PG net is a strong, but also elastic stress-bearing structure, which has an average cut-off value for the passage of globular proteins of about 50 kDa and works as a sieve with holes of a mean diameter about 2 nm, reaching in a few cases a maximal diameter of 4 nm (Delcour et al., 1999; Demchick and Koch, 1996; Dijkstra and Keck, 1996; Höltje, 1998; Jordan et al., 2008). PG of Gram-negative bacteria is located in the periplasm and covalently linked to the OM by Braun's lipoproteins (Fig. I.4A; Braun and Sieglin, 1970; Dijkstra and Keck, 1996). Gram-positive bacteria have several layers of PG forming a structure that can be about 50 nm thick surrounding the cell CM. It can be up to 10 times as thick as the PG of Gram-negative bacteria. The Gram-positive PG sacculus is interspersed with WTA that can be either tethered to the membrane (lipoteichoic acids (LTA)) or covalently linked to the sugar backbone of the PG sacculus (Delcour et al., 1999; Foster and Popham, 2002). WTA are poly-anionic, phosphate-rich linear polymers mainly responsible for the overall negative net charge of the Gram-positive cell surface (Fig. I.7). WTA have a particular affinity for divalent cations (Bhavsar et al., 2004; Weidenmaier and Peschel, 2008).

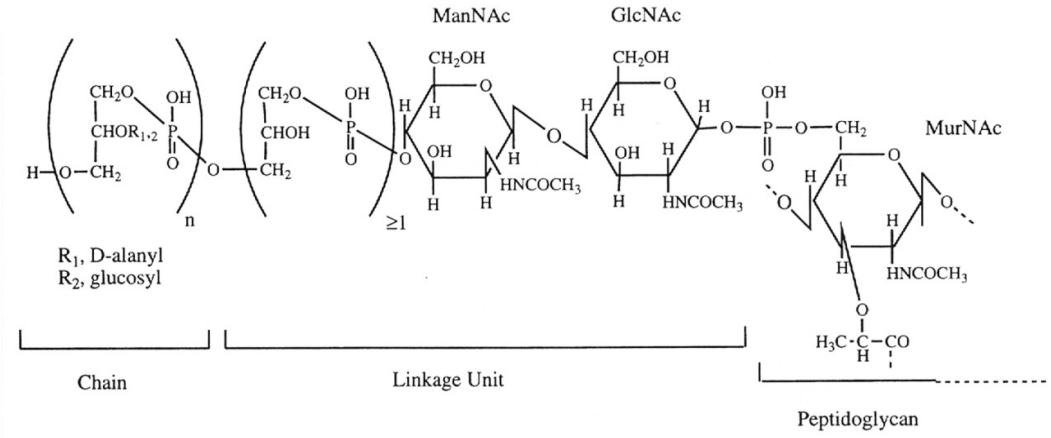

Fig. I.7. Structure of the major glycerol teichoic acid of *B. subtilis* strain 168. Man*N*Ac, *N*-acetylmannosamine. Adapted from Foster and Popham, 2002.

The PG meshwork embeds also sugar polymers, proteins and lipoproteins. Although the structure of cell wall protects bacteria from attacks by environmental stresses, including other biological entities, most of the Gram-positive cell wall components may serve as receptors for phages (Vinga et al., 2006a; Young, 2010).

I.4.2. Cytoplasmic membrane

The bacterial CM is composed of lipids assembled in a bilayer containing integral and peripheral membrane proteins, carbohydrates, ions (K^+, Na^+), and water (Finean et al., 1984). There is a large difference of lipid composition among the CM of bacterial species. For most bacteria the predominant zwitterionic phospholipid is phosphatidylethanolamine (PE). In general, Gram-negative bacteria have a higher content of PE than Gram-positive bacteria. The predominant anionic lipids in bacterial membranes are phosphatidylglycerol and cardiolipin (Epand and Epand, 2009). The CM is hydrophobic and fluid in nature. It acts as a semi-permeable barrier to prevent leakage of the hydrophilic constituents from the cytoplasm and to protect the internal milieu of the cell from external environmental insults. Importantly, the CM is impermeable to protons allowing the cell to conserve the energy of electron-transfer as proton electrochemical gradient ($\Delta\mu_H^+$) across the membrane. This form of energy is used to drive reactions such as adenosine triphosphate (ATP) synthesis, bacterial motility and active transport across the CM. The CM has many other important functions in cellular processes like cell-cell recognition, signal transduction, chemotaxis, chromosome replication, lipid synthesis, and cell division (for a review see Fyfe et al., 2001; Weiner and Rothery, 2007).

I.4.3. Outer membrane of Gram-negative bacteria

The OM is a distinguishing feature of Gram-negative bacteria. The primary function of the OM is to act as a permeability barrier for cytotoxic compounds and to control the access of solutes to the periplasm.

The OM is an asymmetric bilayer – the inner leaflet is composed of phospholipids, while the outer one consists mainly of lipopolysaccharides (LPS) (Fig. I.4A) (Nikaido, 1996). LPS, a toxic compound for animals, often serves as a phage receptor. LPS plays a critical role in the barrier function of the OM (Raetz and Whitfield, 2002). The LPS molecule can be structurally divided into three parts: a lipid moiety - lipid A, a nonrepeating "core" oligosaccharide and a hydrophilic polysaccharide called the O-antigen which differs from species to species (Madigan et al., 1997; Osborn et al., 1964). LPS molecules bind each other avidly, especially if cations like Ca^{2+} and Mg^{2+} are present to neutralize the negative charge of phosphate groups present on the molecule. The acyl chains are largely saturated, and this facilitates tight packing. The nonfluid continuum formed by the LPS molecules is a very effective barrier for hydrophobic molecules (Nikaido, 2003).

To ensure the influx of cell necessary nutrients from extracellular environment and for the extrusion of waste products from cell cytoplasm, the OM contains a number of transmembrane proteins: nonspecific porin channels and specific channels. These outer membrane proteins (OMPs) are formed essentially by β sheets that are wrapped into cylinders delimiting hydrophilic pores. Porins function as channels for traffic of hydrophilic low-molecular-weight substances (with an exclusion limit for molecules of ≥ 700 Da (Nikaido et al., 2003). Specific channels gate the diffusion of specific classes of nutrients.

OMPs are frequently phage receptors. Several OMPs have been identified by this feature (e.g. FhuA (or TonA receptor for phages T1, T5), Bfe (or BtuB; phage BF23), LamB (phage λ) and Tsx (Phage T6) (Heller, 1992).

Another class of OM proteins are lipoproteins. Lipoproteins contain lipid moieties that anchor them in the inner leaflet of the OM (Sankaran and Wu, 1994). As mentioned before, Braun's lipoproteins link the periplasmic thin layer of PG to the OM, but the function of most of the 100 OM lipoproteins found in *E. coli* is not known (Miyadai et al., 2004).

I.4.4. Bacterial surface structures

Bacterial surface structures that protrude from the cell surface are key players in adhesion, motility, chemotaxis, bacterial conjugation, biofilm and S-layer formation. These structures include the glycocalyx (capsular polysaccharides and slime layer), various adhesins, flagella and S-layer proteins.

Surface proteins called adhesins have the ability to adhere to host tissue, to solid surfaces or to other cells. Microbial adhesins are often assembled into complex polymeric organelle structures (fimbriae, curli, pili), although adhesins linked to the cell surface as monomers or simple oligomers also exist. Fimbriae are rod-shaped adhesive surface organelles (Klemm and Krogfelt, 1994). Curli are heteropolymeric proteinaceous filamentous appendages that play a role on the adherence properties of several biofilm-forming *E. coli* strains (Olsén et al., 1989). The F conjugative pilus is involved in horizontal gene transfer from a donor to a recipient cell during bacterial conjugation. In Gram-positive bacteria adhesins are usually attached covalently to stem peptides within the PG layers or sometimes via noncovalent ionic interactions to PG or teichoic acids (Silhavy et al., 2010). Another type of surface structures are those involved in cell motility - long rotating appendages anchored in CM called flagella. Some pili, designated type IV pili, can also generate motile forces (Mattick, 2002). Microbial adhesins and flagella are surface determinants of bacterial biofilm formation (van Houdt and Michiels, 2005).

The S-layer is a paracrystalline array found outside the PG layer in some Gram-positive or on top of the OM in several Gram-negative species. This self-assembling uniform lattice structure is usually composed of a single protein, but may also have attached carbohydrates. It completely envelops the bacterium. Each S-layer has a specific cut-off value and thus may act as molecular sieve to exclude agents that might damage the cell. Although present in many different bacteria and archaea, the functions of S-layers are poorly understood (Young, 2010 and references therein).

Bacterial pili, flagella, capsular and slime polysaccharides can serve as receptors for bacteriophages. Polymerization and depolymerization of pili is exploited by phages to approach the bacterial surface (Dreiseikelmann, 1994; Manchak et al., 2002).

I.5. Bacteriophage entry in the host cell

Like all other viruses, bacteriophages are obligate intracellular parasites. Therefore successful delivery of the virion genome to the bacterial cell is an essential early step for host infection. Phages use different strategies to deliver their genetic information across the bacterial envelope to the cell cytoplasm where their genome is expressed and replicated. The details of how viral DNA transits from the virion to the host cytoplasm and of how the cellular environment catalyzes and possibly organizes the entire process remain poorly understood. This process encompasses specific virion-host recognition, passage of the virion across the different cell envelope barriers and establishment of optimal conditions for virus multiplication in the host cytoplasm.

I.5.1. Phage adsorption

Phage infection is initiated by specific interaction of the virion with receptors at the host surface. The first contact with the bacterial surface usually leads to reversible binding of the virus particle that is not saturable. It allows for dissociation of viable phages from the bacterium. In a second step, phages attach irreversibly to cell envelope receptor committing to infection of the host. This process is normally saturable due to a limited number of active receptors accessible for the irreversible interaction at the cell surface. Reversible and irreversible adsorption can target the same receptor or involve different surface components. The most recent list of known receptors is described by Vinga et al., (2006a).

I.5.1.1. Bacterial receptors

Structures employed as phage receptors likely include most if not all molecules or molecular assemblies exposed at the cell surface. However, each bacteriophage species is known to be able to infect just a narrow host range. Such specificity is due to the phage ability to interact only with specific receptor structures exposed on the bacterial cell surface. The distinct envelopes of Gram-negative and Gram-positive bacteria impose different barriers to virus attack (section I.4).

Gram-negative bacteria

Various LPS sites and OMP's may serve as receptors for bacteriophages infecting Gram-negative bacteria (Fig. I.4A; Table I.2; Vinga et al., 2006a).

Table I.2. Overview of bacteriophage receptors in Gram-negative bacteria.

Phage	Phage host	Phage primary receptor	Phage secondary receptor	Cellular functions of receptors	Reference
T4	*Escherichia coli*	LPS (for *E. coli* B); OmpC (for *E. coli* K-12)	LPS core heptose residues	LPS: OM stability and protection and is an endotoxin to animals; OmpC: influx/efflux of small molecules	Mosig and Eiserling, 2006; Yu and Mizushima, 1982
K20	*Escherichia coli*	LPS	OmpF	LPS confers OM stability and protection and is an endotoxin to animals; OmpF confers influx/efflux of small molecules	Silverman and Benson, 1987; Traurig and Misra, 1999
TLS	*Escherichia coli*	LPS	TolC	LPS confers OM stability and protection and is an endotoxin to animals; TolC is component of efflux system	German and Misra, 2001
T5	*Escherichia coli*	LPS	FhuA	LPS confers OM stability and protection and is an endotoxin to animals; FhuA confers transport of ferrichrome	Heller and Braun, 1982; Heller and Schwarz, 1985; Plançon et al., 1997
T7	*Escherichia coli*	LPS	LPS	LPS confers OM stability and protection and is an endotoxin to animals;	Lindberg, 1973; Weidel, 1958
Rtp	*Escherichia coli*	LPS	LPS	LPS confers OM stability and protection and is an endotoxin to animals;	Wietzorrek et al., 2006
P22	*Salmonella typhimurium*	LPS	LPS	LPS confers OM stability and protection and is an endotoxin to animals;	Baxa et al., 1996; Steinbacher, 1996
ϕX174	*Escherichia coli*	LPS	LPS	LPS confers OM stability and protection and is an endotoxin to animals;	Feige and Stirm, 1976

ϕ13	*Pseudomonas syringae*	LPS	LPS	LPS confers OM stability and protection and is an endotoxin to animals;	Qiao et al., 2000
T1	*Escherichia coli*	FhuA	FhuA/TonB*	Transport of ferrichrome	Letellier et al., 2004
λ	*Escherichia coli*	LamB	LamB/ManY*	Uptake of maltose	Ryter et al., 1975; Szmelcman and Hofnung, 1975
BF23	*Escherichia coli; Salmonella typhimurium*	BtuB	BtuB	Transport of vitamin B12	Di Masi et al., 1973
T-even like	*Escherichia coli*	OmpA	OmpA	Integrity of the outer membrane, efficient conjugation	Morona et al., 1985
Gifsy-1 and Gifsy-2	*Salmonella typhimurium*	OmpC	OmpC	Influx/efflux of small molecules	Ho and Slauch, 2001
PRD1	*Pseudomonas aeruginosa; Pseudomonas fluorescens; Pseudomonas putida; Acinetobacter calcoaceticus; Escherichia coli; Proteus mirabilis; Vibrio cholerae; Salmonella typhimurium*	Proteins encoded by conjugative drug-resistance plasmid of incompatibility groups P, N or W	Proteins encoded by conjugative drug-resistance plasmid of incompatibility groups P, N or W	Conjugation	Olsen et al., 1974
M13 f1 fd	*Escherichia coli*	Pilus tip	Coreceptor: TolA	Pilus confers conjugation and attachment to host; TolA confers integrity of OM	Jacobson, 1972; Webster, 1996
MS2	*Escherichia coli*	Pilus side	Pilus side	Conjugation and attachment to host	Date, 1979; van Duin, 1988
Qβ					van Duin, 1988
ϕ6	*Pseudomonas syringae*	Pilus side	Phospholipids	Pilus confers attachment to host; Phospholipids are major components of all cell membranes	Bamford et al., 1976; Cvirkaite-Krupovic et al., 2010a; Romantschuk and Bamford, 1985

*Cell envelope proteins shown to be required for phage genome entry are also indicated for some examples.

In many cases the complete adsorption process of phages requires both types of molecules (Lindberg, 1973). LPS serves frequently as reversible receptor in conjunction to one of the OMPs (Table I.2; Vinga et al., 2006a). After reversible adsorption to LPS, tailed dsDNA phages K20, TLS and T5 adsorb irreversibly to non-selective porins OmpF, TolC and ferrichrome transporter FhuA respectively (German and Misra, 2001; Heller and Braun, 1982; Heller and Schwarz, 1985; Plançon et al., 1997; Silverman and Benson, 1987; Traurig and Misra, 1999; Yu and Mizushima, 1982). Phage BF23 adsorbs irreversibly to vitamin B12 transporter BtuB which is also the receptor of colicins E1 and E3 (Di Masi et al., 1973). Phages T7 (Lindberg, 1973; Weidel, 1958), P22 (Baxa et al., 1996; Steinbacher 1996), ϕX174 (Feige and Stirm, 1976) and ϕ13 (Qiao et al., 2000) use different LPS segments for both reversible and irreversible binding. There are phages that adsorb directly to OMPs. For example, the receptor to the temperate phage λ is the *E. coli* maltoporin receptor LamB (Ryter et al., 1975; Szmelcman and Hofnung, 1975). T-even like phages adsorb to OmpA (Morona et al., 1985) and *Salmonella* infecting phages Gifsy-1 and Gifsy-2 to OmpC (Ho and Slauch, 2001). Bacteriophage PRD1 and its close relatives (*Tectiviridae*) attach to the protein complex encoded by a conjugative drug-resistance plasmid of incompatibility groups P, N or W (Olsen et al., 1974).

Filamentous ssDNA phages (e.g., M13, f1, and fd) (Webster, 1996), icosahedral ssRNA phages (e.g., MS2 and Qβ) of *E. coli* (van Duin, 1988), and enveloped bacteriophage ϕ6 of *Pseudomonas syringae* (Bamford et al., 1976; Romantschuk and Bamford, 1985) use the bacterial pilus to dock to the bacterium. Filamentous phages interact specifically with the tip of the host cell F-pilus (Jacobson, 1972) whereas bacteriophage ϕ6 and icosahedral ssRNA phages attach to the side of the pili (Bamford et al., 1976; van Duin, 1988). Recently, Cvirkaite-Krupovic et al., (2010a) showed that phospholipids act as secondary receptors during the entry of the phage ϕ6. Interestingly, closely-related phages can use different receptors for phage entry. This is the case of the enveloped dsRNA phage ϕ13 (related

to the phage ϕ6) that uses LPS as receptors. Closely-related tailed dsDNA phages T1, Rtp and TLS adsorb irreversibly to FhuA/TonB, LPS and TolC respectively (Vinga et al., 2006a; Wietzorrek et al., 2006).

Polysaccharide capsules or slime may block access of bacteriophage to receptors localized in the cell wall but can, in turn, be also used for adsorption of phages. Typically, these phages have enzymatic activities associated with the tail structure permitting the phage access to the surface of the OM, where they probably bind to a secondary receptor (Scholl et al., 2005).

Gram-positive bacteria

Bacteriophages infecting Gram-positive bacteria can use PG, WTA, LTA or proteins exposed to the bacterial surface as their receptors. PG-associated sugars such as glucosamine, rhamnose or ribose are receptors for *Streptococcus thermophilus* and *Lactococcus lactis* phages (Table I.3; Geller et al., 2005; Quiberoni et al., 2000).

Table I.3. Overview of bacteriophage receptors in Gram-positive bacteria.

Phage	Phage host	Phage primary receptor	Phage secondary receptor	Cellular functions of receptors	Reference
A511	*Listeria monocytogenes*	PG	PG	Preserve cell integrity and shape	Wendlinger et al., 1996
A118	*Listeria monocytogenes*	N-glucosamine and rhamnose residues of WTAs	N-glucosamine and rhamnose residues of WTAs	Ionic properties of the cell wall	Wendlinger et al., 1996
LL-H	*Lactobacillus delbrueckii*	LTAs associated glucose	LTAs associated glucose	Cell pathogenicity, adhesion and wall hydrophobic properties	Räisänen et al., 2004; 2007
ϕ25	*Bacillus subtilis*	Glucosylated polyglycerol phosphate of WTAs	Glucosylated polyglycerol phosphate of WTAs	Ionic properties of the cell wall	Young, 1967
ϕ29	*Bacillus subtilis*	Glucosylated polyglycerol phosphate of WTAs	Putative CM component	Ionic properties of the cell wall	Jacobson and Landman, 1977; Young, 1967
ϕ3T	*Bacillus subtilis*	Poly-(glucosyl-N-acetylgalactosamine 1-phosphate)	Poly-(glucosyl-N-acetylgalactosamine 1-phosphate)	Ionic properties of the cell wall	Estrela et al., 1991
γ	*Bacillus anthracis*	GamR	GamR	Putatively involved in cobalt transport	Davison et al., 2005
c2	*Lactoccocus lactis*	PG	Pip	PG - preserve cell integrity and shape; Pip-unknown	Geller et al., 1993; Monteville et al., 1994
SPP1	*Bacillus subtilis*	Glucosylated polyglycerol phosphate of WTAs	YueB	WTAs confer ionic properties of the cell wall; YueB-unknown	Baptista et al., 2008; São José et al., 2004; Yasbin et al., 1976

The broad-host-range virulent *Listeria monocytogenes* infecting phage A511 uses PG as primary receptor while A118, a phage of *Listeria*, uses WTA rhamnose and glucosamine for adsorption (Wendlinger et al., 1996). Glucosylated WTAs are essential for the adsorption of numerous phages to *B. subtilis*, *Staphylococcus aureus* and *Lactobacillus plantarum* bacteria (Vinga et al., 2006a and the references therein).

Lactobacillus delbrueckii phage LL-H recognizes and adsorbs to LTA associated glucose (Räisänen et al., 2004, 2007). Bacteriophages ϕ25 and ϕ29 use the major *B. subtilis* WTA - glucosylated polyglycerol phosphate as receptor (Young, 1967), but Jacobson and Landman, 1977 proposed that phage ϕ29 irreversible binding to *B. subtilis* is mediated by a bacterial CM component. Another *B. subtilis* phage ϕ3T adsorbs to a minor WTA, poly-(glucosyl-*N*-acetylgalactosamine 1-phosphate) (Estrela et al., 1991). In contrast to Gram-negative hosts, only a few membrane receptors for phages infecting Gram-positive bacteria were identified. Phage γ that infects *Bacillus anthracis* adsorb to the cell wall anchored protein GamR (Davison et al., 2005). *Lactococcus lactis* phages of the c2 group and *B. subtilis* phage SPP1 interact reversibly with host cell wall carbohydrate polymers (Monteville et al., 1994) and glucosylated poly (glycerolphosphate) WTAs (Baptista et al., 2008) respectively. This reversible interaction allows for irreversible attachment of phages to the bacterial membrane proteins Pip (Geller et al., 1993) or YueB (São-José et al., 2004), respectively. Pip and YueB belong to the family of YueB-related membrane proteins.

YueB-related membrane proteins

YueB is an integral membrane protein of *B. subtilis*. It contain five transmembrane segments at its carboxyl terminus and a large ectodomain forming a 36.5 nm long fiber that spans the *B. subtilis* cell wall (Fig. I.8; São-José et al., 2004, 2006).

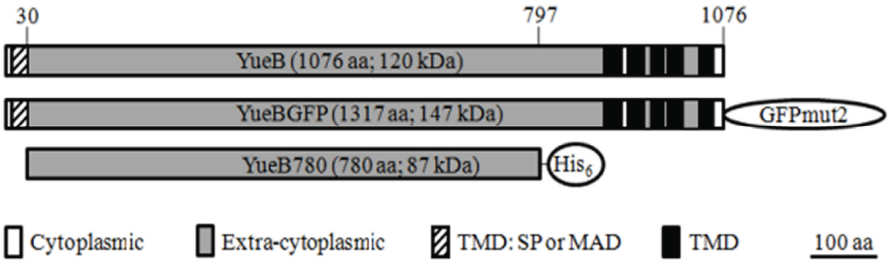

Fig. I.8. Scheme of YueB, YueB-GFP, and YueB780 showing their putative signal peptide (SP), membrane-anchoring domain (MAD) and transmembrane (TMD) segments, extracellular (ectodomain), and cytoplasmic regions. Adapted from Jakutyte et al., 2011.

YueB780 is a dimeric elongated fiber active to trigger SPP1 DNA ejection *in vitro* whose sequence covers most of the ectodomain region of YueB (Fig. I.8; São-José et al., 2006). YueB is an orthologue of Pip (phage infection protein), a membrane protein shown to be required for the irreversible binding of phage c2 to *L. lactis* (Table I.3).

YueB might be part of a putative Type VII secretion system (T7SS) machinery whose components are co-encoded by the *yuk* operon (São-José et al., 2004). The presence of YueB-related proteins is one of the features that characterizes the T7SS of Firmicutes (type VIIb subfamily (Abdallah et al., 2007)).

I.5.1.2. Phage receptor binding proteins

As mentioned before, reversible and irreversible adsorption can target the same receptor or involve different surface components. The two strategies correlate with distinct phage adsorption machineries whose complexity can vary from a single receptor binding protein (RBP) to complex baseplates with several RBPs as found in phages with long tails.

The vast majority of known bacterial viruses (96%; Ackermann, 2009) use a tail device for specific recognition of the host, binding to its surface and delivery of the genome from their icosahedral capsid to the bacterial cytoplasm (order *Caudovirales*). The tail adsorption apparatus can be composed of the distal tail protein (Dit), combined with a tail spike or more complex structures featuring tail fibers, and/or elaborated baseplates. Curiously, some tailed phages encode two alternate tail fiber genes and can switch them to extend their host range (Kamp et al., 1978; Scholl et al., 2001). When phages feature distal fibers, these are frequently used to sense the bacterial cell surface and to interact in a reversible way with host receptors (phages T5, T4, T7). Besides recognition, an activity frequently associated

to tail spikes is the ability to attack the host cell receptor or other surface structures facilitating penetration of the phage through the cell wall (Steinbacher et al., 1996).

Phages belonging to the *Podoviridae* family (P22, ϕ29, ε15; section I.3) bind frequently to host cells through stubby homotrimeric tail spikes that are attached to their short tail. In phage ϕ29, the neck appendages (gp12) of the virion are responsible for the reversible interaction with the *B. subtilis* cell wall (Guo et al., 2003; Villanueva and Salas, 1981). Another tail component, gp13, is proposed to function as a cell-wall degrading enzyme (Xiang et al., 2008).

Adsorption of the *Myoviridae* family phages T4, P2 or Mu to their bacterial hosts is normally mediated by long and short tail fibers or tail-spike proteins attached to the complex baseplate found at the tip of the contractile tail. Phage T4 host recognition occurs through a reversible adsorption of at least three long tail fibers to the LPS or OmpC found at the bacterial surface. This interaction leads to transmission of a signal to the baseplate, causing the extension of the homotrimeric short fibers (protein gp12) and irreversible interaction with LPS (Kanamaru et al., 2002). Recently, Bartual et al., (2010) presented the crystal structure of the receptor-binding tip of the bacteriophage T4 long tail fiber. This protein is highly homologous to the tip of bacteriophage λ side tail fibers as revealed by sequence similarity analysis.

Siphoviridae (e.g. phages p2, TP901-1, SPP1, λ, T5) use baseplates, straight tail fibers or tail spikes for host receptor recognition. Phage λ uses the tip of its straight tail fiber, formed by protein gpJ, to bind to LamB (Berkane et al., 2006; Wang et al., 2000) while phage T5 protein pb5, located in the tip of the tail conical region, mediates irreversible binding to FhuA (Heller and Schwarz, 1985). All known *L. lactis* siphophages possess a baseplate at the tip of their tail involved in host recognition and attachment (Sciara et al., 2010 and references therein). Recently Sciara et al., 2010 reported the structure of the lactococcal phage p2 baseplate and proposed a mechanism for baseplate activation during attachment to the host cell. The

baseplate is composed of three protein species, including six trimers of the RBP. In the presence of Ca^{2+}, the RBPs rotate, presenting their binding sites to the host. Subsequently a channel opens at the bottom of the baseplate for DNA passage. Phage SPP1 uses an adsorption device located at the tail fiber (Plisson et al., 2007). Interestingly, several tail components of the SPP1 show significant sequence and fold similarity to equivalent proteins from lactococcal phages which possess a baseplate at the tail tip (Veesler et al., 2010a,b). Recently, Goulet et al., (2011) determined the cryo-EM structure of a complex formed by two SPP1 proteins, distal tail cap gp19.1 (Dit) and N-terminus of the gp21 (Tal). Remarkably, in Dit-Tal complexes a Dit hexamer associates with Tal trimers that can be display a "closed" conformation or an "open" conformation delineating a central channel. The two conformational states dock nicely into the EM map of the SPP1 cap domain, respectively before and after DNA release (Goulet et al., 2007; Plisson et al., 2007). Moreover, the open/closed conformations of Dit-Tal are consistent with the structures of the corresponding proteins in the siphophage p2 baseplate, where the Tal protein (ORF16) attached to the ring of Dit (ORF15), was also found to adopt these two conformations (Sciara et al., 2010). Therefore, Goulet and co-workers proposed that this is a prevalent mechanism for the tail opening in siphophages infecting Gram-positive bacteria.

A striking structural and functional similarity was shown between the Type VI secretion system (T6SS) and bacteriophage tail components (Bönemann et al., 2010; Leiman et al., 2009; Pell et al., 2009; Veesler et al., 2010a). Secretion is fundamental to bacterial virulence. Bacterial pathogens use at least 7 distinct extracellular protein secretion systems to export proteins through their cell envelope and in some cases into the host eukaryotic cell or another bacterium (Hood et al., 2010; Schwarz et al., 2010). Several components of the of the T6SS are structurally very similar to those that make up the long tail of bacteriophages. Using crystallographic, biochemical, and bioinformatic analyses, there 3 T6SS components, were shown to be homologous to bacteriophage T4 tail proteins. These include the tail tube protein, the membrane-

penetrating needle, and a protein associated with the needle and tube (Leiman et al., 2009). A remarkable structural similarity was also shown between bacteriophage λ major tail protein and a component of the bacterial T6SS (Pell et al., 2009). The structural similarity observed between phage tail and the T6SS proteins, strongly supports the hypothesis that phage tails and T6SS are evolutionarily related. These components of a membrane-penetrating nanomachines most possibly evolved first in the context of a phage tail and bacteria evolving to use parts of phages for their own advantage. The question, how these structurally related machines perform similar but clearly distinct tasks: phage DNA ejection into the cell cytoplasm and delivery of bacterial virulence factors, remain to understand.

Filamentous bacteriophages (fd, M13, f1, Ike, CTXΦ, IF1) use different domains (N1 and N2) of their pIII protein to bind to cellular receptors (Stengele et al., 1990). The initial binding of the pIII N2 domain to a pilus is followed by the irreversible interaction with the C-terminal domain of host protein TolA. The latter interaction is mediated through the domain N1 of pIII (Lorenz and Schmid, 2011; Lubkowski et al., 1998; Riechmann and Holliger, 1997).

Membrane containing bacteriophages belonging to the *Cystoviridae* (e.g. phage ϕ6), *Tectiviridae* (e.g. phage PRD1) and *Corticoviridae* (e.g. phage PM2) families (Table I.1) and icosahedral tailless ssDNA phage ϕX174 use spike proteins as receptor-binding proteins (Abrescia et al., 2008; Bamford et al., 1987; Kawaura et al., 2000; Mindich et al., 1982; Romantschuk and Bamford, 1985; Suzuki et al., 1999).

The ssRNA containing phages of *Leviviridae* family bind to the host cell receptor via a maturation protein (van Duin and Tsareva, 2006).

I.5.2. Cell wall passage

Bacteriophages have to cross the cell wall of their host bacterium for genome delivery to the host cytoplasm. The major classes of PG hydrolases contain unrelated enzymes as lysozymes, amidases, transglycosylases or endopeptidases. Several phages possess genes encoding PG hydrolysing enzymes with lytic domains which are conserved between bacteriophages and plasmid genomes (Koonin and Rudd, 1994; Lehnherr et al., 1998). Bacteriophages are known to have lytic cell wall hydrolysis proteins for phage entry and lytic enzymes for phage progeny escape (endolysins), but their function and roles in virus cycle are different. Contrary to endolysins which are synthesized at the late stage of the lytic cycle, virions often harbor PG hydrolases that locally degrade the PG in order to facilitate the entry of phage DNA during infection. The action of PG hydrolyzing enzymes must be well controlled and cause only transient openings in the PG sacculus to maintain the bacterial cell envelope integrity. In all cases phage entry enzymes are components of the phage particles (Moak and Molineux, 2004). These can be either associated with the tail structure or be an internal head protein, as phage T4 tail protein gp5 and T7 protein gp16, respectively, suggesting a role in cell wall penetration during cell wall passage (Kanamaru et al., 2002; Kao and McClain, 1980; Moak and Molineux, 2000; Nakagawa et al., 1985). Bacteriophage T5 Pb2 is a multifunctional protein that carries fusogenic and PG hydrolysing activities in addition to its tape measure role (Boulanger et al., 2008). Protein P17 of *Staphylococcus aureus* phage P68 was shown to have both receptor binding and PG hydrolysing activities (Takác and Bläsi, 2005). The tail tip protein gp13 of bacteriophage ϕ29 has also two PG hydrolyzing activities: the N-terminus domain is a lysozyme, while the C-terminus is an endopeptidase (Xiang et al., 2008). Interestingly, it was shown that residues in the active site and the structural pattern are conserved among bacterial lysostaphin homologs (autolysins) and bacteriophage ϕ29 gp13 C-terminal endopeptidase domain (Cohen et al., 2009).

Membrane-containing bacteriophages PRD1 and ϕ6 contain lytic activities associated with the virion structure (Caldentey and Bamford, 1992; Mindich and Lehman, 1979; Rydman and Bamford, 2000). The PRD1 internal membrane protein P7 and the ϕ6 nucleocapsid protein P5 facilitate the phage nucleic acid transfer across the cell wall during entry.

I.5.3. CM passage and DNA entry in the cytoplasm

The last barrier for virus entry to the cytoplasm is the CM. The diverse phage particles structural organization correlates with different strategies to cross this barrier.

I.5.3.1. Genome ejection through a specialized vertex

The majority of bacteriophages have an icosahedral capsid that protects their dsDNA genome. Most of the virions deliver their dsDNA to the host through a structure localized at a specialized vertex of the icosahedron characterized by presence of a portal gatekeeper. In case of tailed phages interaction of the phage tail RBPs with cell surface receptor generates a signal transmitted along the tail structure to trigger DNA ejection (Aksyuk et al., 2009; Boulanger et al., 2008; Plisson et al., 2007). dsDNA exits from the capsid through the tail tube to reach the cell cytoplasm.

Phages of Gram-negative bacteria

After binding to the host, bacteriophage T4 (*Myoviridae*) undergoes major structural rearrangements that cause the sheath around the tail tube to contract and drive the central tube through the OM (Aksyuk et al., 2009; Leiman et al., 2003; Moody, 1973). The detailed mechanism of how the linear 169 kbp long dsDNA genome crosses the CM of the host in 30 seconds remains to be elucidated, yet it is

clear that the process requires proton electrochemical gradient on the CM (Labedan and Goldberg, 1979).

Binding of bacteriophage T5 (*Siphoviridae*) to its receptor FhuA, results in conformational changes and membrane insertion of the tape-measure protein Pb2, an elongated protein that is released from the phage tail tube interior at the beginning of infection, preceeding the release of DNA from the virion (Boulanger et al., 2008). The genome transfer proceeds in two steps. First, 8% of the genome is transferred to the cytoplasm. Then there is a pause during which two early proteins (A1 and A2) are synthesized. Transfer of the rest of phage DNA is dependent on the presence of proteins A1 and A2 in the cytoplasm (Letellier et al., 1999).

The tape measure protein of the *Siphoviridae* phage λ, gpH*, may also have a role in forming the channel for DNA passage across the CM (Roessner and Ihler, 1984). Additionally, the CM protein ManY (component of the mannose PTS system) facilitates phage λ DNA penetration by interaction with gpH* (Esquinas-Rychen and Erni, 2001).

The tail of phage T7 (*Podoviridae*) is too short to span the cell envelope of its Gram-negative host cell. Thus one of the first steps of T7 infection is ejection of three viral internal core proteins (see Fig. I.3 for position of the T7 core inside the capsid) proposed to form a continuous channel structure from the tip of the phage tail to the cell cytoplasm (Chang et al., 2010; Molineux, 2001). First, about 850 bp of the genome are transferred into the host. Promoters located on the leading part of the DNA allow the *E. coli* RNA polymerase to initiate transcription and to pull about 7 kb of the genome into the cytoplasm. From these early transcripts the T7 RNA polymerase is then synthesized. Its transcription activity on T7 specific promoters pulls the remaining part of the genome into the cell (García and Molineux, 1995, 1996; Molineux, 2001). This multistep translocation of the T7 genome takes about 10 min at 30 °C (García and Molineux, 1995).

Recently, the structural changes accompanying infection of bacteria *Salmonella anatum* and *Prochlorococcus marinus*, by podoviruses ε15 and P-SSP7, respectively, were studied by single particle cryo-electron tomography (Chang et al., 2010; Liu et al., 2010). In the first stage of infection the tailspikes of ε15 attach to the surface of the host cell. Next, the tail hub attaches to a putative cell receptor and establishes a tunnel through which core proteins exit the virion. A tube spanning the periplasmic space is formed for viral DNA passage, presumably resulting from the rearrangement of the phage core or from cellular proteins. After DNA ejection, the tube and portal seals, and the empty bacteriophage remains at the cell surface. Liu et al., (2010) suggest that upon binding of phage P-SSP7 to the host cell, the tail fibers induce a cascade of structural alterations of the portal vertex complex that triggers DNA release.

The tailless dsDNA containing bacteriophage PRD1 (*Tectiviridae*) infects various Gram-negative cells that carry an IncP-type conjugative plasmid. PRD1 has an internal membrane between the genome and the capsid. It was suggested that this phage, like tailed phages, delivers its genome to the host through a specific vertex leaving the empty capsid outside the cell (Grahn et al., 2002). Receptor recognition and binding triggers structural rearrangements at one of the PRD1 capsid vertices. The phage spherical membrane then transforms into a tube-like structure which serves as a channel for genome traffic to the host cytoplasm (Bamford et al., 1995; Grahn et al., 2002).

Icosaedral ssDNA (e.g., ϕX174, *Microviridae*) and ssRNA (e.g., f2, MS2, Qβ, *Leviviridae*) phages were proposed to transfer their genome from the capsid to the bacterial cytoplasm through a genome delivery apparatus located at one of the vertices (Brown et al., 1971; Jazwinski et al., 1975; van Duin and Tsareva, 2006).

Phages of Gram-positive bacteria

The information regarding penetration of the phage genome in Gram-positive bacteria is very scarce comparatively to Gram-negative systems. In case of the tailed phages infecting the Gram-positive bacterium *B. subtilis*, DNA passage to the cell cytoplasm is relatively well studied only for the short-tailed dsDNA containing bacteriophage ϕ29 (*Podoviridae*). In a first step, ~60 % of the phage DNA is pushed into the cell, presumably by the pressure built inside the phage capsid. The remaining 40 % of the genome is pulled from inside the cell by an energy-requiring molecular machinery. Early viral proteins synthesized from the initial portion were proposed to play a central role during the second step of genome penetration (González-Huici et al., 2004).

The tailless dsDNA phage Bam35 (*Tectiviridae*) infects *B. thuringiensis* cells and contains an internal membrane in its capsid. Tube-like structures similar to the ones observed for phage PRD1 (see above), have been detected during Bam35 entry (Laurinmäki et al., 2005; Ravantti et al., 2003), suggesting that the viral membrane is involved in delivery of the phage genome into the host cell. Although the PRD1 and Bam35 virion architectures are very similar, the mechanisms of genome penetration to the cell cytoplasm differs (Gaidelyte et al., 2006). PRD1 entry does not cause CM depolarization, whereas Bam35 entry does (Daugelavicius et al., 1997; Gaidelyte et al., 2005). The Bam35 genome transport across the CM depends on presence of divalent cations in the growth medium, whereas phage adsorption and degradation of PG do not show this requirement (Gaidelyte et al., 2006).

I.5.3.2. Capsid dissociation at the cell envelope

This strategy of entry is employed by filamentous bacteriophages (e.g., f1, fd, M13, *Inoviridae*) infecting Gram-negative bacteria. The minor viral protein pIII localized at one end of filamentous ssDNA bacteriophages is associated with the host

CM during both virus assembly and entry (Bennett and Raconjac, 2006). The infection of filamentous bacteriophages depends on a primary receptor that captures the virus to the cell surface and a co-receptor that induces the uncoating event (Click and Webster, 1997; Riechmann and Holliger, 1997). As mentioned before, interaction of the pIII N2 domain with host cell pili as primary receptor, makes the pIII domain N1 available for the secondary binding site at the cell envelope (or co-receptor), the CM protein TolA (Riechmann and Holliger, 1997). This interaction triggers the virion uncoating leading to the insertion of the viral major capsid proteins into the bacterial CM, resulting in the phage genome entry into the bacterial cytoplasm (Bennett and Raconjac, 2006; Click and Webster, 1998).

The protein coat of enveloped dsDNA bacteriophage PM2 (*Corticoviridae*) (Table I.1) also dissociates at the host cell envelope. Proteins P1 and P2 composing the capsid of bacteriophage PM2 were found to be released into the medium upon genome internalization (Kivelä et al., 2004). It was proposed that the viral membrane fuses with the host OM and the genome is released into the periplasmic space (Kivelä et al., 2008). The PM2 genome thus enters to the host cytoplasm in a unique, Ca^{2+}-dependent manner (Cvirkaite-Krupovic et al., 2010b).

I.5.3.3. Fusion and endocytosis-like penetration

The internalization of an entire viral capsid rarely occurs in bacteria. The best studied case is the dsRNA bacteriophage ϕ6 (*Cystoviridae*) that has evolved a mechanism similar to endocytosis to cross the host CM. Entry of ϕ6 involves viral envelope fusion with the host cell OM (Bamford et al., 1987), cell wall degradation inside the periplasmic space by a viral enzyme (Caldentey and Bamford, 1992; Mindich and Lehman, 1979), and endocytic-like host CM penetration (Bamford et al., 1987; Romantschuk et al., 1988; Poranen et al., 1999). As endocytosis is not a

common way for periplasmic material uptake in bacterial cells, it is likely that the CM membrane curvature formation is induced by viral proteins.

Phages of the *Plasmaviridae* family infect mycoplasmas which are small, wall-less bacteria. Adsorption of pleomorphic membrane containing dsDNA bacteriophage L2 to the receptor leads to the fusion of phage membrane and host CM, leading to deliver viral genome into the host cytoplasm (Maniloff and Dybvig, 2006).

I.5.3.4. Forces driving tailed phages dsDNA entry in the cytoplasm

The bacterial cell cytoplasm is crowded by high concentrations of macromolecules. A turgor pressure (ΔP between the cell interior and exterior) of 1-5 atm was found for Gram-negative bacteria like *E. coli*. Gram-positive cells, such as *B. subtilis* have much higher turgor: ~ 19 atm (Poolman and Glaasker, 1998; Whatmore and Reed, 1990). Therefore, cell turgor poses a formidable barrier for phage DNA entry. Pressure built by DNA packing inside virions is largely insufficient for entire genome delivery into the bacterial cytoplasm (São-José et al., 2007).

Several models for phage DNA transport have been formulated. Hershey and Chase (1952) suggested that the phage coat acted like a hypodermic syringae. Other authors (Stent, 1963) believe that phage nucleic acid is packed into the phage coat under constraint and forces is way out when the tail tube is uncorked. Also, thermal rotation of T-even head, causing the centrifugal force on phage DNA, was considered (Ore and Pollard, 1956) to be a possible energy source for DNA injection. On the other hand, Zaribnicky (1969) suggested that the mechanism of T-even phages DNA injection into a bacterium was result of internal pressure caused by the thermal agitation of polypeptides and polyamines inside the phage head. It was proposed that the tight packed phage DNA under high pressure in the capsid is spontaneously ejected upon infection and then pulled by interactions with macromolecules in the cytoplasm to the host cell interior (Earnshaw and Casjens, 1980; Evilevitch et al.,

2003; González-Huici et al., 2004; Grayson et al., 2006; Molineux, 2001; São-José et al., 2007). Another model is based on the chemiosmotic theory of DNA transport in which the electrochemical gradient of protons generated across the host CM by the electron transfer chain would be the driving force for DNA transport (Grinius, 1980). However, later studies revealed that the membrane potential is rather required for opening of a voltage-gated "DNA channel" than for the transport of DNA (Boulanger and Letellier, 1988). Finally, it was recently proposed the hydrodynamic model of DNA ejection. According to this theory, the osmotic pressure difference between the cytoplasm and external fluids might provide a force for phage DNA ejection. This osmotic pressure gradient is counter-balanced by a hydrostatic pressure differential (turgor). During the phage induced channel opening there is the stream of water molecules moving along the osmotic gradient from the medium, through the phage virion into the cell cytoplasm, that drags the phage genome along with it (Grayson and Molineux, 2007; Molineux, 2006; Panja and Molineux, 2010).

I.5.3.5. Ion fluxes accompanying phage infection

The initial steps of phage infection are usually associated with depolarization of the host CM and/or the release of intracellular K^+ ions (Letellier et al., 1999; Poranen et al., 2002). The timing and pattern of ion leakage is different among phages, providing a fingerprint for infection by each virus species (Letellier et al., 1999). Depolarization of the CM and K^+ leakage can be the result of creation of a hydrophilic channel for DNA passage or of opening of existing ion-permeable channels in the CM triggered by phage infection. It is yet not known, if K^+ leakage and depolarization of the CM play a physiological role in infection or if they are side effects accompanying phage entry.

Infection of *E. coli* by tailed phages T4 (*Myoviridae*) and T5 (*Siphoviridae*) leads both to CM depolarization and to K^+ efflux (Boulanger and Letellier, 1992;

Grinius and Daugelavicius, 1988; Kalasauskaite et al., 1983; Labedan and Letellier, 1981; Letellier and Labedan, 1984). It was shown that bacteriophage T4 infection causes a fast efflux of internal K^+, but another coliphage T5 induces K^+ efflux in two steps. These results correlate with fast T4 DNA entry (30 s) and two distinct steps of T5 DNA entry in *E. coli*, respectively (reviewed in Letellier et al., 1999; 2004). However, T4-induced channels remain open after phage entry and T4 ghosts are able to induce similar changes of the cell envelope permeability (Boulanger and Letellier, 1988; Duckworth and Winkler, 1972; Grinius and Daugelavicius, 1988; Winkler and Duckworth, 1971).

Bacteriophage PRD1 (*Tectiviridae*) uses an internal membrane device for DNA delivery to the host cytoplasm and leads to an efflux of K^+ but no membrane depolarization is observed during phage entry (Daugelavicius et al., 1997; Grahn et al., 2002). In case of the PRD1 closely related phage Bam35 that infects the Gram-positive bacterium *B. thuringiensis*, the CM depolarization and the leakage of intracellular K^+ occur simultaneously starting at 2 min p. i. (Gaidelyte et al., 2006).

Genome passage of bacteriophage PM2 (*Corticoviridae*) through the host envelope of *Pseudoalteromonas* causes depolarization of the CM with accompanying leakage of the intracellular K^+ into the medium (Kivelä et al., 2004).

The *B. subtilis* phage SPP1 (*Siphoviridae*) cause a very fast depolarization of the infected cell CM, with a maximal level of CM depolarization reached at ~1 min post-infection (p.i.) (Vinga et al., 2006b).

I.6. Bacteriophage SPP1

Bacteriophage SPP1 that belongs to the *Siphoviridae* family (Table I.1) infects the Gram-positive rod-shape soil bacterium *B. subtilis*. SPP1 was first described by Riva et al., (1968). The virion contains an icosahedral capsid and a flexible non-

contractile tail with a tail fiber at the tip (Fig. I.9). The linear ~45.9 ds DNA molecule tightly packed inside the capsid is terminally redundant including the 44007 bp SPP1 genome and a sequence repetition at its extremities. This topology is generated by a mechanism of genome headful packaging (Tavares et al., 1996). The SPP1 capsid icosahedral lattice is composed of the major capsid protein gp13 and of the decoration protein gp12. The capsid contains also the non-essential minor capsid protein gp7 that supports correct routing of the phage genome to the host cell cytoplasm (Vinga et al., 2006b). The tail is attached to the capsid through the head-to-tail connector, which contains a portal gatekeeper protein structure to control DNA release from the capsid (Fig. I.9; Orlova et al., 2003; Plisson et al., 2007). Recently, the pseudoatomic structure of a complete portal system was reported (Lhuillier et al., 2009). The SPP1 gatekeeper is composed of dodecamers of the portal protein gp6, the adaptor gp15, and the stopper gp16 (Lurz et al., 2001; Orlova et al., 2003). Binding of gp15 and gp16 to the portal protein after encapsidation is essential to avoid leakage of packaged DNA. Gp16 closes the channel through which DNA exits the capsid upon DNA ejection (Orlova et al., 2003; Lhuillier et al., 2009). The connector is attached to the tail end forming a head-to-tail interface characterized by presence of gp17 protein (Plisson et al., 2007; Chagot et al., 2011). The SPP1 tail tube is composed of gp17.1 and gp17.1* proteins with an internal tape measure protein gp18 inside the lumen of the tube (Plisson et al., 2007). The recently published structure of the distal SPP1 tail protein Dit (gp19.1), suggested that Dit is a docking platform for the tail adsorption apparatus and forming the cap interface between the tail-tube and the tail-fiber (Veesler et al., 2010a). Despite that the structure of the complete tail fiber remains unsolved, the tail fiber protein gp21 was assigned a function in receptor recognition at the host surface (Baptista, 2009).

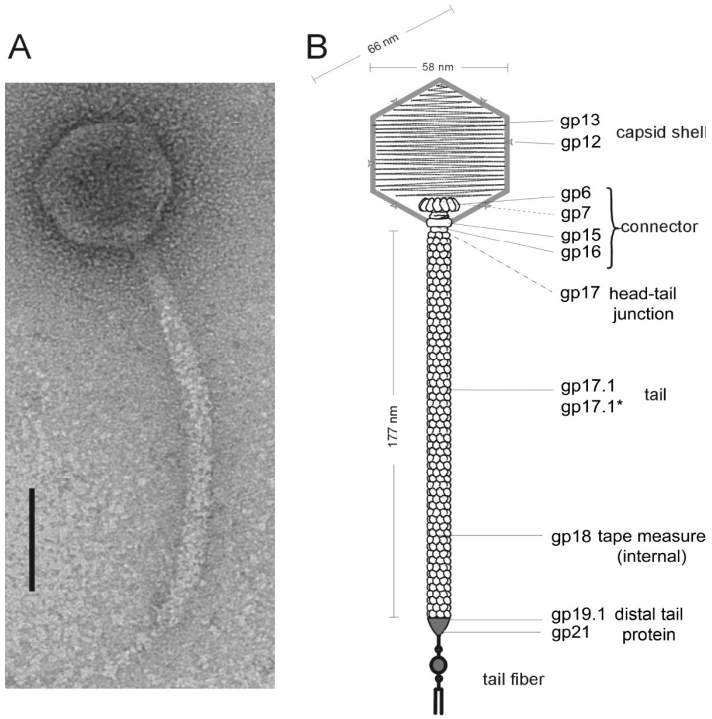

Fig. I.9. Structure of bacteriophage SPP1. (A) Electron microscopy. The bar represents 50 nm. (B) a scheme of the mature virion showing dimensions and structural proteins. Adapted from Alonso et al., 2006.

Bacteriophage SPP1 infection is initiated by the SPP1 reversible binding to glucosylated poly(glycerolphosphate) cell WTA (Baptista et al., 2008). This reversible interaction allows for fast attachment of phages to the bacterium facilitating two-dimensional scanning of its surface for the SPP1 receptor YueB (Baptista et al., 2008). The strong interaction of SPP1 with YueB commits the phage to infection (São-José et al., 2004, 2006). YueB is an integral membrane protein with five transmembrane segments at its carboxyl terminus and a large ectodomain forming a 36.5 nm-long fiber that spans the thick *B. subtilis* cell wall to expose the SPP1 receptor domain at the bacterial surface (São-José et al., 2004, 2006). Binding of the SPP1 adsorption apparatus to YueB triggers a sequence of conformational changes in the phage tail structure (Plisson et al., 2007) that culminates in genome release from viral particles through the tail tube (São-José et al., 2006, 2007). SPP1 DNA is found

inside *B. subtilis* at 3 min p.i. at 37 °C in rich medium (Burger, 1980 and references therein). Viral DNA transcription and replication initiates rapidly afterwards. Transcription is carried out by the *B. subtilis* RNA polymerase (Esche, 1975; Esche et al., 1975; Milanesi and Cassani, 1972). Replication of phage DNA mediated by the host DNA polymerase III by rolling circle replication and takes place in close association with the membrane (Alonso et al., 2006; Burger, 1980). Concatemers of the phage genome are detected 8 min after infection (Burger, 1980; Missich et al., 1997 and references therein). Expression of late genes coding for morphogenetic proteins initiates at 10-12 min p.i., followed by SPP1 DNA packaging and formation of ~200 infective viral particles per cell that are released by cell lysis occurring between 30 min and 60 min p.i. under optimal infection conditions (Alonso et al., 2006).

THESIS GOALS

The mechanism of genome transfer from the virion to the host cytoplasm is critical to understand and control the beginning of viral infection. Given the accumulated knowledge in the molecular biology of SPP1 and its host, we have selected bacteriophage SPP1 and *B. subtilis* system as a model to study the initial steps of phage infection of Gram-positive bacteria. The goal of this study was to define requirements for entry of the tailed bacteriophage SPP1 into this host Gram-positive rod-shaped bacterium *B. subtilis* and to study the initial steps of infection in space and time. The specific aims of this PhD thesis work were :

- ✓ to define sequential steps in SPP1 DNA entry in the cell;
- ✓ to define changes in cytoplasmic membrane (CM) permeability during the initial steps of bacteriophage SPP1 infection;
- ✓ to determine the localization of the SPP1 receptor protein YueB on the surface of *B. subtilis* cells;
- ✓ to determine the spatial-temporal program of bacteriophage SPP1 attachment, DNA penetration and replication inside the host cytoplasm.

II. MATERIALS AND METHODS

II.1. Bacterial strains and bacteriophages

All biological material used in this work are listed in Table II.1.

TABLE II.1. *B.subtilis* strains and bacteriophages used in this work

Strains, phages	Genotype and/or relevant features[a]	Source or reference
***B. subtilis* strains**		
YB886	*B. subtilis* 168 derivative freed of prophages PBSX and SPβ; wild-type strain; SPP1 indicator strain	(Yasbin et al., 1980)
YB886.Δ6	YB886 derivative with deleted *yueB* (Δ6 deletion); contains an *eryR* marker inserted in the *amyE* locus; Ery^r (0.5 µg ml^{-1})	(Jakutyte et al., 2011)
YB886.PspacYB	YB886 derivative expressing *yueB* under the control of the promoter P_{spac} (inducible with IPTG); Ery^r (0.5 µg ml^{-1})	(Jakutyte et al., 2011)
YB886.Δ6.PxylYB	YB886. Δ6 derivative with P_{xylA}-driven expression of *yueB* (inducible with xylose); Neo^r (7.5 µg ml^{-1})	(Jakutyte et al., 2011)
YB886.YBGFP	YB886 derivative driving native expression of *yueB-gfp*, *yueB*ΩpCB-GFP; Spc^r (100 µg ml^{-1})	(Jakutyte et al., 2011)
YB886.Δ6.PxylYBGFP	YB886.Δ6 derivative with P_{xylA}-driven expression of *yueB-gfp* (inducible with xylose); Neo^r (7.5 µg ml^{-1}) Spc^r (100 µg ml^{-1})	(Jakutyte et al., 2011)
MMB357	Expression of *lacI-cfp*; *thrC*::(P_{pen}-*lacIΔ11-cfp(W7)mls* Ery^r (0.5 µg ml^{-1}) Lin^r (12.5 µg ml^{-1})	A.D. Grossman
GSY10000	YB886 derivative; expression of *lacI-cfp*; *thrC*::(P_{pen}-*lacIΔ11-cfp(W7)mls* Ery^r (0.5 µg ml^{-1}) Lin^r (12.5 µg ml^{-1})	(Jakutyte et al., 2011)
12A	Asporogenic strain; *trpC2 spoOA12*	(Hoch and Spizizen, 1969)
***B. subtilis* phages**		
SPP1	Lytic siphophage	(Riva et al., 1968)
SPP1*delX110lacO*$_{64}$	SPP1 derivative carrying deletion *delX110* (Tavares et al., 1992) and an array of *lacO* operators	(Jakutyte et al., 2011)
SP01	Lytic myophage	(Okubo et al., 1964)
ϕ29	Lytic podophage	(Anderson et al., 1966)

[a]Ery^r, erythromycin resistance; Spc^r, spectinomycin resistance; Neo^r, neomycin resistance; Lin^r, lincomycin resistance.

II.2. Microbiology methods

II.2.1. General methods

B. subtilis strains (Table II.1) were grown in Luria-Bertani (LB) medium with appropriate antibiotics/supplements.

Development of competence and transformation were carried out according to the method of Boylan et al., (1972). Briefly, 10 ml of GM1 (100 ml of Spizizen's minimal medium (SP1) (1.4% K_2HPO_4, 0.6% KH_2PO_4, 0.1% Tri-sodium citrate × $2H_2O$, 0.2% $(NH_4)_2SO_4$, 0.02% $MgSO_4$ × $7H_2O$, 0.5% glucose) (Spizizen, 1958) supplemented with 0.02% acid-hydrolyzed casein, 0.1% yeast extract, and 50 μg ml^{-1} of methionine and tryptophan) medium was inoculated 1:50 from an overnight culture in extent of the desired *B. subtilis* strain and incubated with shaking at 37 °C. The turbidity of the culture was followed at hourly intervals for the first 3 h, and at 30 min intervals thereafter. Turbidity was plotted as a function of logarithm until growth departed from a linear relationship (t_0). At 90 min after t_0 (at this stage cells can also be supplemented with 20% glycerol and freezed at -80 °C) the cells were diluted 1:10 into GM2 medium (GM1 supplemented with 0.5 mM $CaCl_2$ and 2.5 mM $MgSO_4$) and incubated for 60 min at 37 °C with strong aeration. Culture was supplemented with 20 mM $MgCl_2$ and incubated with 1 μg ml^{-1} DNA for an additional 30 min at 37 °C with aeration. Cells were pelleted, resuspended in LB medium and spread on plates with appropriate antibiotics.

Phages SPP1 and SP01 were multiplied in *B. subtilis* YB886 (Yasbin et al., 1980) and phage ϕ29 in *B. subtilis* 12A (Hoch and Spizizen, 1969) grown in LB medium and supplemented with 10 mM $CaCl_2$ (for SPP1, SP01 and ϕ29) and 10 mM $MgCl_2$ (for ϕ29) just before infection (Santos et al., 1984; Chen and Guo, 1997). Isolated phages plaques (10^5-10^6 pfu) were used to generate confluent plate lysates (10^8-$5x10^8$) and then phages were amplified sequentially in small and large scale

culture infections. Cell debris were pelleted at 8,000 *g* for 15 min at 4 °C. In large scale preparations the lysates were centrifuged overnight at 8,000 *g* to sediment phage particles. Phages were then purified by isopycnic centrifugation in a discontinuous gradient with layers of 1.7, 1.5 and 1.45 g cm^{-3} of CsCl prepared in TBT buffer (100 mM Tris-HCl, 100 mM NaCl, 10 mM $MgCl_2$, pH 7.5, (Biswal et al., 1967)). Gradients were run in a SW41Ti rotor (Beckman Coulter) at 32,000 rpm for 6 h at 20 °C and the phage blue band was collected with a syringe and a needle by lateral perforation of the tube (Sambrook et al., 1989). Phages were dialysed against TBT and stocked in this buffer. Titrations were carried out using *B. subtilis* YB886 as indicator strain unless stated otherwise.

II.2.2. Measurement of SPP1 adsorption to *B. subtilis* cells

The measurements of reversible and irreversible adsorption of phage SPP1 to *B. subtilis* were adapted after the protocols São-José et al., (2004) and Baptista et al., (2008) with the following modifications. *B. subtilis* cells were collected from exponentially growing cultures (A_{600} of 0.8; ~10^8 colony forming units per ml (cfu/ml)). Cells were supplemented with the concentrations of $CaCl_2$ or/and EGTA indicated in the text (section III.2.) and 50 µg ml^{-1} of chloramphenicol. Chloramphenicol ensured the arrest of cell growth and phage multiplication throughout the experiments.

For measuring SPP1 **reversible adsorption (R_{ads})** to strain YB886Δ6 (unable to adsorb irreversibly) cells were equilibrated for 5 min at 0 °C. Phage SPP1 was added to the samples in order to obtain ~10^7 pfu/ml. Adsorption was measured at defined times of cell/phage contact by rapidly sedimenting cells from 100 µl mixture samples (15,000 × *g*; 0.5 to 1 minute centrifugation, room temperature) and titrating the free phages present in the supernatant (pfu/ml). At 50 min after phage addition the culture was transferred to 37 °C. Reversible adorption was calculated using the

formula $R_{ads} = ln(P_0/P)/\Delta t$, where P_0 is the phage input and P the fraction of free phages after a Δt period. The adsorption rate constant (k_1) is the ratio between R_{ads} and the bacterial cell mass expressed as A_{600} (equal to 0.8 in k_1 determinations).

For measuring SPP1 **irreversible adsorption** cells were equilibrated for 5 min at 37 °C. Phage SPP1 was added to the samples in order to obtain ~10^7 pfu/ml and at defined time points 10 µl aliquots were diluted 100-fold in TBT buffer supplemented with 10% chloroform. After vigorous vortexing during 5 seconds the mixtures were allowed to equilibrate for 5 min at room temperature, centrifuged (15,000 x *g*; 5 min) and the supernatants recovered for the enumeration of free phages (unadsorbed phages plus virions that were reversibly bound). The irreversible adsorption constant k_{ads} was calculated as the ratio between the irreversible adsorption rate and the bacterial cell mass expressed as A_{600} ($k_{ads} = \ln(P_0/P)/\Delta t A_{600}$, where P_0 is the phage input and P the fraction of free phages after a Δt period).

Control mixtures without added cells were used to confirm the phage input in each experiment.

All adsorption measurements were carried out by Dr Catarina Baptista and Dr Carlos São-José (Instituto de Medicina Molecular and Faculdade de Farmácia da Universidade de Lisboa, Portugal).

II.3. Molecular biology and genetics methods

II.3.1. General recombinant DNA techniques

PCR amplification of DNA fragments was carried out in a Biometra thermocycler using *Taq* DNA polymerase (Invitrogen) or *Pfu* polymerase (Stratagene) as recommended by the suppliers. All the oligonucleotides used in this work were purchased from Eurofins MWG GmbH or Invitrogen. PCR products were purified from the PCR mixtures using the QIAquick PCR Purification Kit 50 (QIAGEN).

DNA sequencing services were purchased from GATC Biotech AG, Germany. Restriction endonuclease digestions (New England Biolabs, MBI Fermentas, TaKaRa Biomedicals) and DNA ligations (T4 DNA Ligase, New England Biolabs) were performed according to the supplier's instructions.

II.3.2. DNA separation by gel electrophoresis

DNA molecules were separated by conventional agarose gel electrophoresis (Sambrook and Russel, 2001) in TAE buffer (Ogden and Adams, 1987) as gel/running buffer. Agarose gels 0.8 % (w/v) were stained for 30 min with ethidium bromide. The DNA molecular weight standard used was the 1Kb*plus* DNA Ladder (Invitrogen). DNA bands were visualized under U.V. lightening and images captured by a digital camera.

II.3.3. Bacterial strains construction

II.3.3.1. Construction of YB886 isogenic strains carrying the *yueB* Δ6 deletion and *yueB* conditional mutants

YB886 strains expressing different *yueB* forms were obtained by transformation of wild type YB886 with genomic DNA constructs of *B. subtilis* L16601 derivatives (Baptista, 2009; São-José et al., 2004). The *yueB* Δ6 deletion was introduced in YB886 using CSJ4 DNA as donor (São-José et al., 2004) and selecting for erythromycin and SPP1 resistance (ery^R at the *amyE* locus). The resulting strain was named YB886.Δ6 (Fig. II.1). This strain served as recipient for transformation with CSJ6 DNA (São-José et al., 2004), yielding strain YB886.Δ6.PxylYB that allows ectopic expression of *yueB* under the control of the P_{xylA} promoter (Fig. II.1). Strain

YB886.PspacYB was obtained by transformation of YB886 with DNA of CSJ3 (São-José et al., 2004), which expresses *yueB* under the control of the P_{spac} promoter.

Strain construction was carried out by Dr Catarina Baptista and Dr Carlos São-José (Instituto de Medicina Molecular and Faculdade de Farmácia da Universidade de Lisboa, Portugal).

II.3.3.2. Expression of *yueB-gfp* fusions

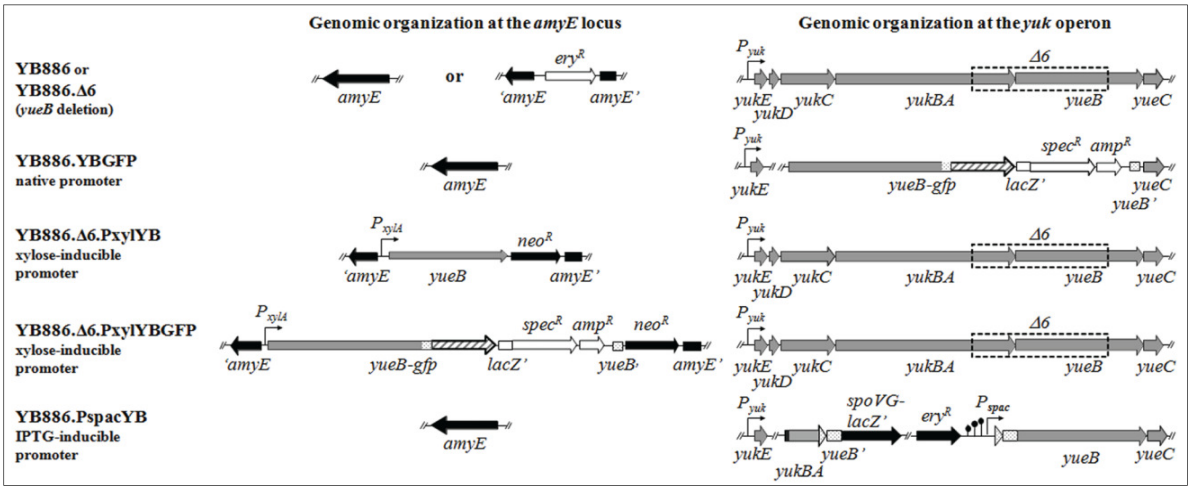

Fig. II.1. Relevant genomic organization of strains used in the present study, with different levels of *yueB* or *yueB-gfp* expression. The *yueB-gfp* fusion was cloned under the control of the native *yukE* promoter (strain YB886.YBGFP) or of the inducible P_{xylA} promoter at the ectopic *amyE* locus (strain YB886.Δ6.PxylYBGFP). Adapted from Jakutyte et al., 2011.

For expression of *yueB-gfp* fusions the *gfp mut2* gene was PCR amplified from vector pEA18 (Quisel et al., 1999) (primer pair gfp 30D and gfp 749R; AGTAAAGGAGAAGAACTTTTCACTGGAG and GATCCTCGAGGAATTCTTATTTGTATAGTTCATCCATGC; the *Xho*I and *Eco*RI sites are underlined) and fused, by overlap extension PCR, to another PCR product that carried the 3' end of *yueB* except for the stop codon (using the primer pair YB GFP-1 and YB GFP-2; CGTTATTCGGAATTCCTCGAGTCCTTGTCGGACTTA

and
CTCCAGTGAAAAGTTCTTCTCCTTTACTGTTGTTGTTGTTCGCTTCATACGT
TTCATCGCTTTCTGCTGT; sites *Xho*I and *Eco*RI are underlined). Note that in the overlapping PCR only the flanking primers (YB GFP-1 and gfp 749R) carry restriction sites. The fusion product was cleaved with *Eco*RI and cloned in vector pUS19 digested with the same enzyme (Benson and Haldenwang, 1993). The resulting plasmid, pCB-GFP, was checked for sequence correctness and used to transform *B. subtilis* L16601 and CSJ6, yielding strains CBM-GFP and CBM191, with native or P_{xylA}-dependent expression of *yueB-gfp*, respectively (Baptista, 2009). Strains YB886.YBGFP and YB886.Δ6.PxylYBGFP were obtained by transforming YB886 with CBM-GFP DNA and YB886.Δ6 with CBM191 DNA, respectively (Fig. II.1; Baptista, 2009). The k_{ads} of SPP1 to these strains was determined as described (section II.2.2; Baptista et al., 2008; São-José et al., 2004).

Strain construction was carried out by Dr Catarina Baptista and Dr Carlos São-José (Instituto de Medicina Molecular and Faculdade de Farmácia da Universidade de Lisboa, Portugal).

II.3.3.3. Expression of *lacI-cfp* fusions

B. subtilis MMB357 (Lemon and Grossman, 2000; Table II.1) producing the fusion protein LacI-CFP was kindly provided by Prof Alan D. Grossman and Dr Cathy Lee (MIT, Cambridge, USA). The cassette coding for the fusion protein was transferred to *B. subtilis* YB886 by SPP1 transduction (Yasbin and Young, 1974) to obtain the isogenic strain GSY10000 (Table II.1). In brief, a lysate of SPP1 multiplied in MMB357 was used to infect 0.3 ml of a late logarithmic phase culture (A_{600} of 1.5; ~$4x10^8$ cfu/ml) of the receptor strain YB886 supplemented with 10 mM $CaCl_2$. The culture infected with an input multiplicity (i.m.) of 1 was incubated for 10 min at 37 °C, mixed with 2 ml of prewarmed LB medium and further incubated with shaking

for an additional 10 min. Bacteria were sedimented and resuspended in prewarmed medium containing 20 µL of anti-SPP1 serum to inactivate free phages. Bacteria were further incubated for 30 min, sedimented and resuspended in 0.3 ml LB medium. Serial dilutions of the culture were plated in solid medium supplemented with 12.5 µg ml^{-1} lincomycin and 0.5 µg ml^{-1} erythromycin to select for transductants resistant to antibiotics of the macrolide, lincosamide, and streptogramin families (*mls*). The new strain was tested for tryptophan, methionine and threonine auxotrophy, for phenylalanine prototrophy, for absence of PBSX and SPβ bacteriophages (Dröge and Tavares, 2000), and for LacI-CFP fluorescence signal in SPP1*delX110lacO*$_{64}$ infections (see below).

II.3.4. Construction of bacteriophage SPP1*delX110lacO*$_{64}$

An array of *lacO* operators situated between *Nhe*I and *Xba*I restriction sites of plasmid pFX276 kindly provided by Dr François-Xavier Barre (CGM, Gif-sur-Yvette, France) (Lau et al., 2003), was amplified by PCR using primers 124-2 (*5´*-AAGAGCATGCATTACGTAATGGATCCACTTTATGCTTCCGGCTCG-*3´*; restriction sites *Sph*I, *Sna*BI, and *Bam*HI are underlined) and 125-2 (*5´*-AAGAGCATGCATCTCGAGGATGTGCTGCAAGGCG-*3´*; sites *Sph*I and *Xho*I are underlined) and digested with *Sph*I. The PCR fragment was cloned into the genome of bacteriophage SPP1*delX110* (Tavares et al., 1992) cleaved at its unique *Sph*I site 39721-39726 bp (EMBL accession code X97918 (Alonso et al., 1997); Fig.II.2). The ligation reaction was transformed into *B. subtilis* competent cells (section II.2.1; Boylan et al., 1972). Single phage plaques were titrated to re-obtain single plaques corresponding to pure clones. Insertion of the *lacO* operators cassette was confirmed by PCR and DNA sequencing. PCR was routinely used to check for stability of the insert during multiplication of the SPP1*delX110lacO*$_{64}$ phage.

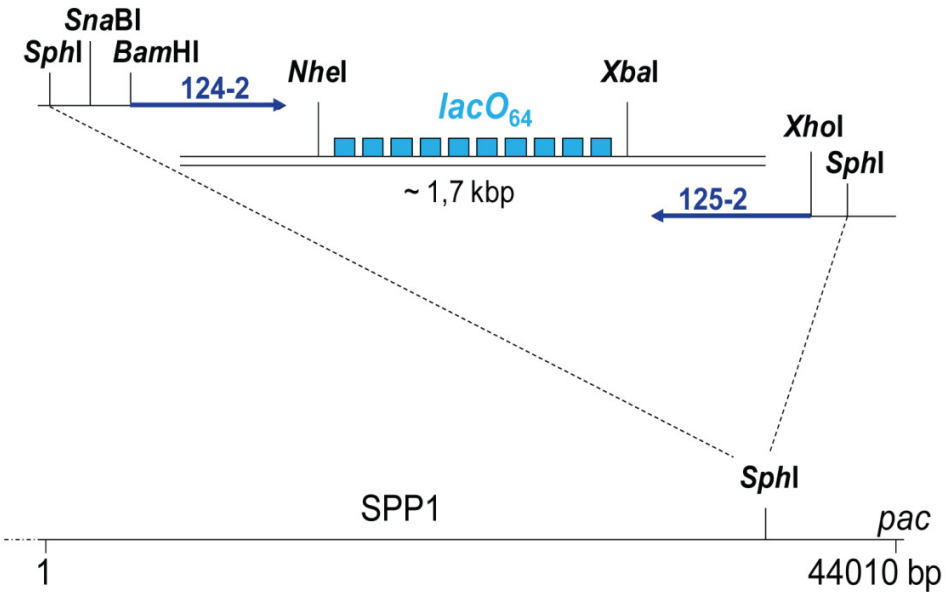

Fig. II.2. Scheme of bacteriophage SPP1*delX110lacO*$_{64}$ construction. Primers 124-2 and 125-2 are shown in blue arrows.

II.4. Biochemical methods

II.4.1. Protein analysis by SDS-PAGE and Western blotting

Adequate volumes of protein samples were analyzed by electrophoresis on SDS-PAGE gels (Laemmli, 1970). Proteins were visualized by Coomassie Blue staining (Sambrook and Russel, 2001). Protein blotting onto nitrocellulose membranes (Whatman) was routinely performed in a semi-dry transfer apparatus (Biometra). Western blot with polyclonal/monoclonal anti-sera were carried out as described (São-José et al., 2004; Towbin et al., 1979). Immuno-detection of the receptor YueB780 was performed with rabbit polyclonal sera diluted 1:30,000. Green Fluorescence Protein (GFP) fusion proteins were detected using an anti-GFP mouse monoclonal antibody (Clontech), following the suppliers' instructions. Phage biotinylation was detected using a Streptavidin-HRP conjugate dye (Invitrogen) diluted 1:1000. Antigen/antibody complexes were detected with the enhanced

chemiluminescence (ECL) detection reagent (Amersham Biosciences), according to the manufacturer's instructions.

II.4.2. Fractionation of *B. subtilis* extracts and Western blot of YueB engineered versions

The method was adapted from São-José et al. (São-José et al., 2004). Strains YB886, YB886.Δ6, YB886.YBGFP, YB886.Δ6.PxylYBGFP, and YB886.Δ6.PxylYB (Table II.1; Fig. II.1) were grown overnight at 30 ºC in LB medium. Cultures were then diluted 1:100 in 500 ml of LB medium (containing 0.5 % xylose in case of P_{xyl}-driven expression) and grown at 37 ºC to an A_{600} of 0.8. Bacteria were sedimented and resuspended in 10 ml of lysis buffer (50 mM Hepes, 300 mM NaCl, pH 8, supplemented with 1 mg ml^{-1} lysozyme and a protease inhibitor cocktail at the concentration described by the supplier (complete EDTA-free; Roche Applied Science)). The sample was homogenized by sonication (45 s / 60 % / 0.5 pulse with 1 min interval, 10 cycles). An aliquot of 500 µL was taken (*total extract* sample) and the remaining volume was centrifuged at 20,000 *g*, for 20 min at 4 ºC to clear the lysate removing large aggregates and non-lysed bacteria. After saving 500 µL of the supernatant (*soluble extract* fraction), 5 ml of supernatant were submitted to ultracentrifugation (120,000 *g*, 90 min, 4 ºC). A 700 µL aliquot of the supernatant was carefully removed (*cytoplasmic extract* fraction) and the rest of the supernatant discarded. The membrane-enriched pellet was resuspended in 250 µL lysis buffer supplemented with 0.1 % Triton and centrifuged at 10,000 *g*, for 20 min, at 4 ºC to eliminate insoluble material. The supernatant was used as the *membrane extract* fraction.

The total protein in different fractions was quantified by NanoDrop (ND-1000 Spectrophotometer, Nuciber) and the amounts of protein specified in the section III.3.2. were loaded into 8 % SDS-PAGE gels, stained with Coomassie Blue to

monitor the reproducibility of the fractionation procedure (not shown) or used for Western blot as described (São-José et al., 2004).

Fractionation of *B. subtilis* extracts and their analysis were carried out by Dr Catarina Baptista (Instituto de Medicina Molecular and Faculdade de Farmácia da Universidade de Lisboa, Portugal).

II.4.3. SPP1 phages disruption

Suspensions of CsCl-purified phage particles were disrupted by incubation with 50 mM EDTA, pH 8.0, at 55 °C for 30 min (Tavares et al., 1996). After addition of 100 mM $MgCl_2$, DNA was digested for 1 h at 37 °C with 0.4 U μL^{-1} of Benzonase (Merck).

II.4.4. Chemical modification of bacteriophages

A 10 mM stock of EZ-Link® Sulfo-NHS-LC-Biotin (sulfosuccinimidyl-6-[biotin-amido]hexanoate) (PIERCE) was made in Milli-Q water (Millipore) (Edgar et al., 2008). The solution was mixed with CsCl-purified SPP1*delX110lacO*$_{64}$ phage particles previously dialysed against 20 mM Hepes-Na, pH 7.0, 100 mM NaCl, 10 mM $MgCl_2$ to yield a final concentration of 24 μM biotinylation reagent. After 30 min at room temperature the reaction was stopped by the addition of glycine to a final concentration of 0.025%. The concentration of Sulfo-NHS-LC-Biotin was optimized to have minimal effect on phage viability as tested by direct plaque assay (> 80 % phage viability). Labeling of phage proteins was tested by Western blot using streptavidin-HRP conjugate dye. Determination of the irreversible adsorption constant (k_{ads}) of control and modified phages to *B. subtilis* YB886 was carried out as described in section II.2.2.

II.5. Fluorescence microscopy

II.5.1. Phage binding localization

Overnight cultures of *B. subtilis* YB886 and YB886.Δ6 strains were diluted 1:50 in fresh LB medium and grown at 37 °C to mid-exponential phase (A_{600} of 0.8). To stain the bacterial membrane, the non-toxic vital membrane dye FM1-43FX (Invitrogen, Eugene, USA) was added 2 min before infection to a final concentration of 5 μg ml^{-1}. To inhibit DNA synthesis, one of the culture samples was supplemented with 6 (*p*-Hydroxyphenylazo)-Uracil (HPUra) (kindly provided by NC Brown, GLSynthesis, Worcester, USA) to a final concentration of 200 μM and incubated for 2 min at 37 °C. A Qdot655 streptavidin conjugate (Invitrogen) was added to the biotynilated bacteriophage SPP1*delX110lacO*$_{64}$ (section II.4.4), immediately prior to use, to obtain a Qdot streptavidin conjugate concentration of 10 nM. The mix was incubated 5 min at room temperature and centrifuged for 5 min at 5,000 × *g*. The supernatant containing Qdot655-labeled bacteriophage SPP1*delX110lacO*$_{64}$ was used to infect *B. subtilis* cultures supplemented with 10 mM $CaCl_2$. The cultures infected with an i.m. of 6 infective phages *per* bacterium (pfu/cfu) (i.m.; Adams, 1959; Jakutyte et al., 2011) were incubated for 2 min at 37 °C, fixed with glutaraldehyde to a final concentration of 0.5 %, and further incubated at room temperature for 2 min. To obtain only stably adsorbed phages, fixed bacteria/phage mixtures were diluted 100-fold with phosphate buffered saline (PBS) (Sambrook et al., 1989), sedimented for 5 min at 5,000 *g* and resuspended in 10 μL of PBS. An aliquot of bacteria (2 μL) was immediately mounted on a thin film of 1.2 % agarose (SeaKem GTG Agarose, Cambrex Bio Science Rockland) in water, on microscope slides (MARIENFELD, Lauda-Königshofen, Germany) and overlaid with a coverslip (MENZEL-GLÄSER, Thermo Fisher Scientific). Cells were immediately imaged by contrast and fluorescence microscopy. Preparation for microscopy was identical for all culture samples described below.

II.5.2. Internal YueB localization

Strains producing YueB-GFP fusions were diluted 1:50 from an overnight culture in fresh LB medium. Strain YB886.Δ6.PxylYBGFP was grown in presence of 0.5 % xylose, added immediately after dilution of the overnight culture, for induction. Cells were grown at 37 ºC to mid-exponential phase (A_{600} of 0.8). To stain the bacterial membranes the vital membrane dye FM4-64FX was used as described above.

II.5.3. External YueB localization

Overnight cultures of *B. subtilis* YB886.YBGFP and YB886.Δ6.PxylYBGFP strains were diluted 1:50 in fresh LB medium and grown at 37 ^{o}C. Bacteria (500 µL) were collected during exponential growth (A_{600} of 0.8) by centrifugation, resuspended in 500 µL of prewarmed LB medium containing 2 % bovine serum albumin (BSA) and then incubated for 10 min at 30 ^{o}C with shaking. Anti-YueB780 purified polyclonal IgGs (São-José et al., 2006) (12 µg ml^{-1}) were added and incubated at 30 ^{o}C for 10 min. Bacteria were centrifuged, washed once with 800 µL of LB, and resuspended in 400 µL of a 1:2000 dilution of anti-rabbit IgG Alexa Fluor 546 fluorescent dye conjugate antibody (Molecular Probes) as a secondary antibody in BSA-LB. After incubation at 30 ^{o}C for 5 min, cells were washed with 800 µL of LB, resuspended in 500 µL of LB and immediately imaged as described above. Alternatively, samples of exponentially growing bacteria (500 µl) were fixed for 15 min at room temperature with 4% (w/v) paraformaldehyde and 0.02% glutaraldehyde in PBS. Fixed cells were washed twice with 800 µl of PBS and resuspended in 400 µl of PBS containing 2% (w/v) BSA. After incubation at 4 °C for 20 min the cells were sedimented, resuspended in 400 µl of BSA-PBS containing anti-YueB polyclonal antibodies (12 µg ml^{-1}), and incubated at 4 °C for 1 h. Cells were washed twice with

800 µl of PBS followed by incubation with secondary antibody and imaging as described above for non-fixed cells.

II.5.4. Phage DNA detection

For SPP1 phage DNA localization, an overnight culture of *B. subtilis* GSY10000 strain producing LacI-CFP was diluted 1:50 in fresh LB medium and grown at 37 ^{o}C to A_{600} 0.8. The culture was supplemented with 10 mM $CaCl_2$, infected at an i.m. of 3 with SPP1*delX110lacO*$_{64}$ followed by incubation for 2 min at 37 ^{o}C and microscopy at room temperature.

II.5.5. Image acquisition

Image acquisition of contrast and fluorescence observations was performed using a Leica DMRA2 microscope coupled to a Sony CoolSnap HQ cooledCCD camera (Roper Scientific). The digital images were acquired and analyzed with METAMORPH™ version 6 software. Where indicated, images of fluorescent samples were deconvolved within METAMORPH™. Overlays of micrographs were assembled using METAMORPH™ before exporting the images to Adobe PHOTOSHOP™ version CS4. Linear adjustment of contrast was sometimes applied to entire images equally, for better visualization of weak signals or to obtain a better signal-to-noise ratio in images taken at early times of p.i.. No other electronic enhancement or manipulation was applied to our images.

II.6. Measurements of ion fluxes and determination of the membrane voltage

Measurements of ion fluxes were adapted for studying the infection of *B. subtilis* with SPP1 after the protocols of Daugelavicius et al. (1997) and Vinga et al. (2006b) with the following modifications. To describe the early changes in CM permeability of phage infected cells, the overnight cultures of *B. subtilis* strains were diluted 1:50 in fresh LB medium, pH 8.0 (pH adjusted with NaOH) supplemented with appropriate antibiotics (Jakutyte et al., 2011) and grown at 37 °C to mid-exponential phase (A_{600} of 0.8). Bacteria were collected by centrifugation, resuspended in LB, pH 8.0 to obtain a ~150-fold concentration of the original cell culture volume, and kept at room temperature until used (maximum four hours). $2.5x10^9$ cfu were added simultaneously to two - four 5 ml thermostated (37 °C) reaction vessels containing 5 ml of LB, pH 8.0, supplemented with 3 μM tetraphenylphosphonium (TPP^+) chloride and 5 mM $CaCl_2$, incubated for five minutes, and infected. Phages were added at the desired i.m. of total phage particles *per* cell. At the end of the experiment the CM was permeabilized by the addition of gramicidin D (GD) to a final concentration of 5 μg ml^{-1} in order to estimate both the amount of TPP^+ accumulated in ΔΨ-dependent manner and the amount of TPP^+ irreversibly bound to the cells. The composition of the medium was varied as described in results (section III.1). The concentrations of TPP^+ and K^+ in the medium were monitored using selective electrodes (Daugelavicius et al., 1997; Grinius et al., 1980). TPP^+ chloride and GD were purchased from Sigma.

II.7. Electron microscopy

Phages and phage-related structures were negatively stained with uranyl acetate for electron microscopy (EM) observation (Steven et al., 1988).

To quantify Qdot labeled SPP1 virions, the Qdot streptavidin conjugate stock solution (1 µM) (Invitrogen) was centrifuged at 5000 g for 3 minutes followed by dilution of the supernatant in water to 5, 10, 20 and 50 nM. A 1 µL aliquot of each dilution was incubated with 9 µL of biotinylated SPP1*delX110lacO*$_{64}$ for 5 min at room temperature. The reaction mixture was centrifuged at 5000 *g* for 3 min followed by negative staining of the supernatant with uranyl acetate and electron microscopy.

All electron microscopy work was carried out by Dr Rudi Lurz (Max-Planck-Institut für Molekulare Genetik, Berlin, Germany).

III. RESULTS

III.1. SPP1 - induced changes in the host cell CM

Delivery of viral DNA through the bacterial envelope is in most cases associated with the alterations in the transmembrane difference of electrical potential (membrane voltage, $\Delta\Psi$) and with the efflux of intracellular potassium ions (Letellier et al., 1999; Poranen et al., 2002). The cytoplasmic membrane (CM) of bacterial cells is not permeable to inorganic ions such, as K^+ and H^+, but permeable to lipophilic cations, such as TPP^+. After TPP^+ addition to the cell suspension, this indicator ion crosses the cell envelope and distributes between the incubation medium and the cytosol according to the $\Delta\Psi$. At equilibrium conditions the ratio of TPP^+ concentrations in the cytosol and in the medium correlates with the $\Delta\Psi$. Therefore, distribution of the lipophilic cation TPP^+ across the CM can be used to follow the changes in $\Delta\Psi$ of bacterial cells (Rottenberg, 1989).

The goal of this part of the study is to understand the trigger and significance of CM depolarization during SPP1 infection.

III.1.1. Optimization of the conditions for SPP1-induced CM depolarization

In order to define the role of medium composition and temperature on SPP1-induced depolarization, as well as to optimize conditions for infection experiments, these parameters were varied and TPP^+ measurements were carried out. The concentration of TPP^+ in the medium was registered during the first minutes of SPP1 infection with an i.m. of 5. The results are summarized in Table III.1.

Table III.1. Effects of medium composition and pH on TPP^+ accumulation by *B. subtilis* cells and bacteriophage SPP1-induced CM depolarization.

Medium	pH	$CaCl_2$, mM	TPP^+ uptake	SPP1-induced CM depolarization
100 mM Na - phosphate	8.0	5	low	-
100 mM Na - phosphate	8.0	-	low	very low
100 mM Tris-HCl	8.0	5	very high	-
100 mM Tris-HCl	8.0	-	very high	low
25 mM Tris-HCl + 10% LB	7.0	5	low	very low
25 mM Tris-HCl + 10% LB	7.0	-	low	very low
25 mM Tris-HCl + 10% LB	8.0	5	high	low
LB	7.0	5	low	high
LB	8.0	5	high	high
LB	8.0	-	high	very high

Cells were grown in LB medium to an A_{600} of 0.8, collected, and resuspended in the medium or buffer indicated at a density of $5x10^8$ cfu/ml. The cell suspension was incubated at 37 °C for 6 min in medium containing 3 µM TPP^+ and infected with SPP1 (i.m. 5). At the end of the experiment (5 minutes p.i.), GD was added to a final concentration of 5 µg ml^{-1} to estimate the amount of TPP^+ accumulated in ΔΨ-dependent manner.

Sodium phosphate buffer was not suitable for the measurements due to reduced TPP^+ uptake (Table III.1). The highest TPP^+ uptake in *B. subtilis* was observed in Tris-HCl at pH 8.0, but the depolarization observed upon SPP1 addition was low. Thus for the following studies we have used LB medium (pH 8.0). Ca^{2+} was added to 5 mM $CaCl_2$, following previous knowledge that Ca^{2+} ions play an important role in SPP1 infection (Santos et al., 1984). This concentration was used instead of 10 mM $CaCl_2$ usually used for SPP1 infection, as the latter concentration of Ca^{2+} led to lower initial TPP^+ accumulation by the cells and a reduced depolarization in response to SPP1 infection compared to experiments carried out in presence of 5 mM $CaCl_2$ (not shown). Cells were added to LB supplemented with 3 µM TPP^+ and 5 mM $CaCl_2$, incubated for six minutes, and infected. Phages were added at the desired i.m. of total phage particles *per* cell. At the end of the experiment, the CM was permeabilized by the addition of GD, an ionophore for monovalent cations (Nicholls and Ferguson, 2002), in order to estimate both the amount of intracellular TPP^+ and of TPP^+ irreversibly bound to the cells. The experimental conditions for measurements are schematized in Fig. III.1. It shall be noted, that the level of the initial TPP^+ uptake and consequently the amplitude of phage-induced CM depolarization can show some variations among experiments. Therefore comparison of measurements in different

conditions were carried out to a maximum extent in parallel and using the same initial culture.

At 37 °C SPP1-induced CM depolarization occurs immediately after addition of phages to bacterial suspension (Fig. III.1). At 25 °C – 37 °C temperatures the initiation of phage-induced CM depolarization was fast but the kinetics of TPP^+ leakage was slower. The maximal level of SPP1-induced CM depolarization was reached at ~1 min p. i. at 37 °C, ~2 min p.i. at 30 °C, while at 25 °C the leakage of TPP^+ ions continued for at least 3 min. At 20 °C and 15 °C TPP^+ uptake into cells was low, preventing reliable studies of SPP1 induced CM changes.

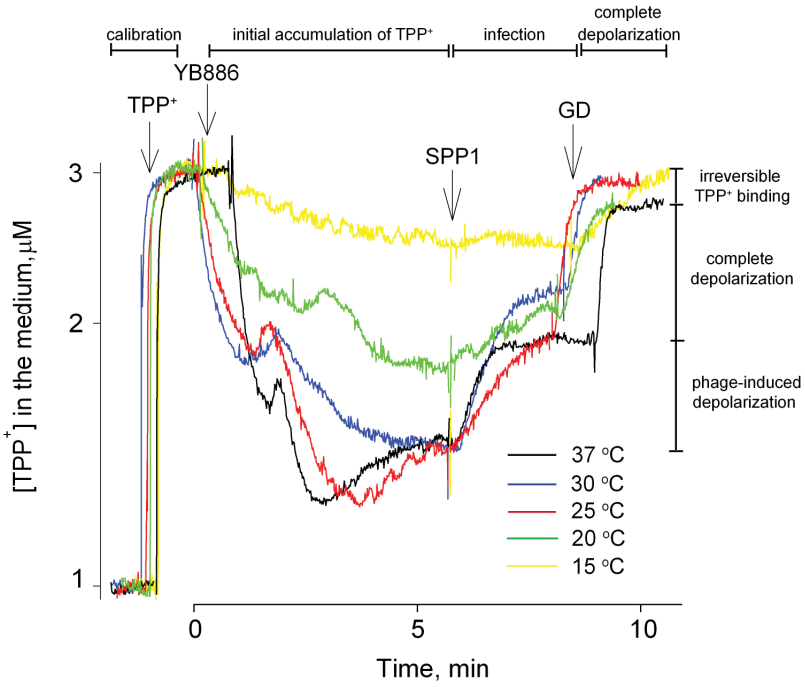

Fig. III.1. Effects of temperature on SPP1-induced CM depolarization of *B. subtilis* YB886 cells. Cells (5×10^8 cfu/ml) were incubated for 6 min in LB, pH 8.0, containing 5 mM $CaCl_2$ and 3 µM TPP^+ and infected with SPP1 (i.m. of 5). Measurements were carried out at the temperatures indicated. Arrows denote the addition of TPP^+, bacteria, phages and GD (final concentration of 5 µg ml^{-1}). The experiment different steps are identified on top of the figure. The levels of depolarization observed for the infection at 37 °C (black curve) are labeled on the right of the figure. Similar results were obtained in two independent experiments.

The depolarizing activity of the phage decreases with the increase of osmotic pressure of the medium (created by addition of sucrose). The SPP1-induced depolarization was totally blocked when osmolarity of the medium was 0.8 OsM and higher (not shown). This might result from reduced diffusion of the phages in high osmolarity solution. Exposure of bacteria to high osmolarity leads to dehydration and shrinkage of the cytoplasm, this can have an effect on cells homeostasis. These factors can affect the interaction of the phage and bacterial cell, on the other hand high osmolarity of the medium can lead to inhibition of DNA exit from the phage capsid.

Medium composition, osmotic pressure and temperature can affect SPP1-induced CM depolarization. All subsequent TPP^+ efflux measurements were performed at 37 °C in LB, pH 8.0 supplemented with 5 mM $CaCl_2$, unless stated otherwise.

III.1.2. Comparison to other *B. subtilis* phages

To establish if the features of CM depolarization caused by infection with SPP1 are specific to this phage, we studied the depolarization caused by infection with other *B. subtilis* tailed phages. Cultures of *B. subtilis* YB886 were split and infected in parallel with SPP1 (Riva et al., 1968), a member of the *Siphoviridae* family, *Podoviridae* phage ϕ29 (Anderson et al., 1966), and *Myoviridae* phage SP01 (Okubo et al., 1964) (Fig III.2A). As found previously, phage SPP1 caused a very fast depolarization of the infected cell CM (Vinga et al., 2006b), with a maximal level of CM depolarization reached at ~1 min p.i. (Fig. III.2B). In case of phages ϕ29 and SP01 a lag period between the addition of phages and the CM depolarization was observed (Fig. III.2B). At 37 °C the maximal level of depolarization was achieved at ~3.5 min p.i. with phage SP01, while bacteriophage ϕ29 caused a slow continuous efflux of TPP^+ ions from the cytoplasm after a lag of ~2 min. At 27 °C the kinetics of SPP1 induced CM depolarization was slower, while for ϕ29 and SP01 a very weak leakage of the

indicator cation was observed starting the 5th min of infection (Fig. III.2C). Depolarization indicates an effect on the CM permeability triggered by phage infection. The delay and low amplitude of ϕ29 and SP01-induced TPP^+ leakage at 27 °C shows that there is at least one temperature-dependent step at their initial stages of infection. This could result of the activation energy required to trigger DNA ejection from SPP1 virions (Raspaud et al., 2007), of an effect on the membrane, or of an enzymatic process.

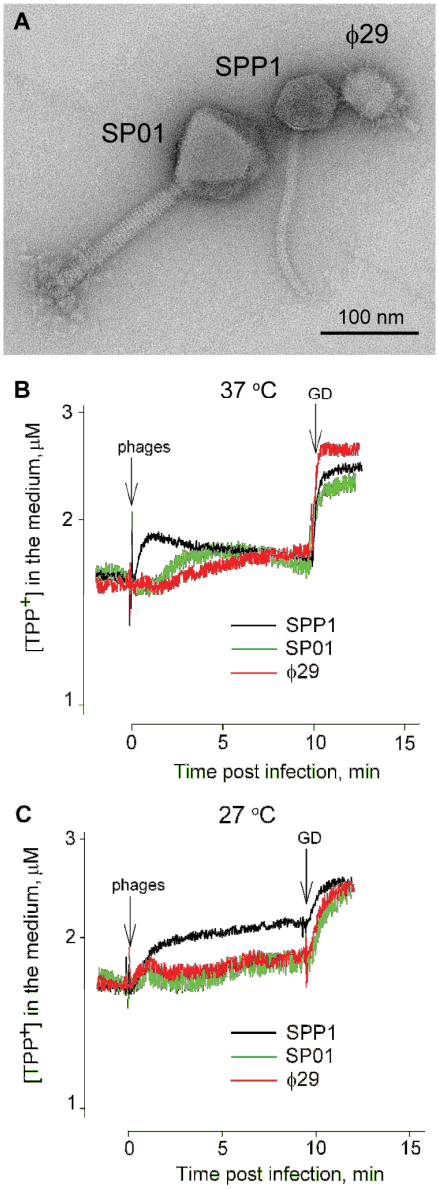

Fig. III.2. Depolarization of the CM caused by SPP1, SP01 and ϕ29 infection of *B. subtilis* YB886. (**A**) SPP1, SP01 and ϕ29 phages observed by EM after negative staining. (**B**,**C**) Variation of extracellular TPP^+ concentration in cultures of *B. subtilis* YB886 cells infected with SPP1 (black), SP01 (green) and ϕ29 (red) at 37 °C (**B**) and 27 °C (**C**). Infections were carried out at an i.m. of 6 pfu/cfu and the measurement of TPP^+ concentration in the medium was carried out as described in the Fig. III.1. Arrows denote the addition of phages and GD (final concentration of 5 µg ml^{-1}). Similar results were obtained in three independent experiments.

III.1.3. CM depolarization caused by SPP1 infection requires the phage receptor YueB and depends on its abundance at the bacterial surface

The fast depolarization of *B. subtilis* cells caused by SPP1 infection can be a result of the initial interaction between the virion and bacterial surface receptors. Therefore the TPP^+ efflux was monitored upon SPP1 interaction with three different *B. subtilis* strains: wild type cells (strain YB886), cells that do not synthesize the receptor YueB but allow reversible attachment of SPP1 particles to WTAs (Baptista et al. 2008; São-José et al. 2004), and cells that overproduce YueB (São-José et al. 2004) (Fig. III.3A). No phage-induced leakage of TPP^+ was observed in cells lacking YueB indicating that the reversible binding of SPP1 to WTAs has no effect on the energetic state of the CM. In case of cells overproducing YueB the SPP1-induced depolarization had reproducibly higher amplitude than in wild type bacteria. This difference correlates with the significantly higher density of YueB at the surface of the overproducing cells (Jakutyte et al. 2011).

Since the amplitude of CM depolarization depends on the amount of YueB, we investigated the effect of the number of infective phage particles *per* bacterial cell (pfu/cfu) on depolarization of wild type and YueB-overproducing cells (Fig. III.3B,C). The CM depolarization of wild type bacteria reached a maximal amplitude at an i.m. of ~12 pfu/cfu being identical at higher i.m.s (Fig. III.3B). The leakage of TPP^+ after GD addition indicated that the CM of infected cells remained partially polarized under these conditions. At i.m.s of 3 or above the depolarization observed for infections of the YueB overproducing cells was higher than the one observed for wild type bacteria when using the same i.m. (Fig. III.3B,C). Furthermore, the increase in phage/bacterium ratio in YueB-overproducing cells correlated with an augmentation in the amplitude of depolarization until the complete CM depolarization was achieved at an i.m. of 48 (Fig. III.3C). The SPP1 infection cycle progresses normally under these conditions with host cell lysis initiating at 30 min p.i. as found in infections at low i.m. (data not shown). Therefore, the strong CM depolarization

does not result from immediate cell lysis due to simultaneous infection of each bacterium by a large number of SPP1 particles ("lysis from without"). The data show that the amplitude of CM depolarization depends on the number of SPP1 phage particles (dependence on i.m.) interacting with the cell and on the amount of YueB exposed on the cell surface for virions binding (dependence on YueB surface concentration) (Fig. III.3B,C). Therefore, the number of YueB receptors is a limiting factor for SPP1–induced CM depolarization in wild-type *B. subtilis*.

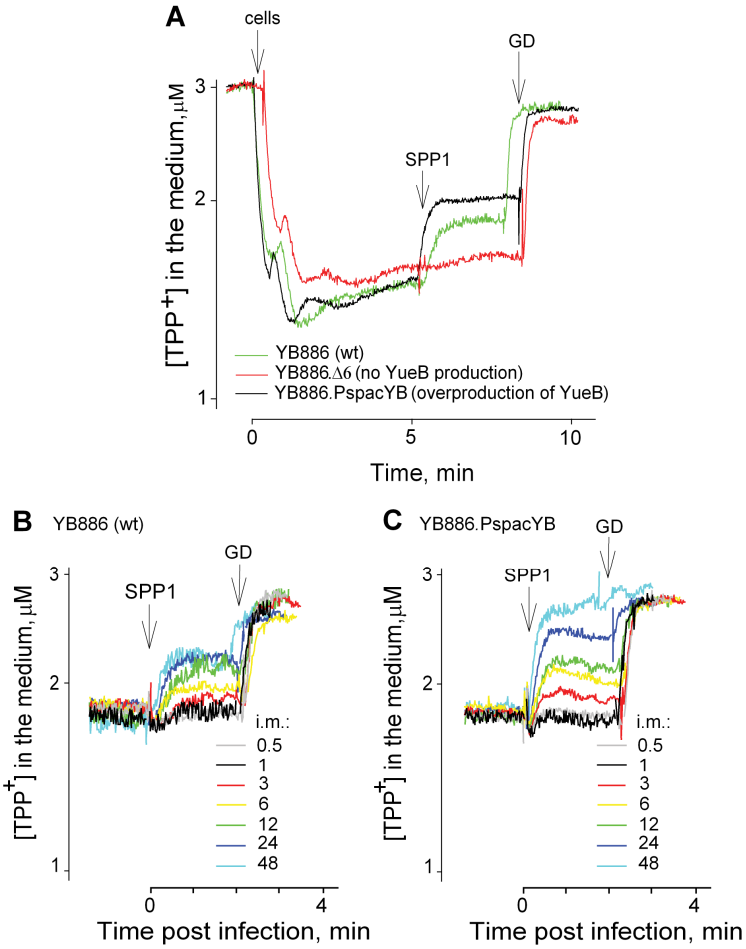

Fig. III.3. Effect of SPP1 infection on TPP^+ ion fluxes across the CM of different *B. subtilis* strains. (**A**) Infection (i.m. of 5 pfu/cfu) of wild type YB886 (green), YB886.Δ6 (no YueB production) (red), and YB886.PspacYB (overproduction of YueB) (black). Similar results were obtained in three independent experiments. Effect of i.m. (pfu/cfu; as indicated in **B** and **C**) on SPP1-induced TPP^+ ion fluxes across the CM of *B. subtilis* YB886 (**B**) and YB886.PspacYB (**C**). Similar results were obtained in two independent experiments.

The finding that irreversible adsorption of SPP1 to *B. subtilis* cells is strictly required to cause CM depolarization led us to investigate if binding of SPP1 particles to *B. subtilis* is sufficient to trigger this effect. Treatment of SPP1 particles with EDTA leads to their dissociation into DNA, empty phages, empty capsids, and tails (Tavares et al. 1996). Tails maintained intact their cell surface binding apparatus (arrows in Fig. III.4A). They also bound to *B. subtilis* with the same efficiency as wild type phages, as assessed by counting intact and disrupted viral particles labeled with quantum dots that remain associated to bacteria after dilution and centrifugation of phage-cells complexes (Fig. III.4B; for description of the methods used see section III.3.1). However, disrupted phage structures did not cause any detectable leakage of TPP^+ when an equivalent to 5 to 50 disrupted particles per bacterium was tested (Fig. III.4C). This result indicates that intact SPP1 particles are required to trigger CM depolarization.

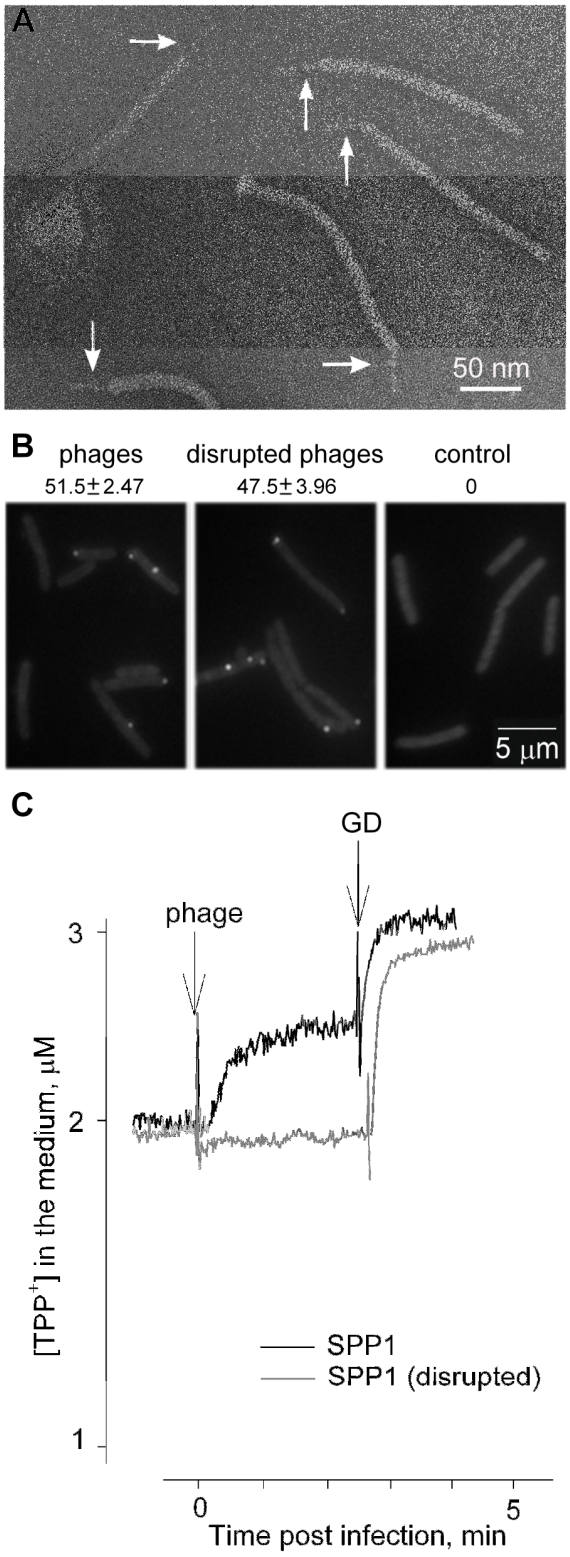

Fig. III.4. Viable and disrupted SPP1 virions binding to *B. subtilis* YB886 cells and effects on TPP^+ ion fluxes across the CM. (**A**) SPP1 phages disrupted with EDTA observed by EM after negative staining. Note that the host adsorption apparatus characterized by presence of the tail spike remains intact (arrows). (**B**) Phages (left) and disrupted phages (center) labeled with quantum dots binding to *B. subtilis* YB886. No unspecific binding of quantum dots to bacteria was observed (right). (**C**) Measurement of TPP^+ concentration in the medium of cells challenged with intact (i.m. of 5 pfu/cfu) or with an equivalent number of EDTA-disrupted particles. Similar results were obtained in three independent experiments.

III.2. Effects of Ca^{2+} ions on SPP1 infection

Divalent cations play a key role in bacteriophage infection (Bonhivers and Letellier, 1995; Cvirkaite-Krupovic et al., 2010b; Geller et al., 2005; Landry and Zsigray, 1980; Sciara et al., 2010; Steensma and Blok, 1979). In case of SPP1 the highest efficiencies of plating (e.o.p.) are obtained in the presence of Ca^{2+} (100 %) and, in decreasing order, with Sr^{2+} (70 to 80 %) and Mg^{2+} (40 to 60 %) (Santos et al, 1984). This raised the question of which step(s) of SPP1 infection depend(s) on the presence of extracellular divalent cations. A detailed analysis of the SPP1 e.o.p. in semi-solid medium showed a reduction to ~60 % when the $CaCl_2$ concentration was reduced from 10 to 5 mM (Fig. III.5A). The e.o.p. is severely compromised at concentrations of 1 mM $CaCl_2$ and below which correlates with a clear small phage plaque size phenotype (Fig. III.5B). No SPP1 plating is observed when no exogenous Ca^{2+} is added to the LB medium that contains ~10 µM Ca^{2+}, as measured using a Ca^{2+} selective electrode (data not shown). This strong dependence on Ca^{2+} explains most probably some variations observed among different laboratories when the e.o.p. of SPP1 is determined in absence of added divalent cations. They are due most probably to different trace amounts of Ca^{2+} found in LB medium and water.

No irreversible SPP1 binding to *B. subtilis* was observed when Ca^{2+} ions in the LB medium were depleted by addition of 0.5 mM EGTA (Fig. III.5C). We observed that the SPP1 irreversible adsorption constant (k_{ads}) was directly proportional to the logarithm of $CaCl_2$ concentration in the range between 0.25 and 10 mM (inset in Fig. III.5C). Since the rate of irreversible binding is highly conditioned by the reversible interaction of SPP1 with WTA (Baptista et al., 2008) we also studied dependence of the latter type of phage binding on Ca^{2+} concentration. Again, Ca^{2+} depletion from LB by EGTA resulted in very low reversible binding, particularly when scored at 37 ºC that favors dissociation of the reversibly bound phages (Fig. III.5D; Baptista et al., 2008).

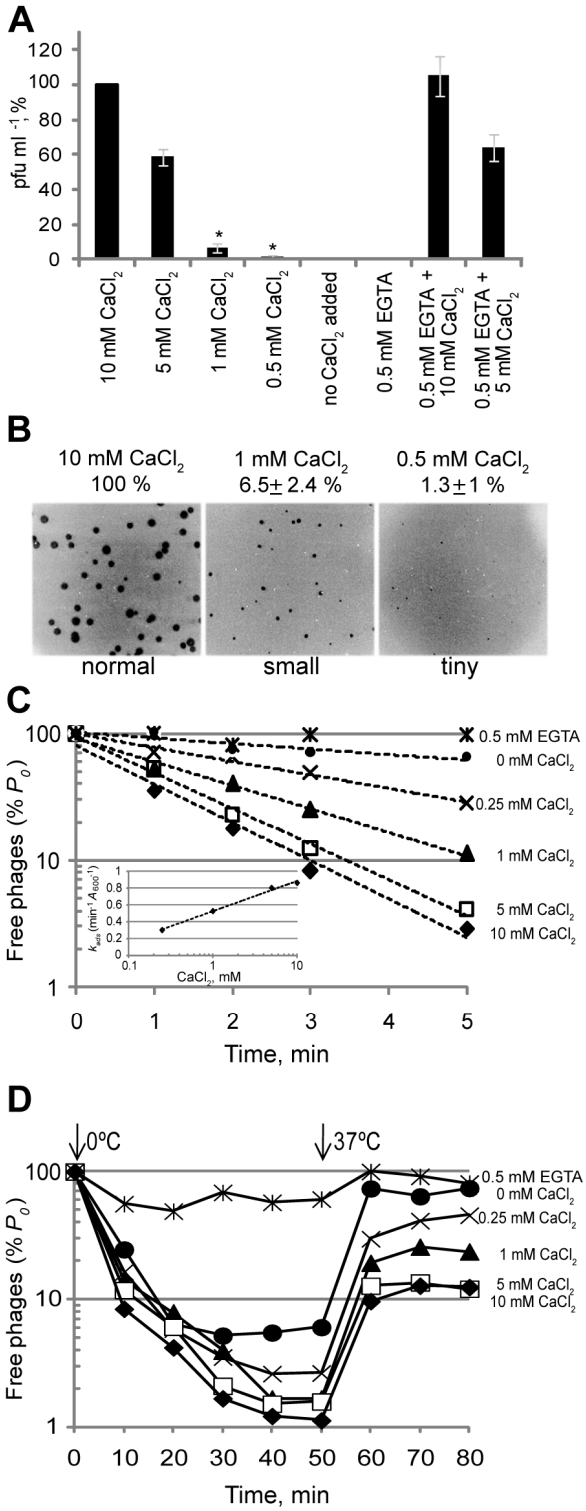

Fig. III.5. Effect of Ca^{2+} on SPP1 infection. (**A**) SPP1 infection of *B. subtilis* YB886 in semi-solid medium (e.o.p.) containing the supplements indicated. The titers are expressed as percentage of the titer obtained in presence of 10 mM $CaCl_2$ ($1.62 \times 10^{12} \pm 3.29$ pfu/ml) and are averages of at least 3 independent experiments. The asterisk indicates a small plaque phenotype dependent on the $CaCl_2$ concentration as illustrated in (**B**). (**C**) SPP1 irreversible adsorption to *B. subtilis* YB886. The irreversible adsorption constant (k_{ads}), determined as described (Baptista et al., 2008), was plotted against the log of $CaCl_2$ concentration (inset). (**D**) SPP1 reversible adsorption. *B. subtilis* YB886.Δ6 (no YueB production) in presence of the indicated $CaCl_2$ concentrations was pre-incubated in melting ice for 10 min. SPP1 was added (i.m. of 0.1) and aliquots taken at different time points to score for viable virions in the culture supernatant as described (Baptista et al., 2008). The culture was switched to 37 °C at 50 min post-infection to favor release of adsorbed phages. Results are plotted as percentage of the initial phage input (P_0).

However, the micromolar Ca^{2+} concentrations present in LB medium were sufficient to sustain reversible binding of more than 90% of the phage input at conditions that disfavor phage desorption (0 ºC, Baptista et al., 2008). At both temperature equilibrium states we observed that the levels of reversibly associated phage particles were higher as the Ca^{2+} concentration increased (Fig. III.5D). However, these results do not allow to discriminate whether Ca^{2+} is necessary exclusively for reversible binding to glucosylated teichoic acids, a requirement for efficient irreversible binding of SPP1 to YueB in liquid medium, or if the divalent cations also play a role directly in phage/YueB interaction.

Depletion of Ca^{2+} that abolished SPP1 binding to *B. subtilis* prevented also detectable SPP1-induced CM depolarization. This inhibition was readily overcome when the concentration of EGTA was titrated by the 230 µM Ca^{2+} present in the medium (concentration of EGTA $\leq$ 0.05 mM) or by addition of exogenous Ca^{2+} (EGTA $\geq$ 0.05 mM) (Fig. III.6).

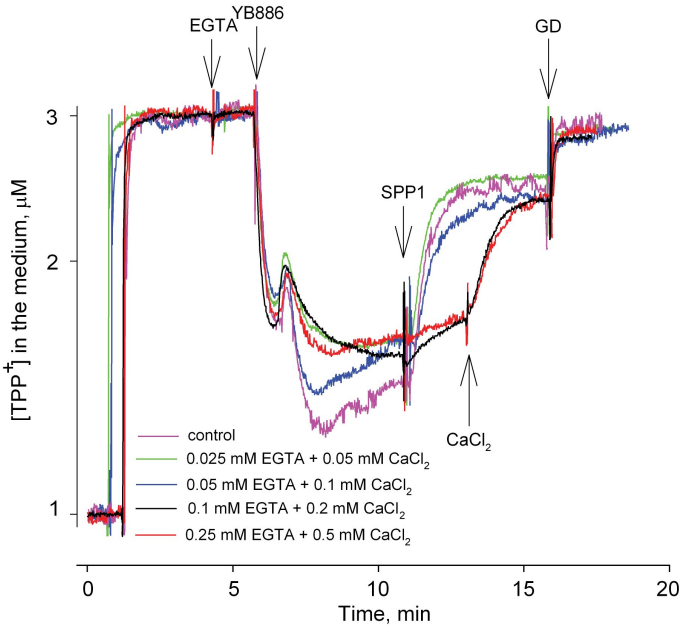

Fig. III.6. Effect of Ca^{2+} ions on SPP1-triggered depolarization of the *B. subtilis* YB886 CM. Cells depleted of extra-cytoplasmic Ca^{2+} with different concentrations of the Ca^{2+}-chelator EGTA were infected with SPP1 (i.m. of 5 pfu/cfu) and at 2 min p.i. a Ca^{2+} supplement was added to yield the concentration indicated: no supplement (control, contains 230 µM Ca^{2+} in the extracellular LB medium as measured with a Ca^{2+} electrode) (purple); supplemented with 0.025 mM EGTA and then with 0.05 mM $CaCl_2$ at 2 min p.i. (green); 0.05 mM EGTA and 0.1 mM $CaCl_2$ (blue); 0.1 mM EGTA and 0.2 mM $CaCl_2$ (black); 0.25 mM EGTA and 0.5 mM $CaCl_2$ (red). Similar results were obtained in two independent experiments.

The LB medium used for depolarization experiments had a concentration of 230 µM Ca^{2+}, higher that the one used in the other experiments described that contained 10 µM Ca^{2+}. Surprisingly, the amplitude of SPP1-induced TPP^+ efflux was higher when the LB medium contained 230 µM Ca^{2+}, than in the presence of 5 mM Ca^{2+} (Fig. III.7). Experiments performed at different i.m.s showed that the increase in phage/bacterium ratio led to the expected increase in amplitude of phage–induced depolarization (Fig. III.7). In LB medium supplemented with 5 mM Ca^{2+} the maximal amplitude of CM depolarization was reached at an i.m. of ~8 and no complete depolarization was observed (Fig. III.7A). In LB medium without additional Ca^{2+} the amplitude of depolarization was significantly higher leading to almost complete CM

depolarization at i.m.s ≥ 8 (Fig. III.7B). The CM depolarization caused by SPP1 thus requires the presence of micromolar concentrations of Ca^{2+}, while millimolar concentrations are inhibitory. The amplitude of SPP1-induced TPP^+ efflux in presence of 5 mM $CaCl_2$ was lower than in the presence of the same concentrations of $MgCl_2$, $BaCl_2$ or $SrCl_2$ (Fig. III.8) indicating that the effect of Ca^{2+} on SPP1-induced depolarization of the CM is specific.

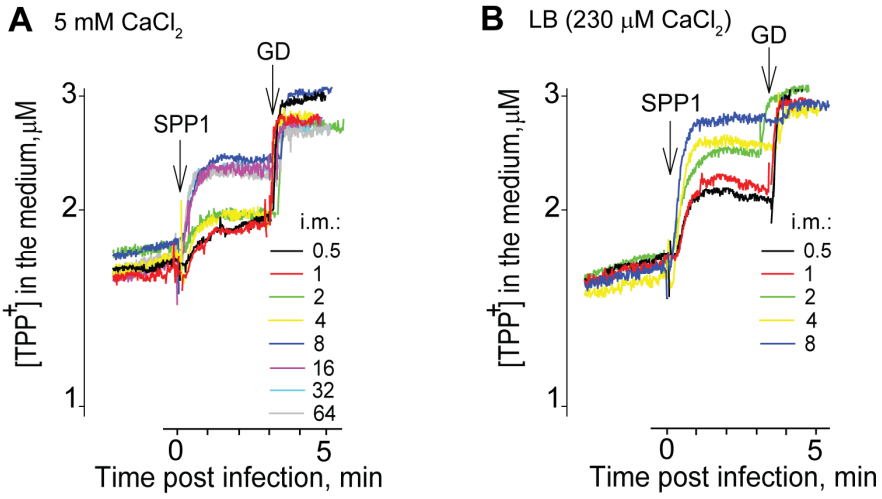

Fig. III.7. Dependence of SPP1-induced CM depolarization on Ca^{2+} concentration. Infections were carried out in LB with 5 mM $CaCl_2$ (**A**) or without supplement (containing 230 µM Ca^{2+} in the extracellular LB medium as measured with a Ca^{2+} electrode) (**B**) at the i.m.s. indicated. Similar results were obtained in three independent experiments.

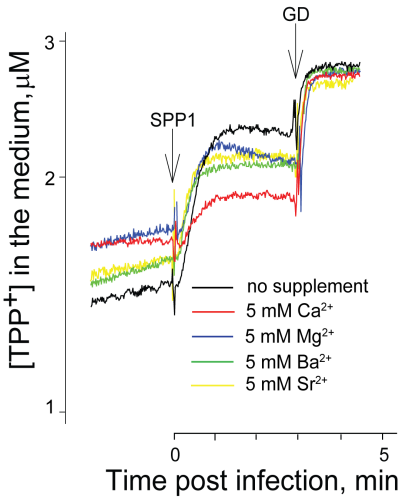

Fig. III.8. Effect of divalent ions on SPP1-induced *B. subtilis* YB886 CM depolarization. Infections with SPP1 were carried out as described in the Fig. III.1 with the concentrations of divalent cations indicated (chloride salts). Similar results were obtained in two independent experiments.

An efflux of cytosolic K^+ usually takes place concomitantly with phage infection (Cvirkaite-Krupovic et al., 2010b; Gaidelyte et al., 2006; Letellier et al., 1999). The addition of SPP1 particles to *B. subtilis* cell suspensions led to a very slow efflux of K^+ ions (Fig. III.9A) when compared to SPP1-induced TPP^+ leakage (Fig. III.9B). The magnitude of K^+ leakage from SPP1-infected cells in LB containing 230 µM Ca^{2+} was higher than in LB supplemented with 5 mM Ca^{2+} as observed also for CM depolarization. These results suggest that SPP1 does not induce K^+-permeable channels upon infection and the slow leakage of K^+ is a result of the CM depolarization.

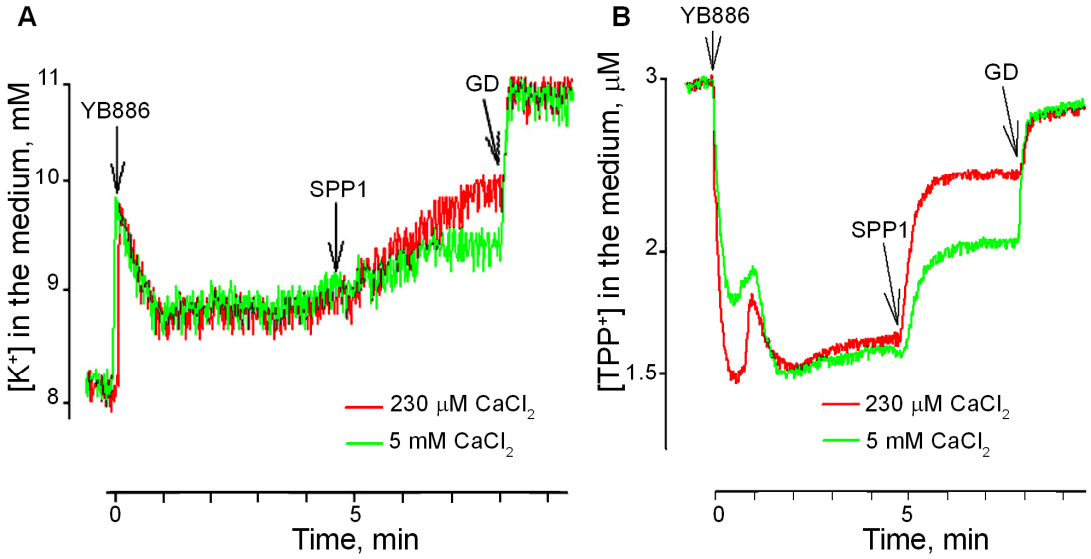

Fig. III.9. K^+ (**A**) and TPP^+ (**B**) ion fluxes across the CM of *B. subtilis* infected with SPP1 (5 pfu/cfu) when no Ca^{2+} is added (red) and in presence of exogenous 5 mM $CaCl_2$ (green). Extracellular ion concentrations were measured with ion specific electrodes. Similar results were obtained in three independent experiments.

III.3. Analysis of SPP1 infection in space and time

Irreversible SPP1 interaction with receptor protein caused distinctively fast physiological changes of *B. subtilus* CM. To establish if those changes accompany phage DNA traffic and to assess factors necessary for efficient initiation of infection, we then aimed to dissect in space and time the sequence of molecular events leading to delivery of the SPP1 genome across the *B. subtilis* cell envelope.

The first steps of tailed phages infection are host recognition and delivery of the genome to the bacterial cytoplasm. SPP1 infection is initiated by the specific interaction between virion RBPs and receptors on the *B. subtilis* surface. SPP1 adsorption involves reversible interaction with the host cell wall glucosylated poly(glycerolphosphate) teichoic acids (Baptista et al., 2008). Reversibly adsorbed phages can be released from cells as infectious particles by dilution. Reversible interaction strongly accelerates irreversible binding to the host cell membrane protein YueB (Baptista et al., 2008; São-José et al., 2004). Irreversibly bound phages commit to infection. Infection then follows encompassing cell wall degradation, passage of the CM and DNA entry in the host bacterium. Linear double stranded SPP1 DNA most likely circularizes in the host cytoplasm before replication of the viral genome initiates. Our interest was to define spatially and temporally the different steps of phage infection.

III.3.1. Localization of SPP1 particles on the surface of *B. subtilis*

We first addressed the distribution of SPP1 phage particles at the *B. subtilis* surface. Fluorescently labeled bacteriophage SPP1*delX110lacO*$_{64}$ particles were produced by chemical attachment of biotin followed by conjugation with streptavidin-coated quantum dots (Qdots, Qdot655-streptavidin), an adaptation of the method of Edgar et al. (2008) used for phages of Gram-negative bacteria. More than 80 % of the labeled SPP1 virions contained one or several Qdots, as assessed by electron

microscopy (Fig. III.10). No detectable difference in titer was found between phages chemically modified and control phages from the same virus preparation diluted in parallel during the labeling reaction (not shown). Biotinylation and Q-dots attachment had thus no effect in viral infectivity. Irreversible adsorption of SPP1*delX110lacO*$_{64}$ to *B. subtilis* YB886 (k_{ads} = 0.52 ± 0.04 min^{-1} A_{600}^{-1}, Table III.2) was slower than SPP1 wild-type (k_{ads} = 0.85 ± 0.03 min^{-1} A_{600}^{-1}). Biotinylation of SPP1*delX110lacO*$_{64}$ particles did not affect significantly their adsorption properties (k_{ads} = 0.43 ± 0.01 min^{-1} A_{600}^{-1}) but subsequent fixation of Qdot655 streptavidin conjugate to modified phages led to a reduction of their k_{ads} to 0.32 ± 0.06 min^{-1} A_{600}^{-1}. This effect on adsorption is probably due to a steric hindrance effect of Qdots bound to the phage tail tip region which affects its interaction with bacterial receptors (São-José et al., 2006). A sub-population of phage particles with Qdots bound to the tip region was indeed observed by electron microscopy (Fig. III.10B,C). The experimental conditions were then optimized for visualization of Qdot-phages bound to bacteria and to compensate for the ~2.7-fold reduction of k_{ads} of Qdot-SPP1*delX110lacO*$_{64}$ particles relative to SPP1 wild-type.

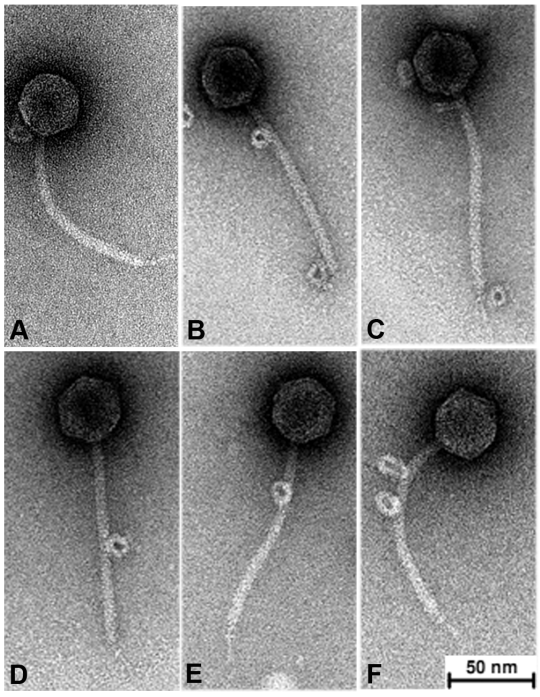

Fig. III.10. Electron micrographs of Qdots-SPP1*delX110lacO*$_{64}$. Phages were chemically modified with biotin using cross-linker EZ-Link Sulpho-NHS-Biotin. Qdots were then added to the biotinylated phages and immediately processed for EM as described in section II.7.

TABLE III.2. SPP1 irreversible adsorption constants (k_{ads}) to host bacteria[a]

Phage	Strain	k_{ads}, min^{-1} A_{600}^{-1}
SPP1*delX110lacO*$_{64}$	YB886	0.52 ± 0.04
SPP1	YB886	0.85 ± 0.03
SPP1*delX110lacO*$_{64}$-biotin	YB886	0.43 ± 0.03
SPP1*delX110lacO*$_{64}$-biotin-Qdot	YB886	0.32 ± 0.06
SPP1*delX110lacO*$_{64}$ + Qdot	YB886	0.49 ± 0.10
SPP1	YB886.Δ6.PxylYB	2.71 ± 0.54
SPP1	YB886.Δ6.PxylYBGFP	2.80 ± 0.48
SPP1	YB886.YBGFP	0.74 ± 0.01

[a]The indicated k_{ads} values are the averages from at least three independent experiments ± standard deviations on the mean.

In order to determine the topology of SPP1 binding to *B. subtilis* cells, the bacterial membrane was stained with the vital green dye FM1-43FX to define the contour individual cells (Fig. III.11A, top panels) and fluorescent virions were added at an i.m. of 6 pfu/cfu. This ratio was optimized to yield a majority of cells with one red fluorescent virion bound *per* cell (Fig. III.11A, bottom panels). Infected bacteria were fixed with glutaraldehyde at 2 min p.i., diluted 100-fold 2 min later, sedimented and resuspended for visualization of virions stably bound to the cell envelope. Control experiments showed that streptavidin-Qdots alone did not attach to *B. subtilis* cells (data not shown). The distribution of Qdot-labelled phages was determined according to the relative distance to the cell poles (d1, the distance to the closest cell end, divided by the cell length, d2, in Fig. III.11B). No correction was made for the total surface available for phage binding in different regions of the cell (e.g. between poles and the bacilli rod) due to cell size variability.

Infection of the *B. subtilis* wild-type strain YB886 yielded 35 % of bacterial cells with bound Qdot-virions (n = 740, from three independent experiments), which localized preferentially at or close to the cell poles (d1/d2 ≤ 0.1, Fig. III.11A,B). Analysis of a subset of cells growing in chains showed that binding to the old bacterial poles was strongly favored (Fig. III.11C). Approximately 20 % of SPP1 virions were found at the closed septal regions corresponding to newly forming poles,

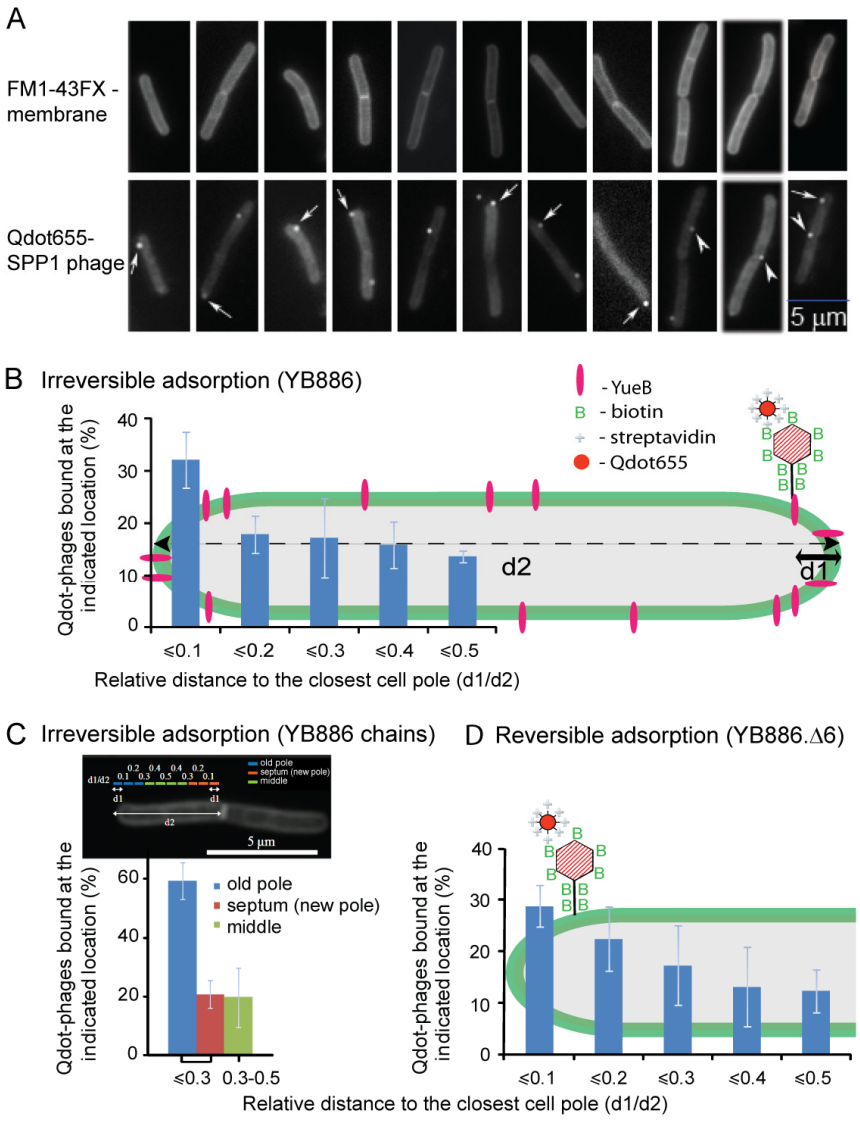

Fig. III.11. Localization of phage SPP1 particles on the surface of *B. subtilis* cells. **A.** Snapshot gallery of wild-type *B. subtilis* YB886 membrane-stained, to define the cell contour (top row) and containing Qdot655-labelled SPP1*delX110lacO*$_{64}$ phages (bottom row). Arrows and arrowheads show Qdot-phages at the cell poles and at septal regions, respectively. **B-D.** Percentage of Qdot-labeled SPP1 particles at the indicated relative distance (d1/d2) to the closest cell pole in the wild-type strain YB886 (**B**); to the old cell pole or to the closed septum in chains of two or more YB886 bacteria (a sub-set of data from **B**) (**C**); and to the closest cell pole in the *B. subtilis yueB* deletion strain YB886.Δ6 (Fig. II.1) (**D**). Infections were carried out at an i.m. of 6 phages *per* bacterium as described in section II.5.1. Results are from three independent infection experiments in which a total number of 400 (**B**), 96 (**C**) and 125 (**D**) cells with a single Qdot phage were measured. Note that the lower number of counts for YB886.Δ6 is due to the lack of irreversible adsorption to these cells explaining why only 8 % of the cells have a Qdot phage.

while the remaining virions adsorbed to more central regions of the cell cylinder (Fig. III.11C). We next visualised reversible binding alone by infecting the *B. subtilis yueB* null mutant (strain YB886.Δ6). Only 8 % of the cells lacking the SPP1 receptor YueB had Qdot-phages bound (n = 767, from three independent experiments). The dilution step used in our experimental setup leads to dissociation of most of the reversibly bound phages (Baptista et al., 2008). Like in wild-type cells, Qdots-labeled phages preferentially bound at the cell poles or in their close neighborhood (Fig. III.11D). Phage binding gradually decreased from the poles towards mid-cell.

The distributions shown in Fig. III.11B and D were found to be similar in a t-test, p-value 0.997 and Two-Sample Kolmogorov-Smirnov test, p-value 0.566. As the computed p-value is greater than the significance level alpha=0.05, one should accept the null hypothesis H_0 (H_0: the two samples follow the same distribution). Statistic analysis obtained using XLSTAT application of Microsoft Office Excel 2007 program (Fig. III.12).

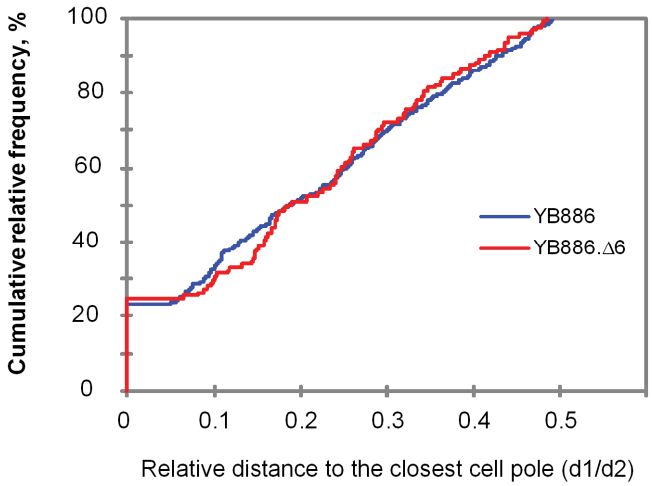

Fig. III.12. Cumulative distributions, of Qdot-labelled SPP1 particles at the indicated relative distance (d1/d2) to the closest cell pole in the YB886 and YB886.Δ6 strains, obtained using two-sample Kolmogorov-Smirnov test with XLSTAT application of Microsoft Office Excel 2007 program.

However, this statistical analysis shall be taken cautiously due to the lower data sampling for phages bound to cells lacking YueB (Fig. III.11D) compared to wild-type bacteria (Fig. III.11B). Taken together, these findings suggested that both reversible and irreversible binding of SPP1 occur preferentially at the cell poles, and thus that reversible adsorption may already target SPP1 for a polar distribution at the *B. subtilis* surface.

When a large i.m. (100 virions/cell) was used to infect wild-type *B. subtilis* cells, a few Qdots-labeled phages were found attached to the bacterial cells at 2 min p.i., again preferentially at their poles (Fig. III.13, top row). In contrast, when cells overproducing YueB were infected, a large number of phages was found stably bound along the length of the bacterial cells, displaying a rather homogeneous punctate distribution on the cell surface (Fig. III.13, bottom row). Since phage binding under our experimental conditions is essentially due to irreversible adsorption (see above), this further suggested that functional YueB available for interaction with SPP1 is present in limiting amounts at the surface of wild-type *B. subtilis* cells (Baptista et al., 2008; São-José et al., 2004).

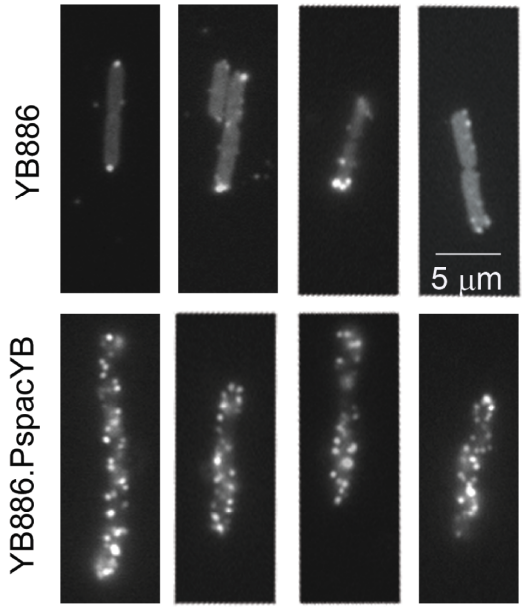

Fig. III.13. SPP1*delX110lacO*$_{64}$ binding to *B. subtilis* cells at high multiplicity of infection. Qdot-labeled phages (100 virions *per* bacterium) were incubated with *B. subtilis* YB886 (upper row) or with the YueB-overproducing strain YB886.PspacYB (bottom row) for 2 min followed by fixation and dilution as described in section II.5.1.

III.3.2. Cellular localization of SPP1 receptor YueB

The polar localization of SPP1 particles at the *B. subtilis* surface might be imposed by the preferential reversible adsorption to bacterial poles (Fig. III.11D) and/or result from the distribution of YueB in the bacterial envelope. YueB is an integral 120 kDa membrane protein found in low amounts in *B. subtilis* (São-José et al., 2004). Its most abundant forms, as detected in extracts of wild-type *B. subtilis* cells by western blot using a polyclonal antibody raised against YueB780 (Fig. I.8; São-José et al., 2006), are truncated polypeptides found associated to membranes after cell fractionation (São-José et al., 2004; Fig. III.14A). These forms did not result from sample degradation (proteolysis) as the same pattern of bands was found when cell extracts were taken directly into trichloroacetic acid to inactivate proteases (Hayashi and Wu, 1983) (data not shown). These observations suggested that YueB is prone to proteolysis *in vivo* or at least immediately after bacterial death, originating the truncated forms observed in Fig. III.14A. The dominant species in western blots corresponded to a doublet of bands (only resolved in long runs of 8 % polyacrylamide gels) with apparent masses around 65 kDa. A less intense band was observed at ~70 kDa, and a faint band that likely corresponds to full-length YueB was detected at ~120 kDa. All these species were absent in the *yueB*$^-$ strain YB886.Δ6 (Fig. III.14A). In cells bearing a GFP fusion to the carboxyl terminus of YueB (Fig. I.8; III.14A), the immunodominant ~65 kDa forms disappeared and a ~90 kDa band, which might correspond to a non-resolved doublet, appeared instead. This indicated that the ~65 kDa species were truncated products of the YueB carboxyl terminus. Western blots developed with anti-GFP antibodies confirmed this assignment (Fig. III.14B). Stronger signals for the same immunoreactive bands were obtained with YueB and YueB-GFP overproducing strains (Fig. III.14A,B, right panels). Note that five-fold less total protein was loaded on these westerns relative to those shown on the left panels of the figure. The region of YueB that binds to SPP1 is not known and no

function was assigned to the individual truncated forms of YueB that are likely present in the cell envelope (Fig. III.14).

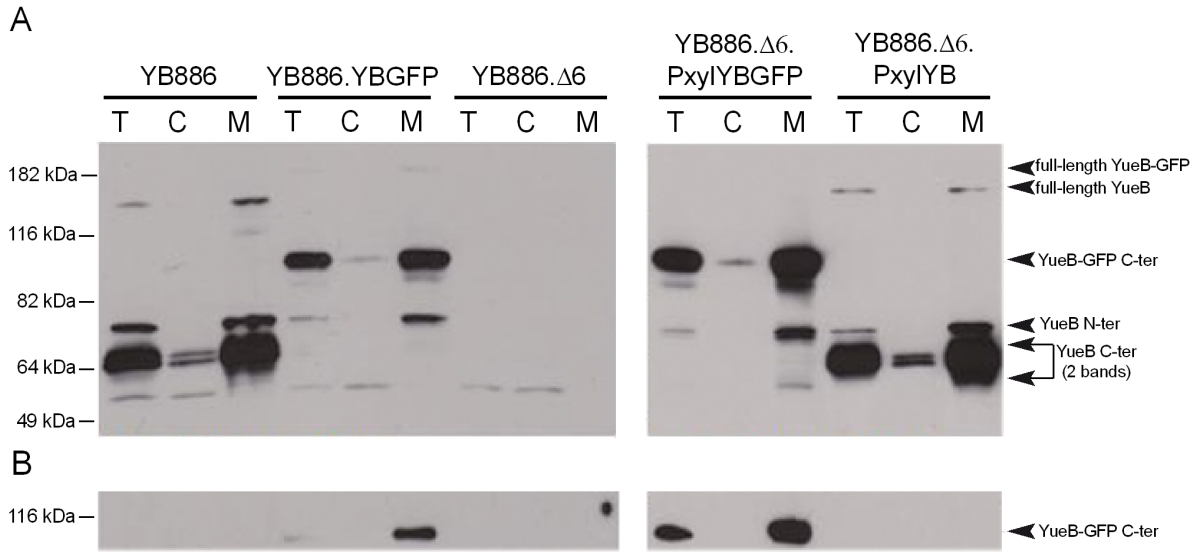

Fig. III.14. Expression of *yueB* and *yueB-gfp* fusions in *B. subtilis*. Production of YueB and YueB-GFP in total cell extracts (T) and after fractionation into cytoplasmic (C) and membrane (M) fractions. Their composition was characterized by western blot using anti-YueB780 (**A**) and anti-GFP (**B**) antibodies. The amount of total protein loaded *per* lane was 30 µg (NanoDrop quantification) for YB886.Δ6.PxylYBGFP and YB886.Δ6.PxylYB (right panels), whereas 150 µg (5-fold) were loaded for YB886, YB886.YBGFP and YB886.Δ6 (left panels) to increase sensitivity. Molecular mass markers are shown on the left. The assignment of YueB-derived bands is shown on the right.

We thus investigated both the localization of the cytoplasmic YueB–GFP fusion in live cells and the surface (extracellular) distribution of YueB by immunofluorescence microscopy (IFM) in non-permeabilised cells to assess the SPP1 receptor topology. The efficiency of SPP1 plating in cells producing YueB-GFP was similar to that found for bacteria producing equivalent amounts of YueB in a titration plate assay (data not shown). Adsorption was only slightly reduced in the strain expressing the *yueB-gfp* fusion under control of the native P_{yuk} promoter (Fig. II.1) relative to the control wild-type strain YB886 while no difference of k_{ads} was found between strains overproducing YueB and YueB-GFP (Table III.2). We concluded that

fusion of GFP to the carboxy-terminus of YueB did not affect receptor activity. Surface localization of YueB by IFM was performed using polyclonal antibodies raised against the extracellular YueB780 fiber region (Fig. I.8; São-José et al., 2006). Pre-incubation of *B. subtilis* cells with anti-YueB780 serum reduced significantly the adsorption constant of SPP1 to bacteria (São-José et al., 2006), showing that the antibodies recognized regions of YueB at the cell surface that are necessary for its SPP1 receptor activity.

Expression of *yueB* driven from its native promoter as the single gene copy coding for YueB in the cell led to a relatively weak surface labeling in IFM of fixed cells (Fig. III.15A). A significant proportion of cells showed a peripheral spotted pattern along the cell cylinder and a strong fluorescence signal at the cell poles (Fig. III.15A). A weak fluorescence signal displaying a similar distribution was also obtained for the YueB-GFP fusion when its coding gene was expressed under control of the P_{yuk} native promoter (Fig. III.15B). Membrane staining defining the contour of individual cells in bacterial chains revealed accumulation of YueB-GFP at old cell poles. The pattern of fluorescent protein distribution was particularly prominent when images were deconvolved (Fig. III.15B, right panels). Although the fluorescence signals in both cases were weak, consistent with the low endogenous levels of YueB (São-José et al., 2004), the similarity of the localization pattern of YueB-GFP and extracellular YueB (IFM experiments) lent support to a discrete localization of YueB along the bacterium sidewalls and its accummulation at the old cell poles. It also indicated that the surface distribution of the YueB ectodomain is similar to that displayed by the transmembrane segments and the cytoplasmic tail at its carboxyl terminus.

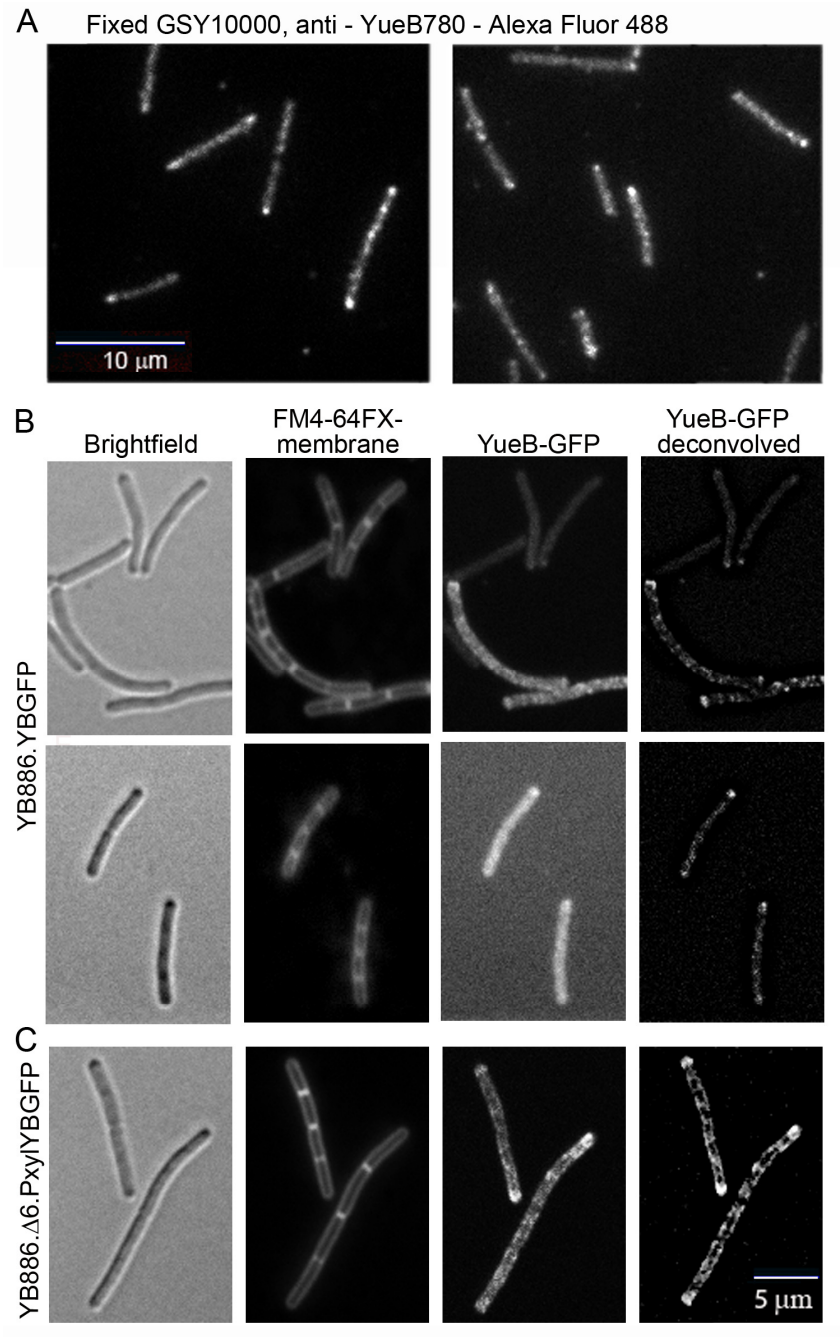

Fig. III.15. Localization of YueB in *B. subtilis*. **A.** Labeling of YueB at the cell surface of fixed GSY10000 cells labeled with polyclonal anti-YueB780 antibodies. **B,C.** Cytoplasmic localization of YueB in *B. subtilis* YB886.YBGFP (expression of the *yueB-gfp* fusion under the native P_{yuk} promoter; Fig. II.1) (**B**) and YB886.Δ6.PxylYBGFP (*yueB-gfp* fusion under the control of a strong xylose inducible promoter; Fig. II.1) (**C**). The YueB cytoplasmic carboxyl terminus (São-José et al., 2004, 2006) was fused to GFP (Fig. II.1). Columns in **B,C** show, from left to right, brightfield; FM4-64FX stained membranes; YueB-GFP fluorescence, and 2D deconvolution of the YueB-GFP signal.

Ectopic overexpression of *yueB-gfp* under control of a xylose-inducible promoter (Fig. II.1; III.14A) gave a more distinct and intense fluorescence signal in the ensemble of the bacterial population (Fig. III.15C). The increased signal-to-noise ratio made the distribution of YueB-GFP along the sidewalls clearly visible, revealing a punctate/banded pattern, and further confirming the enrichment of YueB at cell poles (Fig. III.15C). Again, visualisation of the signal in chains of cells showed that accumulation occurred at the old cell poles in particular. Colocalization of the surface labeling of YueB by IFM and of the YueB-GFP fusion (Fig. III.16) suggested that the ectodomain and the cytoplasmic carboxyl terminus of the protein (despite the presence of several truncated forms, Fig. III.14A) are physically associated in most YueB molecules. Integrity of the YueB dimer (São-José et al., 2006) might be maintained by inter- and intra-subunit interactions between the truncated polypeptides within the YueB quaternary structure explaining the observed similar distribution in the cell envelope.

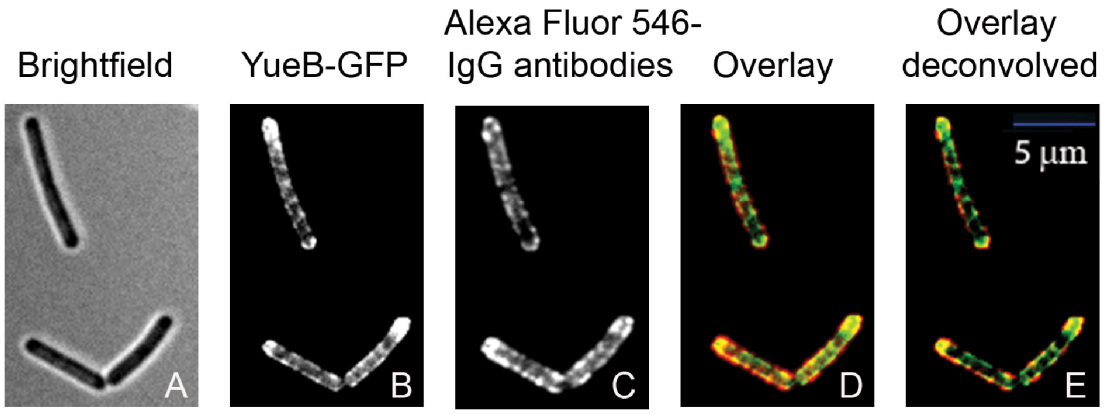

Fig. III.16. Colocalization of YueB on the cytoplasmic side of the membrane and at the cell surface in *B. subtilis* YB886.Δ6.PxylYBGFP (Fig. II.1) using a GFP fusion to the YueB cytoplasmic region (**B,D,E**) and immunostaining with anti-YueB antibodies (surface labelling) (**C-E**), respectively. Overlays of the images are shown in **D** and **E** (deconvolved), where YueB-GFP is in green and anti-YueB antibodies are in red.

III.3.3. Localization of SPP1 DNA in infected cells

The preferential binding of SPP1 phages to the *B. subtilis* cell poles and the enrichment of the YueB receptor at these sites suggested that phage DNA entry might also be polar. In order to visualize SPP1 DNA entry, we cloned an array of *lacO* repeats at the unique *Sph*I site of the bacteriophage SPP1*delX110* genome (Fig. II.2). The repeat of *lacO* (21 bp) operators used was spaced by 10 bp random sequences to prevent genetic instability (Lau et al., 2003). SPP1*delX110*, which encapsidates viral chromosomes of wild-type length (Tavares et al., 1992), carries a 3417 bp *delX* deletion (Chai et al., 1993) within a non-essential region of its genome. Insertion of the *lacO* repeat array in a dispensable region of the phage genome combined with the *delX* deletion lead to no net increase in size of the genome and resulted in viable phages (SPP1$delX110lacO_{64}$). The repetitive segment of DNA was maintained stably in the SPP1 genome and had no deleterious effect in phage multiplication (data not shown). SPP1$delX110lacO_{64}$ was titrated with *B. subtilis* cells producing a LacI-CFP soluble fusion (strain GSY10000) in the presence or in the absence of 1 mM IPTG. IPTG leads to dissociation of LacI-CFP from lacO repeats, thus relieving potential arrest of DNA replication or packaging in this region of the genome. Titrations in both conditions gave identical results (data not shown). We concluded that binding of multiple copies of LacI-CFP to the SPP1 genome impairs neither DNA replication nor DNA packaging into viral procapsids.

Time-lapse observations of SPP1$delX110lacO_{64}$ infecting strain GSY10000 were carried out following the experimental setup schematized in Fig. III.17A. These experiments showed the appearance of intracellular fluorescent foci upon infection (Fig. III.17B). Their size increased with time, which correlated with an increase of their fluorescence intensity and a reduction in the cell background fluorescence (i.e. increased signal-to-noise ratio) (Fig. III.17B). This presumably resulted from the clustering of the LacI-CFP fusion on phage DNA undergoing replication, which initiates at ~3 min p.i. at 37 °C (Burger, 1980; Missich et al., 1997 and references

therein). Consistently, no increase of phage DNA foci fluorescence was found in infected cells treated with HPUra (white arrows in Fig. III.17C), which inhibits bacterial DNA polymerase III - the host enzyme that replicates the SPP1 DNA (Rowley and Brown, 1977). In some cells, the SPP1 replication centers disappeared with time, possibly due to abortive phage multiplication processes (arrowhead in Fig. III.17B). Taken together, these observations indicated that SPP1 genome replication initiates and proceeds at defined foci ('replication factories').

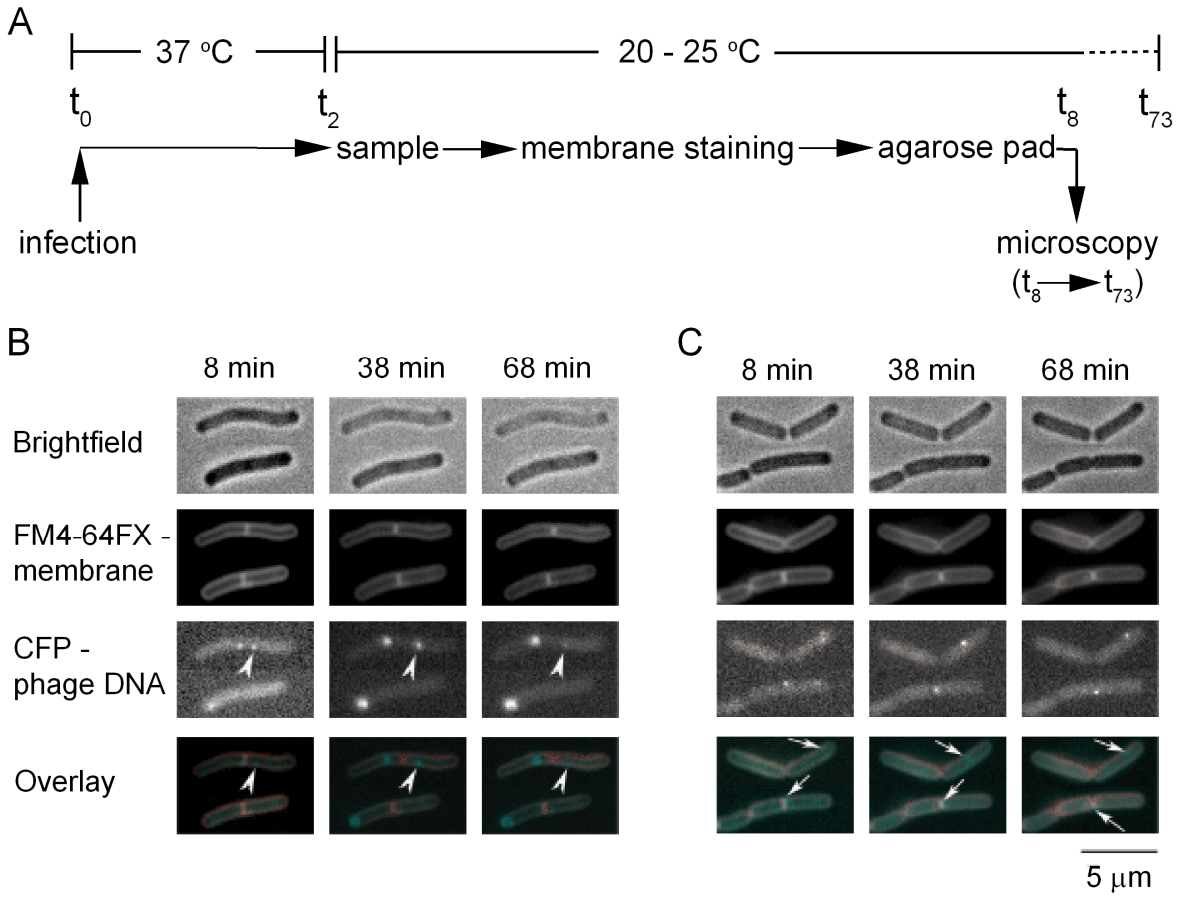

Fig. III.17. Time-lapse of bacteriophage SPP1*delX110lacO64* infection. **A.** Experimental setup. t_0, infection; t_2, 2 min p.i., $t_{8\text{-}73}$, 8 to 73 min p.i. **B, C.** Images of *B. subtilis* producing LacI-CFP infected by phage SPP1*delX110lacO64* (i.m. of 3) in the absence (**B**) or presence of HPUra (**C**) were taken at the p.i. times indicated. Brightfield (top row); FM4-64FX membrane staining (second row); LacI-CFP (third row). The bottom row shows overlays of membrane staining and CFP fluorescence. The arrowheads show a focus that disappears during infection. The white arrows show small LacI-CFP spots in infected cells treated with HPUra.

Quantitative analysis of the spatial distribution of SPP1 replication foci over time showed that they preferentially localized close to the cell poles, with a wide distribution centered at the pole-cylinder junction (d1/d2 ~ 0.1-0.3) at early infection times (Fig. III.18A, black bars). This distribution was shifted towards a more central position in the cell as infection progressed (Fig. III.18A, grey bars and Fig. III.18B). In chains of cells, a higher number of foci appeared to be present close to old cell poles relative to septal regions and to the middle cell at early times p.i.. An accurate quantification was however hampered by limited sampling of the small size foci and their weak fluorescence (data not shown). Measurement of the length of individual cells (infected and non-infected) at different time points showed that cell growth was not affected by SPP1 infection (data not shown), and that cells kept growing on the microscope slide during the time-lapse experiments (see the elongation of the cells shown in Fig. III.17B over time). However, we could not distinguish whether the increase in distance between foci and cell poles over time is a passive process due to cell elongation or if it results from the active movement of the foci.

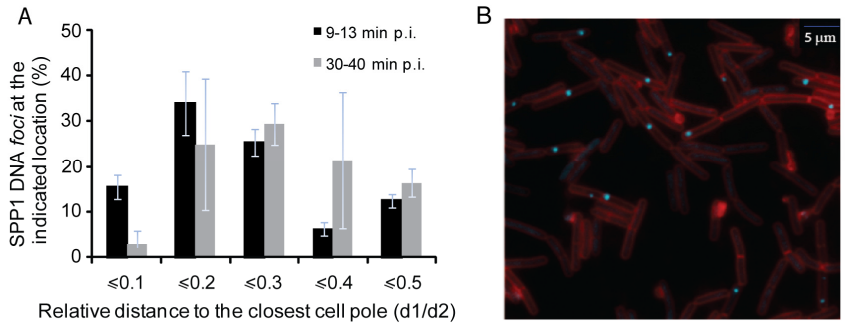

Fig. III.18. Localization of phage SPP1*delX110lacO*$_{64}$ DNA in *B. subtilis* infected cells. **A.** Percentage of SPP1 DNA spots at the indicated distance relative (d1/d2) to the closest cell pole (old cell pole or closed new septum) on the bacterial cell, as observed by fluorescence microscopy (**B**). Measurements from three independent infections were carried out as schematized in Fig. III.11B at early (black bars; 200 cells with a single SPP1 DNA spot were measured from images taken between 9 and 13 min p.i.) and late (grey bars; 200 cells with a single SPP1 DNA spot were measured from images taken between 30 and 40 min p.i.) time-points after infection. **B.** Cells producing LacI-CFP (cyan) were infected by phage SPP1*delX110lacO*$_{64}$ (i.m. of 3) and imaged at a late time point after infection (between 30 and 40 min p.i.). The cell outline was visualized with the vital membrane stain FM4-64FX (red).

III.4. Ca^{2+} ions effect on SPP1 DNA entry

Infectivity of SPP1 assayed by its e.o.p. requires a concentration of Ca^{2+} above 1 mM while detectable adsorption of phage particles to *B. subtilis* occurs at sub-millimolar concentrations (Fig. III.5). This observation shows that Ca^{2+} is necessary at another step of SPP1 infection cycle in addition to its effect on phage adsorption. We have thus investigated if Ca^{2+} ions are necessary for phage DNA transfer from the virion to the bacterial cytoplasm. *B. subtilis* GSY10000 cells producing a LacI-CFP soluble fusion were infected with bacteriophage SPP1*delX110lacO*$_{64}$ that carries an array of 64 *lacO* repeats in its genome (Jakutyte et al., 2011). The appearance of intracellular fluorescent foci (Fig. III.19A) whose size and intensity increase with time shows that viral DNA entered and replicated in the cytoplasm. When *B. subtilis* GSY10000 cells were infected with SPP1*delX110lacO*$_{64}$ at an i.m. of 5 in presence of 5 mM $CaCl_2$, as used in TPP^+ measurements, 65±9.7 % of the cells had an intracellular fluorescent focus (Fig. III.19A,E). Percentage of cells having foci decreased to 20.3±6.6 %, when concentration of $CaCl_2$ was decreased to 1 mM (Fig. III.19B,E). In presence of sub-millimolar $CaCl_2$ concentrations appearance of fluorescent phage DNA foci was strongly affected: only 4.5±3 % and 1.1±0.3 % of infected cells had fluorescent DNA foci in the presence of additional 0.25 mM or without additional $CaCl_2$, respectively (Fig. III.19C,D,E).

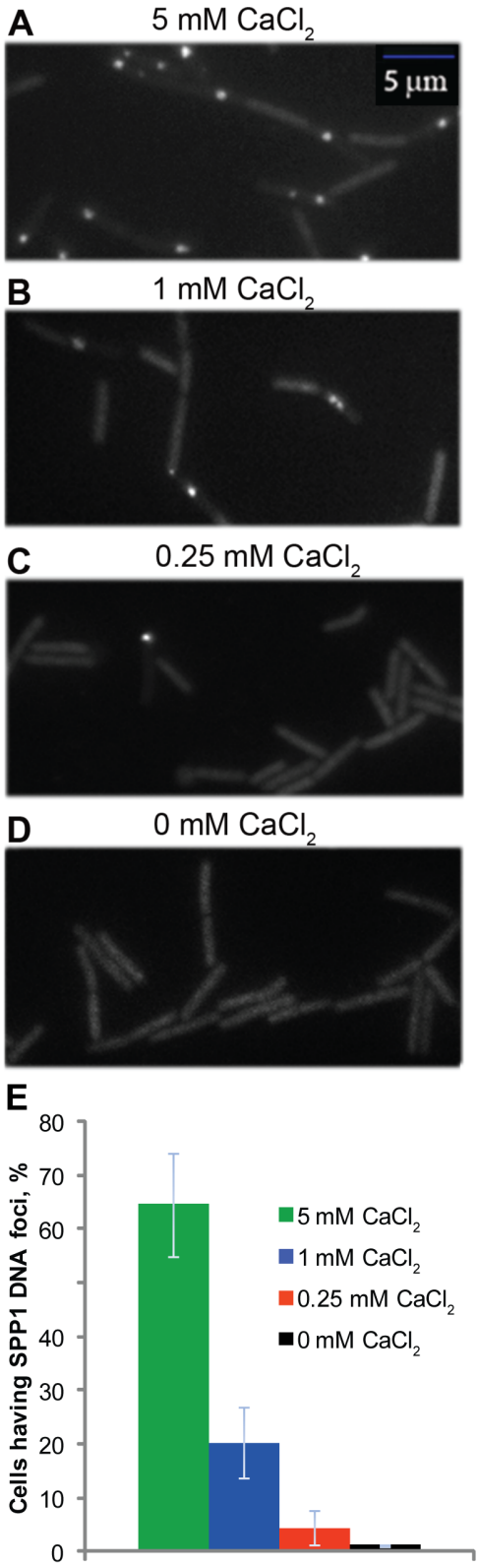

Fig. III.19. Visualization of SPP1 DNA in *B. subtilis* infected cells. (**A-D**) Cultures of *B. subtilis* producing LacI-CFP supplemented with 5 (**A**), 1 (**B**), 0.25 mM $CaCl_2$ (**C**) and without additional $CaCl_2$ (**D**), infected by phage SPP1*delX110lacO*$_{64}$ (i.m. of 5), and imaged at 20-40 min p.i. The endogeneous concentration of Ca^{2+} in the LB medium used was ~10 µM. (**E**) Percentage of cells having SPP1 DNA foci after 20-40 min of infection in presence of the supplements indicated. Results are from four independent infection experiments in which a total number of 412 (**A**), 525 (**B**), 634 (**C**) and 405 (**D**) cells were counted.

IV. DISCUSSION

Bacteriophages use a variety of strategies to deliver their genome across the bacterial envelope to the cell cytoplasm where their genetic information is expressed and replicated. The first contact with the bacterial surface usually leads to reversible binding. In a second step virions attach irreversibly to specific cell envelope receptors committing to infection of the host. Reversible and irreversible binding can be to the same receptor or involve different surface components (section I.5.1.1). Phage particles frequently possess a cell wall degradation activity to drill the PG and to access the CM (section I.5.2). Phage genome passage through the CM requires formation of a pore preceding transfer of DNA from the virion to the cytoplasm. DNA entry can be a very fast process, e.g., it can take less than 30 seconds as found for phage T4 (Letellier et al., 1999), but can also be significantly slower as in the case of phage T7 whose complete genome internalization takes about one third of the infection cycle duration (García and Molineux, 1996). Different durations of phage DNA entry likely result from diverse mechanisms of DNA transfer to the cytoplasm. The question of how a large, hydrophilic, and polyanionic phage DNA molecule crosses the bacterial envelope is still poorly understood.

The information regarding penetration of the phage genome in Gram-positive bacteria is very scarce comparatively to Gram-negative systems. Given the accumulated knowledge in the molecular biology of the tailed bacterial virus SPP1 and its host, our research addresses the cell biology of SPP1 entry and multiplication in the model Gram-positive bacterium *B. subtilis*. The irreversible interaction of SPP1 with receptor protein YueB caused distinctively fast physiological changes of *B. subtilus* CM. The results presented in this PhD thesis established the specific requirements for phage SPP1 infection and dissected its diferent steps in space and time. The sequence of molecular events leading to delivery of a SPP1 genome across the envelope of *B. subtilis* cell was investigated with a variety of experimental approaches (Fig. IV.1).

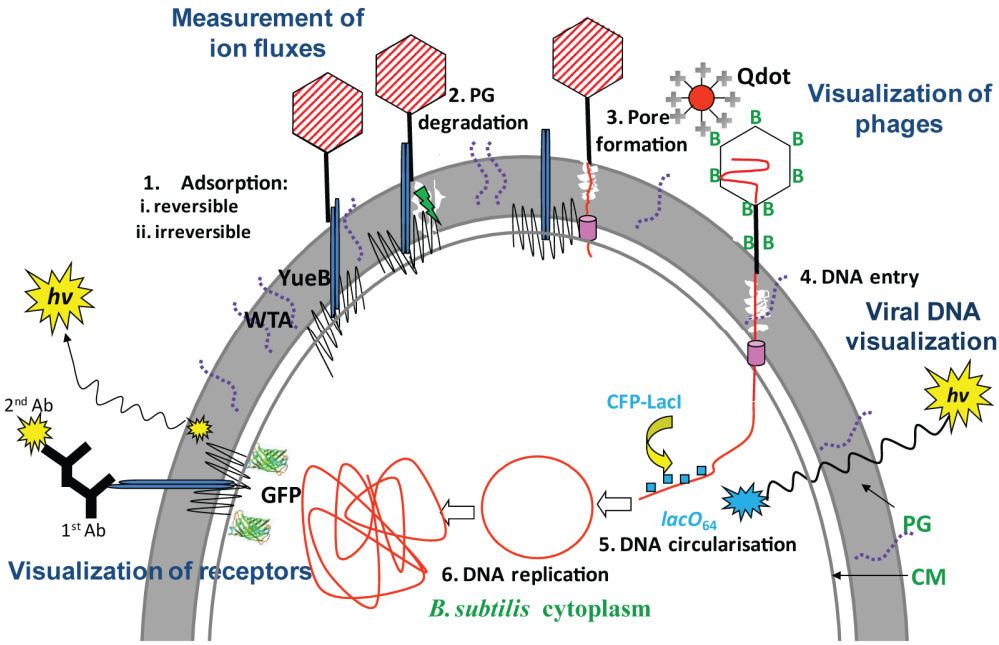

Fig. IV.1. *B. subtilis* infection by bacteriophage SPP1. Bacteriophage entry steps (in black) and experimental assays used in this study (in blue). (1) reversible SPP1 adsorption to glucosylated cell wall teichoic acids (WTAs) and irreversible binding to YueB protein, (2) degradation of peptinoglycan layer (PG), (3) pore in cytoplasmic membrane (CM) formation, steps (1-3) were studied using potentiometrical measurements of TPP^+ ion fluxes across CM (section III.1). (4) DNA entry in the cytoplasm, (5) circularisation and (6) replication studied by fluorescence microscopy methods (section III.3.3). Visualization of receptor protein YueB by fusion to Green fluorescent protein (GFP) and immunofluorescence described in section III.3.2. Visualization of phage particles using fluorescent quantum dot particles (Qdot) (section III.3.1). Note that the scheme is not in scale.

IV.1. The interaction of SPP1 with YueB triggers a very fast depolarization of the *B. subtilis* CM.

Virus genome entry in bacteria requires crossing of the cell envelope. This initial step of infection is usually associated with depolarization of the CM and/or the release of intracellular K^+ ions (Letellier et al., 1999; Poranen et al., 2002). The timing and pattern of ion leakage is different among phages, providing a fingerprint for infection by each virus species. It is yet not known, if depolarization of the CM and/or K^+ leakage play a physiological role in infection or if they are side effects accompanying phage entry. Infection of *E. coli* by tailed phages T4 and T5 leads both

to the CM depolarization and to efflux of K^+ (Boulanger and Letellier, 1992; Grinius and Daugelavicius, 1988; Labedan and Letellier, 1981; Letellier and Labedan, 1984). In contrast, bacteriophage PRD1 that uses an internal membrane device for DNA delivery to the host cytoplasm leads to an efflux of K^+ but no membrane depolarization is observed during phage entry (Daugelavicius et al., 1997; Grahn et al., 2002).

Bacteriophage SPP1 binding to *B. subtilis* leads to a rapid (< 1 min) depolarization of the host CM (Fig. III.9B) but only to a slow and weak leakage on intracellular K^+ (Fig. III.9A). SPP1-induced depolarization is significantly faster than the one accompanying infection of *B. subtilis* by tailed phages ϕ29 and SP01 or entry of the membrane-containing phage Bam35 into *B. thuringiensis* (Fig. III.2B; Gaidelyte et al., 2006). In the latter case the CM depolarization and the leakage of intracellular K^+ occur simultaneously starting at 2 min p.i.. SPP1-induced CM depolarization also shows a reduced temperature-dependence compared to the three other phages discussed (Fig. III.2C; Gaidelyte et al., 2006). The sensitivity to temperature can result of the activation energy required to trigger DNA ejection from SPP1 virions (Raspaud et al., 2007), of dependence on an enzymatic process and/or of an effect on the membrane fluidity. Observations of delayed and slow depolarization caused by ϕ29 and SP01 (Fig. III.2C) or Bam35 (Gaidelyte et al., 2006) at 27 °C suggest that there is at least one temperature-dependent step at their initial steps of infection that is less critical in case of SPP1 infection. A possible candidate is digestion of the cell wall following the irreversible binding of phage particles to non-proteinaceous receptors: ϕ29 and SP01 attach to WTA (Yasbin et al., 1976; Young, 1967). While Bam35 binds to *N*-Acetyl-muramic acid (Gaidelyte et al., 2006). SPP1 attaches reversibly to glucosylated WTA (Baptista et al., 2008), but this step does not lead to the CM depolarization (Fig. III.3A). It is the irreversible adsorption of phage particles to YueB, a membrane protein whose ectodomain spans the complete cell wall to expose the SPP1 receptor region (Fig. I.8; São-José et al., 2004, 2006), that is

required to trigger depolarization. Binding of SPP1 directly contacts the CM. On the other hand, the PG layer can have lower rigidity in this region of the cell wall.

The level of *B. subtilis* membrane depolarization increases with the i.m. of phages used for infection *per* bacterium (Fig. III.3B) showing that each phage irreversible adsorption event generates a signal calling for ions flow through the CM. The maximal amplitude of depolarization for the wild type *B. subtilis* strain YB886 was reached at an i.m. of 8 SPP1 virions per bacterium. The CM depolarization observed was only partial, reflecting a limited number of active YueB receptors for SPP1 binding at the bacterial surface (Baptista et al., 2008; Jakutyte et al., 2011; São-José et al., 2004). This conclusion is supported by infection of a strain overproducing YueB that leads to higher amplitudes of TPP^+ efflux which can reach values revealing total depolarization of the CM (Fig. III.3C). The trigger for CM depolarization requires the interaction of intact SPP1 particles with *B. subtilis* (Fig. III.4B) showing that a structural modification in the SPP1 particle, probably the initiation of DNA ejection, is necessary signal for opening of membrane ion channel(s) that lead to CM depolarization. This differs from phage T4 whose virions and particles disrupted by osmotic shock (ghosts) both cause ion effluxes upon interaction with host bacteria (Boulanger and Letellier, 1988; Duckworth and Winkler, 1972; Winkler and Duckworth, 1971).

VI.2. Effect of Ca^{2+} ions in SPP1 infection

Ca^{2+} ions play an essential role at early stages of infection by phages of the SPP1 group (Landry and Zsigray, 1980; Santos et al., 1984; Steensma and Blok, 1979; Figs. III.5, III.19). Here we show that the divalent cation are necessary for phage reversible adsorption to glucosylated WTAs (Fig. III.5D). WTAs together with teichuronic acid are the prime site metal binders in *B. subtilis* accounting for a ratio of Ca^{2+} at the cell wall 100-120-fold higher than in the extracellular medium (Neuhaus

and Baddiley, 2003; Petit-Glatron et al., 1993). The effect of the divalent cation on WTA structure (Neuhaus and Baddiley, 2003) and/or in local surface charge in the cell wall might explain its role on SPP1 reversible binding to the *B. subtilis* envelope. Present data do not allow establishing if Ca^{2+} plays also a role in the subsequent irreversible interaction of SPP1 with YueB that commits the viral particle to infection. Adsorption of SPP1 to *B. subtilis* requires sub-millimolar amounts of Ca^{2+} that are also sufficient for SPP1 particles to trigger CM depolarization (Fig. III.7B). Raising extracellular Ca^{2+} to millimolar levels is essential for effective SPP1 DNA entry in the cytoplasm (Fig. III.19) and thus for normal infection. The amplitude of CM depolarization decreases at this Ca^{2+} concentration, revealing an inhibitory effect on ion fluxes (Figs. III.7 and III.9) that might contribute to maintain homeostasis of the infected *B. subtilis* cell.

This first part of the work established requirements for early steps in SPP1 entry. We have then pursued to understand how the phage exploits the cell envelope architecture for adsorption and viral DNA delivery to the host cytoplasm.

VI.3. Spatio-temporal program of SPP1 entry in *B. subtilis*

Virus binding and entry in the host cell are the critical steps for initiation of infection. These events occur preferentially at or close to the old cell pole of *B. subtilis* during SPP1 infection (Fig. III.11). This topology correlates with the position of viral DNA entry and initiation of replication that occurs in defined foci inside the bacterium (Figs. III.17; III.18).

Reversible adsorption, which targets glucosylated poly(glycerolphosphate) WTA, is independent of the SPP1 protein receptor YueB (Baptista et al., 2008) but occurred also preferentially near the cell poles (Fig. III.11D). This suggested a particular distribution of WTA, or at least of a particular (glucosylated) form of these polymers recognized by SPP1, at the cell surface. Proteins involved in several steps of

WTA synthesis in *B. subtilis* have been reported to localize to division sites and, to a greater or lesser extent, along the lateral sides of the cells in a helix-like pattern but were particularly absent from polar regions (Formstone et al., 2008). As the putative WTA transporter TagGH was virtually absent from old cell poles, it was suggested that the export and hence the incorporation of WTA into the crosswalls occurs during division (septum formation) and is absent after cell separation and formation of the cell poles. This was consistent with the slower turnover of WTA at the cell poles relative to the cell cylinder (Archibald and Coapes, 1976; Clarke-Sturman et al., 1989; Graham and Beveridge, 1994; Kirchner et al., 1988; Mobley et al., 1984). The resulting different properties of cell poles and their highly electronegative character suitable for cation binding (Sonnenfeld et al., 1985) might favour the interaction with SPP1. Alternatively (or simultaneously) if WTA remain at the old poles for several generation times, this might favor the modification (glucosylation) of the WTA favouring SPP1 recognition at these sites.

Reversible binding at the cell pole may then facilitate virus particle search for its receptor YueB, which was found to localize predominantly at the cell poles too (Figs. III.15; III.16). This can be of significant importance because in the absence of glucosylated WTA the time required for SPP1 to recognize and bind YueB increases drastically (Baptista et al., 2008), probably due to the low abundance of this protein in the cell surface (Fig. III.15). Consistently, the kinetic defect can be compensated by overproduction of YueB (Baptista et al., 2008). The ensemble of the data suggests that SPP1 reversible binding to glucosylated WTA at the old poles provides a primary attachment and favourable positioning of SPP1 at the *B. subtilis* surface for rapid interaction with its low abundant receptor YueB.

The localization of endogenous YueB (Fig. III.15A) and of a functional YueB-GFP fusion expressed under control of the native *yueB* promoter as the only copy of YueB in the cell (Fig. III.15B) showed that the receptor concentrates primarily at the old cell pole of wild-type bacteria, although some fluorescence was also detected in

the cell cylinder (Fig. III.15B). Overproduction of YueB confirmed its polar localization and revealed an uneven distribution following a spotted, possibly helix-like, pattern along the cell length (Figs. III.15C; III.16). This organization was found for both the YueB cytoplasmic region fused to GFP and for the receptor region exposed to the cell surface that is accessible to antibody labeling (Fig. III.16). Higher receptor density correlated with a marked increase of phage binding along the sidewalls (Fig. III.13 bottom lane). We hypothesize that the localization along the cell cylinder of the integral membrane protein YueB, whose ectodomain spans across the entire *B. subtilis* cell wall, results from the mechanism of cell wall growth and structure. Indeed, insertion of new peptidoglycan along the sidewalls of in *B. subtilis* has been shown to follow a banded, helical-like pattern (Daniel and Errington, 2003; Tiyanont et al., 2006) and a recent study using atomic force microscopy showed that the sacculus maintains a coiled-coil cabling architecture (Hayhurst et al., 2008). We suggest that the large YueB ectodomain is found within the cell wall polymers and that YueB polar accumulation is facilitated by the low turnover of the polar caps of the bacterium.

YueB might be part of or associate with a putative T7SS machinery whose components are co-encoded by the *yuk* operon (São-José et al., 2004). Presence of YueB-related proteins is one of the features that distinguishes the T7SS of Firmicutes (type VIIb subfamily (Abdallah et al., 2007)). The subcellular localization of YueB in *B. subtilis* cells (Figs. III.15, III.16) and that of one T7SS component in mycobacteria (Carlsson et al., 2009) suggest that this secretion apparatus might be preferentially located at cell poles, like other complex machineries such as the DNA uptake system during transformation (Hahn et al., 2005), components of the Tat secretion system, and chemotaxis proteins complexes (Buist et al., 2006; Meile et al., 2006). The effective presence of a T7SS in *B. subtilis* as well as the physiological role of YueB remain to be elucidated. Since other components of the *yuk* operon are not essential for bacteriophage SPP1 infection (São-José et al., 2004), we conclude that SPP1 uses

the YueB region exposed to the bacterial cell surface for specific docking but that the putative T7SS secretion machinery is not essential for delivery of phage DNA to the bacterial cytoplasm.

We engineered the SPP1 genome with a set of *lacO* repeats to visualize its position in infected *B. subtilis* cells producing LacI-CFP. Interestingly, the phage DNA was found to localize in foci close to the cell poles early in infection (Fig. III.18), which correlated with the preferential polar adsorption of SPP1 (Fig. III.11). The majority of phage DNA foci were not at the tip of the poles but in the pole-cylinder junction region, suggesting that SPP1 might take advantage of particular features of this region of the cell wall for easier penetration towards the bacterial membrane to deliver its genome to the bacterial cytoplasm. A single, well-individualized fluorescent focus was found in individual bacteria infected at low i.m. (Fig. III.18B). The increase of fluorescence of each SPP1 DNA focus over time suggested that genome replication occurs at an intracellular location defined by the position of its entry (Fig. III.17). This might involve an initial association of phage DNA to the membrane for its replication as previously suggested (Burger, 1980). It is interesting to note that plasmid pHP13 replisomes can also cluster in foci located predominantly close to the *B. subtilis* poles (Wang et al., 2004).

In *B. subtilis*, the efficiency of phages SPP1 and ϕ29 genome replication was recently shown to be affected in *mreB* cytoskeleton mutants (Muñoz-Espín et al., 2010). The precise role of MreB in SPP1 replication was not established, and we have shown that its genome replication occurs at a single focus. In contrast, ϕ29 DNA (and components of the ϕ29 replication machinery) localizes in peripheral helix-like structures a topology that depends on MreB leading to the conclusion that this component of the bacterial cytoskeleton organizes phage ϕ29 DNA replication at the membrane (Muñoz-Espín et al., 2009, 2010). ϕ29 uses a terminal protein covalently attached to its linear double-stranded DNA molecule that primes initiation of phage DNA replication (Salas, 2006) whereas phage SPP1 replicates its DNA initially via

the theta mode and later via a rolling circle mode (Alonso et al., 2006). Thus, organization of viral DNA replication by the bacterial MreB cytoskeleton in multiple sites along the periphery of infected cells might be specific to phages using the protein-primed mechanism of DNA replication. In contrast, the replisomes of phages such as SPP1 and λ remain confined to a single replication factory (Edgar et al., 2008; Jakutyte et al., 2011).

Edgar et al. (Edgar et al., 2008) showed that different phages of Gram-negative bacteria adsorb selectively to cell poles and that coliphage λ DNA entry targets a number of cell components at this subcellular localization. The present work reveals that the pole and possibly the pole-cylinder junction are also a preferential target for viral DNA delivery across the Gram-positive envelope. Assembly of a replication focus nearby the polar DNA entry region may spatially constrain the virus genome for optimal functioning of its replication factory.

VI.4. The working model

The work described here defines a sequence of discrete steps necessary for SPP1 passage of the Gram-positive envelope of *B. subtilis* (Fig. IV.2) and spatio-temporal information on the process. SPP1 binding to surface receptors that requires a sub-millimolar concentration of extracellular Ca^{2+} culminates on its irreversible adsorption to YueB (steps 1-2 in Fig. IV.2). This interaction promotes depolarization of the CM. The membrane channel(s) involved in the process is(are) not known. The correlation between the amplitude of depolarization and the concentration of phage-YueB complexes (Fig. III.3) suggests that the channel that opens for ions flux can be (i) formed by the transmembrane segments of YueB (depicted by the conformational switch of YueB between steps 2 and 3 in Fig. IV.2), (ii) a channel associated to YueB that is present in excess amounts relative to YueB (yellow in Fig. IV.2), or (iii) a channel formed by phage or cellular proteins for viral DNA passage (pink channel in

step 3 in Fig. IV.2). The requirement for intact viral particles to trigger depolarization (Fig. III.4) indicates that channel opening/formation depends on a stimulus from the virion bound to YueB. Initiation of the cascade of structural rearrangements leading to DNA ejection from SPP1 particles (depicted by the open interior of the tail from step 3 on in Fig. IV.2) (Raspaud et al., 2007) is the most conceivable possibility. However, achievement of DNA transfer to the cytoplasm is not necessary to cause CM depolarization showing that the two events can be uncoupled at sub-millimolar concentrations of extracellular Ca^{2+} (Figs. III.7 and III.19). The channel's opening is directly or indirectly controlled by the divalent cation. A Ca^{2+}-dependent switch of channel structure is likely at least in the case that ion fluxes leading to depolarization and DNA traffic occur through the same channel. Localized degradation of the ~50 nm-thick cell wall (step 4 in Fig. IV.2) precedes SPP1 DNA delivery to the cytoplasm across a hydrophilic channel formed in the CM either by phage or host protein(s) (step 5). Deletion of YueB carboxyl terminus transmembrane segments still allows for SPP1 infection in semi-solid medium (C.S.-J. and Mário A. Santos, unpublished results) showing that the receptor does not provide the route for SPP1 passage of the CM. Since SPP1 does not infect this strain in liquid medium it was not possible to carry out potentiometric studies to define in CM depolarization results of a membrane channel formed by YueB.

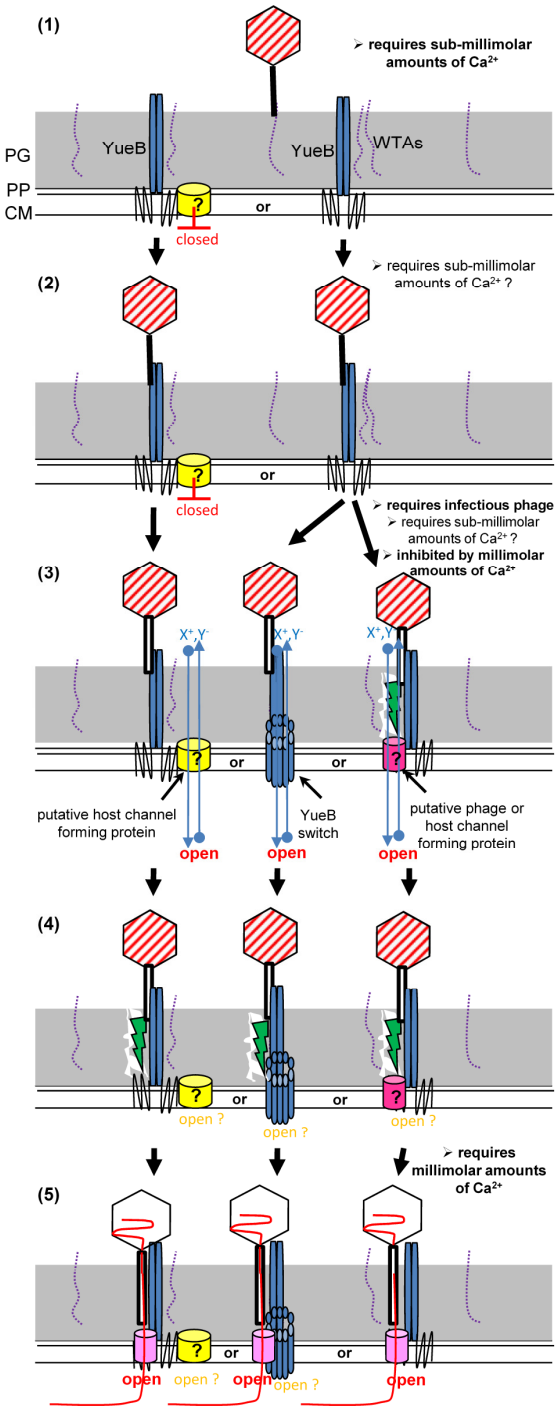

Fig. IV.2. Model for SPP1 entry into the host cell. (1) Reversible adsorption to glucosylated cell wall teichoic acids (WTAs). PG - peptidoglycan layer; PP – periplasm; CM - cytoplasmic membrane. (2) Irreversible adsorption to YueB. (3) Structural modification in the SPP1 phage; generation of signal to trigger CM depolarization. X^+ - positively charged ions; Y^- - negatively charged ions. (4) Cell wall localized degradation. (5) DNA passage through the CM and entry in the cytoplasm. Requirements for Ca^{2+} for each SPP1 entry step are indicated. Details on the ion channels depicted are described in the text.

Virus binding and entry was shown here to occur preferentially at or close to the old cell pole of *B. subtilis* during SPP1 infection (Fig. III.11). Phage SPP1 likely exploits particular features of WTA in this region for preferential adsorption to the bacterium, and uses subsequently the locally enriched surface protein YueB for irreversible binding to the host. This topology correlates with the position of viral DNA entry and initiation of replication that occurs in defined foci inside the bacterium (Figs. III.17; III.18). These findings provide further support to the growing evidence that phages take advantage of the host cell architecture for efficient spatial coordination of the sequential events occurring during infection.

The goal is now set to identify the phage and host effectors acting on these different steps that will provide a framework to understand in molecular detail how SPP1 crosses the Gram-positive cell envelope.

VI.5. Perspectives

The major goal that we proposed was accomplished in this work. We dissected first steps of SPP1 infection, visualized SPP1 binding at the cell surface and DNA entry in real time. The results obtained are anticipated to provide a significant advance of understanding of first steps of phage infection and multiplication *in vivo*. The work is expected also to deliver reagents and relevant novel information for bacterial cell biology.

For the first time we were able to show that a phage of Gram-positive host binds preferentially to the cell poles. The fact that reversible phage binding to the glucosylated WTAs was already directed to the cell poles, shows particular properties of WTAs located in this region. Further experimentation will be required to investigate if *B. subtilis* mutants of the MreB cytoskeleton affect phage distribution on the cell surface, and whether genome entry is also affected spatially and/or kinetically,

as previously was shown that host cytoskeleton elements organizes *B. subtilis* phage ϕ29 DNA replication in bacterial cytoplasm (Muñoz-Espín et al., 2009).

We showed the topology of localization of SPP1 receptor protein YueB on the *B. subtilis* surface, that suggest the localization of T7SS secretion apparatus in rod-shaped Gram-positive bacteria. Our results confirmed that there are limited amounts of YueB protein exposed on the surface of the wild-type *B. subtilis* cells. As, YueB-related proteins are one of the features of T7SS in Firmicutes and their physiological role remain still to be elucidated, we expect that our observations would be useful to the future approaches.

This study has provided us tools to physiologically dissect phage-caused host CM depolarization and viral genome entry, however yet not known, if depolarization of the CM play a physiological role in infection or if it is a side effect. Cell wall hydrolysis is most probably achieved by the bacteriophage tail adsorption apparatus whose enzymatic properties characterization *in vitro* allowing understand the mechanism of phage DNA passage across the cell wall. After leaving the tail, there is a moment in which the DNA of SPP1 is sensitive to external DNAse attack. This dismisses the possibility that a continuous channel is formed between the SPP1 capsid and the bacterial cytoplasm to allow viral DNA entry (Fig. IV.2). Thus, this "moment" of DNAse sensitivity is probably before SPP1 DNA enters the unknown but safe way that leads it into the host cytoplasm. The mechanism can be addressed biochemically by cell fractionation of bacteria infected with phages carrying radioactive proteins to identify labeled phage proteins inserted in the lipid bilayer. A second approach could be the development of a proteoliposome system carrying the YueB receptor, which promotes SPP1 DNA ejection (São-José et al., 2006), to detect also phage protein insertion in the liposome. That would help to reveal and understand the molecular mechanism of tailed bacteriophage genome delivery to the host cell: to define the phage and host factors required for passage of the viral genome through the cell wall and host CM.

The observation that tailed phages assemble viral replication centers loads to the hypothesis that they could leed to assembly of viral assembly factories. Such organization found in eukaryotic viruses requires to characterize the assembly, organization and dynamics of phage DNA multiplication foci (section III.3.3). This organization confines protein synthesis, DNA replication and virus particle assembly to a restricted space optimizing coupling of their associated sequential biochemical reactions. Extensive studies requires to bring together the knowledge of phage and bacteria cell biology. Fluorescence microscopy methods used in this study could be applied to define the composition, architecture and dynamics of the virus multiplication foci throughout virus cycle. Foci can be imaged for the presence of phage components and host proteins identified by a genetic selection approach as being essential for virus multiplication. Foci arrested at specific steps of the virus cycle by drugs or mutation in phage components can provide snapshots of its organization. Time-lapse and photobleaching recovery experiments would deliver information on the dynamics of foci components. Characterization of interactions between host and phage proteins aims to provide additional molecular detail to the resulting model of virus multiplication center.

The detailed understanding of these processes *in vivo* will uncover how such viruses exploit the synergy between their components and host cell machines to assemble infectious particles with remarkable precision and efficiency. These findings provide the growing evidence that phages take advantage of the host cell architecture for efficient spatial coordination of the sequential events occurring during infection. Spatio-temporal program of bacterial virus infection could be the further support to investigate architecture and spatial coordination of the bacterial cells.

REFERENCES

Abdallah, A.M., Gey van Pittius, N.C., Champion, P.A., Cox, J., Luirink, J., Vandenbroucke-Grauls, C.M., Appelmelk, B.J., Bitter, W., 2007. Type VII secretion-mycobacteria show the way. Nat. Rev. Microbiol. 5, 883-891.

Abedon, S.T., 2006. Phage ecology, in: Calendar, R. (Ed.), The Bacteriophages. Oxford University Press, New York, pp. 37-46.

Abedon, S.T., 2009. Phage evolution and ecology. Adv. Appl. Microbiol. 67, 1-45.

Abrescia, N.G., Grimes, J.M., Kivelä, H.M., Assenberg, R., Sutton, G.C., Butcher, S.J., Bamford, J.K., Bamford, D.H., Stuart, D.I., 2008. Insights into virus evolution and membrane biogenesis from the structure of the marine lipid-containing bacteriophage PM2. Mol. Cell. 31, 749-761.

Ackermann, H.W., 1998. Tailed bacteriophages: the order caudovirales. Adv. Virus Res. 51, 135-201.

Ackermann, H.W., 2007. 5500 Phages examined in the electron microscope. Arch. Virol. 152, 227-243.

Ackermann, H.-W., 2009. Phage classification and characterization. Methods Mol. Biol. 501, 127-140.

Adams, M.H., 1959. Bacteriophages. Wiley Interscience, New York.

Aksyuk, A.A., Leiman, P.G., Kurochkina, L.P., Shneider, M.M., Kostyuchenko, V.A., Mesyanzhinov, V.V., Rossmann, M.G., 2009. The tail sheath structure of bacteriophage T4: a molecular machine for infecting bacteria. EMBO J. 28, 821-829.

Alonso, J.C., Lüder, G., Stiege, A.C., Chai, S., Weise, F., Trautner, T.A., 1997. The complete nucleotide sequence and functional organization of *Bacillus subtilis* bacteriophage SPP1. Gene 204, 201-212.

Alonso, J.C., Tavares, P., Lurz, R., Trautner, T.A., 2006. Bacteriophage SPP1, in: Calendar, R. (Ed.), The Bacteriophages, second ed. Oxford University Press, New York, pp. 331-349.

Anderson, D.L., Hickman, D.D., Reilly, B.E., 1966. Structure of *Bacillus subtilis* bacteriophage ϕ29 and the length of ϕ29 deoxyribonucleic acid. J. Bacteriol. 91, 2081-2089.

Archibald, A.R., Coapes, H.E., 1976. Bacteriophage SP50 as a marker for cell wall growth in *Bacillus subtilis*. J. Bacteriol. 125, 1195-1206.

Bamford, D.H., Caldentey, J., Bamford, J.K., 1995. Bacteriophage PRD1: a broad host range DSDNA tectivirus with an internal membrane. Adv. Virus Res. 45, 281-319.

Bamford, D.H., Palva, E.T., Lounatmaa, K., 1976. Ultrastructure and life cycle of the lipid-containing bacteriophage phi 6. J. Gen. Virol. 32, 249-259.

Bamford, D.H., Romantschuk, M., Somerharju, P.J., 1987. Membrane fusion in prokaryotes: bacteriophage phi 6 membrane fuses with the *Pseudomonas syringae* outer membrane. EMBO J. 6, 1467-1473.

Baptista C., 2009. Recognition of *Bacillus subtilis* receptors by bacteriophage SPP1 – a genetic and biochemical approach. Ph.D. thesis. Faculdade de Ciências da Universidade de Lisboa, Lisbon, Portugal.

Baptista, C., Santos, M.A., São-José, C., 2008. Phage SPP1 reversible adsorption to *Bacillus subtilis* cell wall teichoic acids accelerates virus recognition of membrane receptor YueB. J. Bacteriol. 190, 4989-4996.

Barák, I., Muchová, K., Wilkinson, A.J., O'Toole, P.J., Pavlendová, N., 2008. Lipid spirals in *Bacillus subtilis* and their role in cell division. Mol. Microbiol. 68, 1315-1327.

Bartual, S.G., Otero, J.M., Garcia-Doval, C., Llamas-Saiz, A.L., Kahn, R., Fox, G.C., van Raaij, M.J., 2010. Structure of the bacteriophage T4 long tail fiber receptor-binding tip. Proc. Natl. Acad. Sci. U.S.A. 107, 20287-20292.

Baxa, U., Steinbacher, S., Miller, S., Weintraub, A., Huber, R., Seckler, R., 1996. Interactions of phage P22 tails with their cellular receptor, Salmonella O-antigen polysaccharide. Biophys. J. 71, 2040-2048.

Bennett, N.J., Rakonjac, J., 2006. Unlocking of the filamentous bacteriophage virion during infection is mediated by the C domain of pIII. J. Mol. Biol. 356, 266-273.

Benson, A.K., Haldenwang, W.G., 1993. Regulation of sigma B levels and activity in *Bacillus subtilis*. J. Bacteriol. 175, 2347-2356.

Berkane, E., Orlik, F., Stegmeier, J.F., Charbit, A., Winterhalter, M., Benz, R., 2006. Interaction of bacteriophage lambda with its cell surface receptor: an in vitro study of binding of the viral tail protein gpJ to LamB (Maltoporin). Biochemistry. 45, 2708-2720.

Bhavsar, A.P., Erdman, L.K., Schertzer, J.W., Brown, E.D., 2004. Teichoic acid is an essential polymer in *Bacillus subtilis* that is functionally distinct from teichuronic acid. J. Bacteriol. 186, 7865-7873.

Biswal, N., Kleinschmidt, A.K., Spatz, H.C., Trautner, T.A. 1967. Physical properties of the DNA of bacteriophage SP50. Mol. Gen. Genet. 100, 39-55.

Boylan, R.J., Mendelson, N.H., Brooks, D., Young, F.E., 1972. Regulation of the bacterial cell wall: analysis of a mutant of *Bacillus subtilis* defective in biosynthesis of teichoic acid. J. Bacteriol. 110, 281-290.

Bönemann, G., Pietrosiuk, A., Mogk, A., 2010. Tubules and donuts: a type VI secretion story. Mol. Microbiol. 76, 815-821.

Bonhivers, M., Letellier, L., 1995. Calcium controls phage T5 infection at the level of the *Escherichia coli* cytoplasmic membrane. FEBS Lett. 374, 169-173.

Boulanger, P., Jacquot, P., Plançon, L., Chami, M., Engel, A., Parquet, C., Herbeuval, C., Letellier, L., 2008. Phage T5 straight tail fiber is a multifunctional protein acting as a tape measure and carrying fusogenic and muralytic activities. J. Biol. Chem. 283, 13556-13564.

Boulanger, P., Letellier, L., 1988. Characterization of ion channels involved in the penetration of phage T4 DNA into *Escherichia coli* cells. J. Biol. Chem. 263, 9767-9775.

Boulanger, P., Letellier, L., 1992. Ion channels are likely to be involved in the two steps of phage T5 DNA penetration into *Escherichia coli* cells. J. Biol. Chem. 267, 3168-3172.

Braun, V., Sieglin, U., 1970. The covalent murein-lipoprotein structure of the *Escherichia coli* cell wall. The attachment site of the lipoprotein on the murein. Eur. J. Biochem. 13, 336-346.

Brøndsted, L., Hammer, K., 2006. Phages of *Lactococcus lactis*, in: Calendar, R. (Ed.), The Bacteriophages. Oxford University Press, New York, pp. 572-592.

Brown, D.T., MacKenzie, J.M., Bayer, M.E., 1971. Mode of host cell penetration by bacteriophage phi X174. J. Virol. 7, 836-846.

Brüssow H., 2001. Phages of dairy bacteria. Ann. Rev. Microbiol. 55, 283-303.

Buist, G., Ridder, A.N., Kok, J., Kulpers, O.P., 2006. Different subcellular locations of secretome components of Gram-positive bacteria. Microbiology 152, 2867-2874.

Burger, K.J., 1980. Membrane binding of bacteriophage SPP1 DNA. Mol. Gen. Genet. 179, 373-376.

Cabeen, M.T., Jacobs-Wagner, C., 2010. The bacterial cytoskeleton. Annu. Rev. Genet. 44, 365-392.

Caldentey, J., Bamford, D.H., 1992. The lytic enzyme of the *Pseudomonas* phage phi 6. Purification and biochemical characterization. Biochim. Biophys. Acta. 1159, 44-50.

Calendar, R. (Ed.), 2006. The Bacteriophages. Oxford University Press, New York.

Callanan, M.J., Klaenhammer, T.R., 2008. Bacteriophages in industry, in: Encyclopedia of life sciences. John Wiley & Sons, Ltd: Chichester.

Carballido-López, R., 2006. The bacterial actin-like cytoskeleton. Microbiol. Mol. Biol. Rev. 70, 888-909.

Carballido-López, R., Errington, J., 2003. A dynamic bacterial cytoskeleton. Trends Cell Biol. 13, 577-583.

Carlsson, F., Joshi, S.A., Rangell, L., Brown, E.J., 2009. Polar localization of virulence-related Esx-1 secretion in mycobacteria. PLoS Pathog. 5, e1000285.

Casjens, S., Hendrix, R., 1988. Control mechanisms in dsDNA bacteriophage assembly, in: Calendar, R. (Ed.), The Bacteriophages, vol. 1. Plenum Press, New York, pp. 15-91.

Catalano, C.E., (Ed.), 2005. Viral Genome Packaging Machines: Genetics, Structure, and Mechanism. Landes Bioscience/Eurekah, Georgetown, TX; Kluwer Academic/Plenum Publishers, New York.

Chagot, B., Auzat, I., Gallopin, M., Petitpas, I., Gilquin, B., Tavares, P., Zinn-Justin, S., 2011. Solution structure of gp17 from the *Siphoviridae* bacteriophage SPP1: insights into its role in virion assembly. Proteins. DOI: 10.1002/prot.23191.

Chai, S., Szepan, U., Lüder, G., Trautner, T.A., Alonso, J.C., 1993. Sequence analysis of the left end of the *Bacillus subtilis* bacteriophage SPP1 genome. Gene 129, 41-49.

Chang, C.Y., Kemp, P., Molineux, I.J., 2010. Gp15 and gp16 cooperate in translocating bacteriophage T7 DNA into the infected cell. Virology. 398, 176-186.

Chen, C., Guo, P., 1997. Magnesium-induced conformational change of packaging RNA for procapsid recognition and binding during phage phi29 DNA encapsidation. J. Virol. 71, 495-500.

Clarke-Sturman, A.J., Archibald, A.R., Hancock, I.C., Harwood, C.R., Merad, T., Hobot, J.A., 1989. Cell wall assembly in *Bacillus subtilis*: partial conservation of polar wall material and the effect of growth conditions on the pattern of incorporation of new material at the polar caps. J. Gen. Microbiol. 135, 657-665.

Click, E.M., Webster, R.E., 1997. Filamentous phage infection: required interactions with the TolA protein. J. Bacteriol. 179, 6464-6471.

Click, E.M., Webster, R.E., 1998. The TolQRA proteins are required for membrane insertion of the major capsid protein of the filamentous phage f1 during infection. J. Bacteriol. 180, 1723-1728.

Cohen, D.N., Sham, Y.Y., Haugstad, G.D., Xiang, Y., Rossmann, M.G., Anderson, D.L., Popham, D.L., 2009. Shared catalysis in virus entry and bacterial cell wall depolymerization. J. Mol. Biol. 387, 607-618.

Cvirkaite-Krupovic, V., Krupovic, M., Daugelavicius, R., Bamford, D.H., 2010b. Calcium ion-dependent entry of the membrane-containing bacteriophage PM2 into its *Pseudoalteromonas* host. Virology. 405, 120-128.

Cvirkaite-Krupovic, V., Poranen, M.M., Bamford, D.H., 2010a. Phospholipids act as secondary receptor during the entry of the enveloped, double-stranded RNA bacteriophage phi6. J. Gen. Virol. 91, 2116-2120.

d'Hérelle, F., 1917. Sur un microbe invisible antagoniste des bacilles dysentériques. C.R. Acad. Sci. 165, 373-375.

Daniel, R.A., Errington, J., 2003. Control of cell morphogenesis in bacteria: two distinct ways to make a rod-shaped cell. Cell. 113, 767-776.

Date, T., 1979. Kinetic studies of the interaction between MS2 phage and F pilus of *Escherichia coli*. Eur. J. Biochem. 96, 167-175.

Daugelavicius, R., Bamford, J.K., Bamford, D.H., 1997. Changes in host cell energetics in response to bacteriophage PRD1 DNA entry. J. Bacteriol. 179, 5203-5210.

Davison, S., Couture-Tosi, E., Candela, T., Mock, M., Fouet, A., 2005. Identification of the *Bacillus anthracis* (gamma) phage receptor. J. Bacteriol. 187, 6742-6749.

Delcour, J., Ferain, T., Deghorain, M., Palumbo, E., Hols, P., 1999. The biosynthesis and functionality of the cell-wall of lactic acid bacteria. Antonie Van Leeuwenhoek. 76, 159-184.

Demchick, P., Koch, A.L., 1996. The permeability of the wall fabric of *Escherichia coli* and *Bacillus subtilis*. J. Bacteriol. 178, 768-773.

Di Masi, D.R., White, J.C., Schnaitman, C.A., Bradbeer, C., 1973. Transport of vitamin B12 in *Escherichia coli*: common receptor sites for vitamin B12 and the E colicins on the outer membrane of the cell envelope. J. Bacteriol. 115, 506-513.

Dijkstra, A.J., Keck, W., 1996. Peptidoglycan as a barrier to transenvelope transport. J. Bacteriol. 178, 5555-5562.

Domingo, E., Holland, J.J., 1994. Mutation rates and rapid elolution of RNA viruses, in: Morse, S.S. (Ed.), The evolutionary biology of viruses. Raven Press, Ltd., New York, pp. 161-184.

Dramsi, S., Magnet, S., Davison, S., Arthur, M., 2008. Covalent attachment of proteins to peptidoglycan. FEMS Microbiol. Rev. 32, 307-320.

Dreiseikelmann, B., 1994. Translocation of DNA across bacterial membranes. Microbiol. Rev. 58, 293-316.

Dröge, A., Tavares, P., 2000. *In Vitro* packaging of DNA of the *Bacillus subtilis* bacteriophage SPP1. J. Mol. Biol. 296, 103-115.

Duckworth, D.H., Winkler, H.H., 1972. Metabolism of T4 bacteriophage ghost-infected cells. II. Do ghosts cause a generalized permeability change? J. Virol. 9, 917-922.

Earnshaw, W.C., Casjens, S.R., 1980. DNA packaging by the double-stranded DNA bacteriophages. Cell. 21, 319-331.

Edgar, R., Rokney, A., Feeney, M., Semsey, S., Kessel, M., Goldberg, M.B., Adhya, S., Oppenheim, A.B., 2008. Bacteriophage infection is targeted to cellular poles. Mol. Microbiol. 68, 1107-1116.

Epand, R.M., Epand, R.F., 2009. Lipid domains in bacterial membranes and the action of antimicrobial agents. Biochim. Biophys. Acta. 1788, 289-294.

Esche, H., 1975. Gene expression of bacteriophage SPP1. II. Regulatory aspects. Mol. Gen. Genet. 142, 57-66.

Esche, H., Schweiger, M., Trautner, T.A., 1975. Gene expression of bacteriophage SPPI. I. Phage directed protein synthesis. Mol. Gen. Genet. 142, 45-55.

Esquinas-Rychen, M., Erni, B., 2001. Facilitation of bacteriophage lambda DNA injection by inner membrane proteins of the bacterial phosphoenol-pyruvate: carbohydrate phosphotransferase system (PTS). J. Mol. Microbiol. Biotechnol. 3, 361-370.

Estrela, A.I., Pooley, H.M., de Lencastre, H., Karamata, D., 1991. Genetic and biochemical characterization of Bacillus subtilis 168 mutants specifically blocked in the synthesis of the teichoic acid poly(3-O-beta-D-glucopyranosyl-N-acetylgalactosamine 1-phosphate): gneA, a new locus, is associated with UDP-N-acetylglucosamine 4-epimerase activity. J. Gen. Microbiol. 137, 943-950.

Evilevitch, A., Lavelle, L., Knobler, C.M., Raspaud, E., Gelbart, W.M., 2003. Osmotic pressure inhibition of DNA ejection from phage. Proc. Natl. Acad. Sci. U.S.A. 100, 9292-9295.

Fauquet, M., Mayo, M.A., Maniloff, J., Desselberger, U., Ball, L.A., 2005. Virus Taxonomy: VIIIth report of the International Committee on Taxonomy of Viruses. Elsevier Academic Press, San Diego, CA; London, UK.

Feige, U., Stirm, S., 1976. On the structure of the Escherichia coli C cell wall lipopolysaccharide core and on its phiX174 receptor region. Biochem. Biophys. Res. Commun. 71, 566-573.

Finean, J.B., Coleman, R., Michell, R.H., 1984. Membranes and their cellular functions. Blackwell, Oxford.

Fyfe, P.K., McAuley, K.E., Roszak, A.W., Isaacs, N.W., Cogdell, R.J., Jones, M.R., 2001. Probing the interface between membrane proteins and membrane lipids by X-ray crystallography. Trends Biochem. Sci. 26, 106-112.

Formstone, A., Carballido-López, R., Noirot, P., Errington, J., Scheffers, D.-J., 2008. Localization and interactions of teichoic acid synthetic enzymes in Bacillus subtilis. J. Bacteriol. 190, 1812-1821.

Foster, S.J., Popham, D.L., 2002. Structure and synthesis of cell wall, spore cortex, teichoic acids, S-layers, and capsules, in: Sonenshein, A.L., Hoch, J.A., Losick, R. (Eds.), Bacillus subtilis and its closest relatives from genes to cells. ASM Press, Washington, pp. 21-41.

Gaidelyte, A., Cvirkaite-Krupovic, V., Daugelavicius, R., Bamford, J.K., Bamford, D.H., 2006. The entry mechanism of membrane-containing phage Bam35 infecting Bacillus thuringiensis. J. Bacteriol. 188, 5925-5934.

Gaidelyte, A., Jaatinen, S.T., Daugelavicius, R., Bamford, J.K., Bamford, D.H., 2005. The linear double-stranded DNA of phage Bam35 enters lysogenic host cells, but the late phage functions are suppressed. J. Bacteriol. 187, 3521-3527.

Gan, L., Chen, S., Jensen, G.J., 2008. Molecular organization of Gram-negative peptidoglycan. Proc. Natl. Acad. Sci. U.S.A. 105, 18953-18957.

García, L.R., Molineux, I.J., 1995. Rate of translocation of bacteriophage T7 DNA across the membranes of Escherichia coli. J. Bacteriol. 177, 4066-4076.

García, L.R., Molineux, I.J., 1996. Transcription-independent DNA translocation of bacteriophage T7 DNA into Escherichia coli. J. Bacteriol. 178, 6921-6929.

Geller, B.L., Ivey, R.G., Trempy, J.E., Hettinger-Smith B., 1993. Cloning of a chromosomal gene required for phage infection of Lactococcus lactis subsp. lactis C2. J. Bacteriol. 175, 5510-5519.

Geller, B.L., Ngo, H.T., Mooney, D.T., Su, P., Dunn, N., 2005. Lactococcal 936-species phage attachment to surface of Lactococcus lactis. J. Dairy Sci. 88, 900-907.

German, G.J., Misra, R., 2001. The TolC protein of Escherichia coli serves as a cell-surface receptor for the newly characterized TLS bacteriophage. J. Mol. Biol. 308, 579-585.

González-Huici, V., Salas, M., Hermoso, J.M., 2004. The push-pull mechanism of bacteriophage ϕ29 DNA injection. Mol. Microbiol. 52, 529-540.

Goulet, A., Lai-Kee-Him, J., Veesler, D., Auzat, I., Robin, G., Shepherd, D.A., Ashcroft, A.E., Richard, E., Lichière, J., Tavares, P., Cambillau, C., Bron, P., 2011. The opening of the SPP1 bacteriophage tail, a prevalent mechanism in Gram-positive-infecting siphophages. J. Biol. Chem. 286, 25397-25405.

Graham, L.L., Beveridge, T.J., 1994. Structural differentiation of the Bacillus subtilis 168 cell wall. J. Bacteriol. 176, 1413-1421.

Grahn, A.M., Daugelavicius, R., Bamford, D.H., 2002. Sequential model of phage PRD1 DNA delivery: active involvement of the viral membrane. Mol. Microbiol. 46, 1199-1209.

Grayson, P., Evilevitch, A., Inamdar, M.M., Purohit, P.K., Gelbart, W.M., Knobler, C.M., Phillips, R., 2006. The effect of genome length on ejection forces in bacteriophage lambda. Virology. 348, 430-436.

Grayson, P., Molineux, I.J., 2007. Is phage DNA 'injected' into cells-biologists and physicists can agree. Curr. Opin. Microbiol. 10, 401-409.

Grinius, L., 1980. Nucleic acid transport driven by ion gradient across cell membrane. FEBS Lett. 113, 1-10.

Grinius, L., Daugelavicius, R., 1988. Depolarization of Escherichia coli cytoplasmic membrane by bacteriophages T4 and lambda: evidence for induction of ion-permeable channels. Bioelectrochem Bioenerg. 19, 235-245.

Grinius, L.L., Daugelavicius, R., Alkimavicius, G.A., 1980. Study of membrane potential of Bacillus subtilis and Escherichia coli cells by the penetration ions methods. Biokhimiia. 45, 1609-1618.

Guo, S., Shu, D., Simon, M.N., Guo, P., 2003. Gene cloning, purification, and stoichiometry quantification of phi29 anti-receptor gp12 with potential use as special ligand for gene delivery. Gene. 315, 145-152.

Guttman, B., Raya, R., Kutter, E., 2005. Basic phage biology, in: Kutter, E., Sulakvelidze, A. (Eds.), Bacteriophages biology and application. CRC Press, Boca Raton, FL, pp. 29-66.

Hahn, J., Maier, B., Haijema, B.J., Sheetz, M., Dubnau, D., 2005. Transformation proteins and DNA uptake localize to the cell poles in Bacillus subtilis. Cell 122, 59-71.

Hayashi, S., Wu, H.C., 1983. Biosynthesis of Bacillus licheniformis penicillinase in Escherichia coli and in Bacillus subtilis. J. Bacteriol. 156, 773-777.

Hayhurst, E.J., Kailas, L., Hobbs, J.K. Foster, S.J., 2008. Cell wall peptidoglycan architecture in Bacillus subtilis. Proc. Natl. Acad. Sci. U.S.A. 105, 14603-14608.

Heller, K., Braun, V., 1982. Polymannose O-antigens of Escherichia coli, the binding sites for the reversible adsorption of bacteriophage T5+ via the L-shaped tail fibers. J. Virol. 41, 222-227.

Heller, K.J., 1992. Molecular interaction between bacteriophage and the gram-negative cell envelope. Arch. Microbiol. 158, 235-248.

Heller, K.J., Schwarz, H., 1985. Irreversible binding to the receptor of bacteriophages T5 and BF23 does not occur with the tip of the tail. J. Bacteriol. 162, 621-625.

Hendrix, R.W., Smith, M.C.M., Burns, R.N., Ford, M.E. Hatfull, G.F., 1999. Evolutionary relationships among diverse bacteriophages and prophages: All the world‘s a phage. Proc. Natl. Acad. Sci. U.S.A. 96, 2192-2197.

Hershey, A.D., Chase, M., 1952. Independent functions of viral protein and nucleic acid in growth of bacteriophage. J. Gen. Physiol. 36, 39-56.

Ho, T.D., Slauch, J.M., 2001. OmpC is the receptor for Gifsy-1 and Gifsy-2 bacteriophages of Salmonella. J. Bacteriol. 183, 1495-1498.

Hoch, J.A., Spizizen, J., 1969. Genetic control of some early events in sporulation of Bacillus subtilis 168, in: Campbell, L.L. (Ed.), Spores IV. American Society for Microbiology, Bethesda, pp. 112-120.

Hoffmann, C., Leis, A., Niederweis, M., Plitzko, J.M., Engelhardt, H., 2008. Disclosure of the mycobacterial outer membrane: cryo-electron tomography and vitreous sections reveal the lipid bilayer structure. Proc. Natl. Acad. Sci. U.S.A. 105, 3963-3967.

Höltje, J.V., 1998. Growth of the stress-bearing and shape-maintaining murein sacculus of Escherichia coli. Microbiol. Mol. Biol. Rev. 62, 181-203.

Hood, R.D., Singh, P., Hsu, F., Güvener, T., Carl, M.A., Trinidad, R.R., Silverman, J.M., Ohlson, B.B., Hicks, K.G., Plemel, R.L., Li, M., Schwarz, S., Wang, W.Y., Merz, A.J., Goodlett, D.R., Mougous, J.D., 2010. A type VI secretion system of Pseudomonas aeruginosa targets a toxin to bacteria. Cell Host Microbe. 7, 25-37.

Jacobson, A., 1972. Role of F pili in the penetration of bacteriophage fl. J. Virol. 10, 835-843.

Jacobson, E.D., Landman, O.E., 1977. Adsorption of bacteriophages phi 29 and 22a to protoplasts of Bacillus subtilis 168. J. Virol. 21, 1223-1227.

Jakutyte, L., Baptista, C., São-José, C., Daugelavicius, R., Carballido-López, R., Tavares, P., 2011. Bacteriophage infection in rod-shaped gram-positive bacteria: evidence for a preferential polar route for phage SPP1 entry in Bacillus subtilis. J. Bacteriol. 193, 4893-4903.

Jazwinski, S.M., Lindberg, A.A., Kornberg, A., 1975. The gene H spike protein of bacteriophages phiX174 and S13. I. Functions in phage-receptor recognition and in transfection. Virology. 66, 283-293.

Jordan, S., Hutchings, M.I., Mascher, T., 2008. Cell envelope stress response in Gram-positive bacteria. FEMS Microbiol. Rev. 32, 107-146.

Kalasauskaite, E.V., Kadisaite, D.L., Daugelavicius, R.J., Grinius, L.L., Jasaitis, A.A., 1983. Studies on energy supply for genetic processes. Requirement for membrane potential in Escherichia coli infection by phage T4. Eur. J. Biochem. 130, 123-130.

Kamp, D., Kahmann, R., Zipser, D., Broker, T.R., Chow, L.T., 1978. Inversion of the G DNA segment of phage Mu controls phage infectivity. Nature. 271, 577-580.

Kanamaru, S., Leiman, P.G., Kostyuchenko, V.A., Chipman, P.R., Mesyanzhinov, V.V., Arisaka, F., Rossmann, M.G., 2002. Structure of the cell-puncturing device of bacteriophage T4. Nature. 415, 553-557.

Kao, S.H., McClain, W.H., 1980. Baseplate protein of bacteriophage T4 with both structural and lytic functions. J. Virol. 34, 95-103.

Kawaura, T., Inagaki, M., Karita, S., Kato, M., Nishikawa, S., Kashimura, N., 2000. Recognition of receptor lipopolysaccharides by spike G protein of bacteriophage phiX174. Biosci. Biotechnol. Biochem. 64, 1993-1997.

Kirchner, G., Kemper, M.A., Koch, A.L., Doyle, R.J., 1988. Zonal turnover of cell poles of Bacillus subtilis. Ann. Inst. Pasteur Microbiol. 139, 645-654.

Kivelä, H.M., Daugelavicius, R., Hankkio, R.H., Bamford, J.K., Bamford, D.H., 2004. Penetration of membrane-containing double-stranded-DNA bacteriophage PM2 into Pseudoalteromonas hosts. J. Bacteriol. 186, 5342-5354.

Kivelä, H.M., Madonna, S., Krupovic, M., Tutino, M.L., Bamford, J.K., 2008. Genetics for Pseudoalteromonas provides tools to manipulate marine bacterial virus PM2. J. Bacteriol. 190, 1298-1307.

Klemm, P., Krogfelt, K.A., 1994, in: Klemm (Ed.), Fimbriae, Adhesion, Genetics, Biogenesis and Vaccines. CRC Press, Inc., Boca Raton, pp. 9-26.

Koonin, E.V., Rudd, K.E., 1994. A conserved domain in putative bacterial and bacteriophage transglycosylases. Trends Biochem. Sci. 19, 106-107.

Krupovic, M., Bamford, D.H., 2010. Order to the viral universe. J. Virol. 84, 12476-12479.

Kutter, E., Sulakvelidze, A., 2005. Bacteriophages: biology and application. CRC Press, Boca Raton, FL.

Labedan, B., Goldberg, E.B., 1979. Requirement for membrane potential in injection of phage T4 DNA. Proc. Natl. Acad. Sci. U.S.A. 76, 4669-4673.

Labedan, B., Letellier, L., 1981. Membrane potential changes during the first steps of coliphage infection. Proc. Natl. Acad. Sci. U.S.A. 78, 215-219.

Laemmli, U.K., 1970. Cleavage of structural proteins during the assembly of the head of bacteriophage T4. Nature. 227, 680-685.

Landry, E.F., Zsigray, R.M., 1980. Effects of calcium on the lytic cycle of Bacillus subtilis phage 41c. J. Gen. Virol. 51, 125-135.

Lau, I.F., Filipe, S.R., Søballe, B., Økstad, O.-A., Barre, F.-X., Sherratt, D.J., 2003. Spatial and temporal organization of replicating Escherichia coli chromosomes. Mol. Microbiol. 49, 731-743.

Laurinmäki, P.A., Huiskonen, J.T., Bamford, D.H., Butcher, S.J., 2005. Membrane proteins modulate the bilayer curvature in the bacterial virus Bam35. Structure. 13, 1819-1828.

Lehnherr, H., Hansen, A.M., Ilyina, T., 1998. Penetration of the bacterial cell wall: a family of lytic transglycosylases in bacteriophages and conjugative plasmids. Mol. Microbiol. 30, 454-457.

Leiman, P.G., Basler, M., Ramagopal, U.A., Bonanno, J.B., Sauder, J.M., Pukatzki, S., Burley, S.K., Almo, S.C., Mekalanos, J.J., 2009. Type VI secretion apparatus and phage tail-associated protein complexes share a common evolutionary origin. Proc. Natl. Acad. Sci. U.S.A. 106, 4154-4159.

Leiman, P.G., Kanamaru, S., Mesyanzhinov, V.V., Arisaka, F., Rossmann, M.G., 2003. Structure and morphogenesis of bacteriophage T4. Cell. Mol. Life Sci. 60, 2356-2370.

Lemon, K.P., Grossman, A.D., 1998. Localization of bacterial DNA polymerase: evidence for a factory model of replication. Science. 282, 1516-1519.

Lemon, K.P., Grossman, A.D., 2000. Movement of replicating DNA through a stationary replisome. Mol. Cell 6, 1321-1330.

Letellier, L., Boulanger, P., Plançon, L., Jacquot, P., Santamaria, M., 2004. Main features on tailed phage, host recognition and DNA uptake. Front. Biosci. 9, 1228-1339.

Letellier, L., Labedan, B., 1984. Involvement of envelope-bound calcium in the transient depolarization of the Escherichia coli cytoplasmic membrane induced by bacteriophage T4 and T5 adsorption. J. Bacteriol. 157, 789-794.

Letellier, L., Plançon, L., Bonhivers, M., Boulanger, P., 1999. Phage DNA transport across membranes. Res. Microbiol. 150, 499-505.

Lhuillier, S., Gallopin, M., Gilquin, B., Brasilès, S., Lancelot, N., Letellier, G., Gilles, M., Dethan, G., Orlova, E.V., Couprie, J., Tavares, P., Zinn-Justin, S., 2009. Structure of bacteriophage SPP1 head-to-tail connection reveals mechanism for viral DNA gating. Proc. Natl. Acad. Sci. U.S.A. 106, 8507-8512.

Lindberg, A.A., 1973. Bacteriophage receptors. Annu. Rev. Microbiol. 27, 205-241.

Liu, X., Zhang, Q., Murata, K., Baker, M.L., Sullivan, M.B., Fu, C., Dougherty, M.T., Schmid, M.F., Osburne, M.S., Chisholm, S.W., Chiu, W., 2010. Structural changes in a marine podovirus associated with release of its genome into Prochlorococcus. Nat. Struct. Mol. Biol. 17, 830-836.

Lorenz, S.H., Schmid, F.X., 2011. Reprogramming the infection mechanism of a filamentous phage. Mol. Microbiol. 80, 827-834.

Lubkowski, J., Hennecke, F., Plückthun, A., Wlodawer, A., 1998. The structural basis of phage display elucidated by the crystal structure of the N-terminal domains of g3p. Nat. Struct. Biol. 5, 140-147.

Lurz, R., Orlova, E.V., Günther, D., Dube, P., Dröge, A., Weise, F., van Heel, M., Tavares, P., 2001. Structural organisation of the head-to-tail interface of a bacterial virus. J. Mol. Biol. 310, 1027-1037.

Madigan, M.T., Martinko, J.M., Parker, J., 1997. Brock Biology of Microorganisms. Prentice-Hall, Upper Saddle River, NJ.

Manchak, J., Anthony, K.G., Frost, L.S., 2002. Mutational analysis of F-pilin reveals domains for pilus assembly, phage infection and DNA transfer. Mol. Microbiol. 43, 195-205.

Maniloff, J., Dybvig, K., 2006. Mycoplasma phages, in: Calendar, R. (Ed.), The Bacteriophages, second. ed. Oxford University Press, New York, pp. 636-652.

Mattick, J.S., 2002. Type IV pili and twitching motility. Annu. Rev. Microbiol. 56, 289-314.

Meile, J.-C., Wu, L.J., Ehrlich, S.D., Errington, J., Noirot, P., 2006. Systematic localization of proteins fused to the green fluorescent protein in Bacillus subtilis: identification of new proteins at the DNA replication factory. Proteomics 6, 2135-2146.

Milanesi, G., Cassani, G., 1972. Transcription after bacteriophage SPP1 infection in Bacillus subtilis. J. Virol. 10, 187-192.

Mindich, L., Bamford, D., McGraw, T., Mackenzie, G., 1982. Assembly of bacteriophage PRD1: particle formation with wild-type and mutant viruses. J. Virol. 44, 1021-1030.

Mindich, L., Lehman, J., 1979. Cell wall lysin as a component of the bacteriophage phi 6 virion. J. Virol. 30, 489-496.

Minnikin, D.E., 1982. Lipids: Complex lipids, their chemistry, biosynthesis and roles, in: Ratledge, C., Stanford, J. (Eds.), The biology of the mycobacteria, vol 1. Physiology, identification and classification. Academic Press, Inc., New York, pp. 95-184.

Missich, R., Weise, F., Chai, S., Lurz, R., Pedré, X., Alonso, J.C., 1997. The replisome organizer (G38P) of Bacillus subtilis bacteriophage SPP1 forms specialized nucleoprotein complexes with two discrete distant regions of the SPP1 genome. J. Mol. Biol. 270, 50-64.

Miyadai, H., Tanaka-Masuda, K., Matsuyama, S., Tokuda, H., 2004. Effects of lipoprotein overproduction on the induction of DegP (HtrA) involved in quality control in the Escherichia coli periplasm. J. Biol. Chem. 279, 39807-39813.

Moak, M., Molineux, I.J., 2000. Role of the Gp16 lytic transglycosylase motif in bacteriophage T7 virions at the initiation of infection. Mol. Microbiol. 37, 345-355.

Moak, M., Molineux, I.J., 2004. Peptidoglycan hydrolytic activities associated with bacteriophage virions. Mol. Microbiol. 51, 1169-1183.

Mobley, H.L.T., Koch, A.L., Doyle, R.J., Streips, U.N., 1984. Insertion and fate of the cell wall in Bacillus subtilis. J. Bacteriol. 158, 169-179.

Molineux, I.J., 2001. No syringes please, ejection of phage T7 DNA from the virion is enzyme driven. Mol. Microbiol. 40, 1-8.

Molineux, I.J., 2006. Fifty-three years since Hershey and Chase; much ado about pressure but which pressure is it? Virology. 344, 221-229.

Monteville, M.R., Ardestani, B., Geller, B.L., 1994. Lactococcal bacteriophages require a host cell wall carbohydrate and a plasma membrane protein for adsorption and ejection of DNA. Appl. Environ. Microbiol. 60, 3204-3211.

Moody, M.F., 1973. Sheath of bacteriophage T4. 3. Contraction mechanism deduced from partially contracted sheaths. J. Mol. Biol. 80, 613-635.

Morona, R., Krämer, C., Henning, U., 1985. Bacteriophage receptor area of outer membrane protein OmpA of Escherichia coli K-12. J. Bacteriol. 164, 539-543.

Mosig, G., Eiserling, F., 2006. T4 and related phages: structure and development, in: Calendar, R. (Ed.), The Bacteriophages. Oxford Press, New York, pp. 225-267.

Muñoz-Espín, D., Daniel, R., Kawai, Y., Carballido-López, R., Castilla-Llorente, V., Errington, J., Meijer, W.J.J., Salas, M., 2009. The actin-like MreB cytoskeleton organizes viral DNA replication in bacteria. Proc. Natl. Acad. Sci. U.S.A. 106, 13347-13352.

Muñoz-Espín, D., Holguera, I., Ballesteros-Plaza, D., Carballido-López, R., Salas, M., 2010. Viral terminal protein directs early organization of phage DNA replication at the bacterial nucleoid. Proc. Natl. Acad. Sci. U.S.A. 107, 16548-16553.

Nakagawa, H., Arisaka, F., Ishii, S., 1985. Isolation and characterization of the bacteriophage T4 tail-associated lysozyme. J. Virol. 54, 460-466.

Neuhaus, F.C., Baddiley, J., 2003. A continuum of anionic charge: structures and functions of D-alanyl-teichoic acids in gram-positive bacteria. Microbiol. Mol. Biol. Rev. 67, 686-723.

Nicholls, D., Ferguson, S., 2002. Bioenergetics 3, third ed. Academic Press, London.

Nikaido, H., 1996. Outer membrane, in: Neidhardt, F., Curtiss III, R., Lin, E.C.C. et al. (Eds.), Escherichia coli and Salmonella: cellular and molecular biology, vol. 2, second ed. ASM Press, Washington, pp. 29-47.

Nikaido, H., 2003. Molecular basis of bacterial outer membrane permeability revisited. Microbiol. Mol. Biol. Rev. 67, 593-656.

Ogden, R.C., Adams, D.A., 1987. Electrophoresis in agarose and acrylamide gels. Meth. Enzymol. 152, 61-87.

Okubo, S., Strauss, B., Stodolsky, M., 1964. The possible role of recombination in the infection of competent Bacillus subtilis by bacteriophage deoxyribonucleic acid. Virology. 24, 552-562.

Olsén, A., Jonsson, A., Normark, S., 1989. Fibronectin binding mediated by a novel class of surface organelles on Escherichia coli. Nature. 338, 652-655.

Olsen, R.H., Siak, J.S., Gray, R.H., 1974. Characteristics of PRD1, a plasmid-dependent broad host range DNA bacteriophage. J. Virol. 14, 689-699.

Ore, A., Pollard, E., 1956. Physical mechanism of bacteriophage injection. Science. 124, 430-432.

Orlova, E.V., Gowen, B., Dröge, A., Stiege, A., Weise, F., Lurz, R., van Heel, M., Tavares, P., 2003. Structure of a viral DNA gatekeeper at 10 A resolution by cryo-electron microscopy. EMBO J. 22, 1255-1262.

Osborn, M.J., Rosen, S.M., Rothfield, L., Zeleznick, L.D., Horecker, B.L., 1964. Lipopolysaccharide or the Gram-negative cell wall. Science. 145, 783-789.

Panja, D., Molineux, I.J., 2010. Dynamics of bacteriophage genome ejection in vitro and in vivo. Phys. Biol. 7, 045006.

Pell, L.G., Kanelis, V., Donaldson, L.W., Howell, P.L., Davidson, A.R., 2009. The phage lambda major tail protein structure reveals a common evolution for long-tailed phages and the type VI bacterial secretion system. Proc. Natl. Acad. Sci. U.S.A. 106, 4160-4165.

Petit-Glatron, M.F., Grajcar, L., Munz, A., Chambert, R., 1993. The contribution of the cell wall to a transmembrane calcium gradient could play a key role in Bacillus subtilis protein secretion. Mol. Microbiol. 9, 1097-1106.

Plançon, L., Chami, M., Letellier, L., 1997. Reconstitution of FhuA, an Escherichia coli outer membrane protein, into liposomes. Binding of phage T5 to Fhua triggers the transfer of DNA into the proteoliposomes. J. Biol. Chem. 272, 16868-16872.

Plisson, C., White, H.E., Auzat, I., Zafarani, A., São-José, C., Lhuillier, S., Tavares, P., Orlova, E.V., 2007. Structure of bacteriophage SPP1 tail reveals trigger for DNA ejection. EMBO J. 26, 3720-3728.

Poolman, B., Glaasker, E., 1998. Regulation of compatible solute accumulation in bacteria. Mol. Microbiol. 29, 397-407.

Poranen, M.M., Daugelavicius, R., Bamford, D.H., 2002. Common principles in viral entry. Annu. Rev. Microbiol. 56, 521-538.

Qiao, X., Qiao, J., Onodera, S., Mindich, L., 2000. Characterization of phi 13, a bacteriophage related to phi 6 and containing three dsRNA genomic segments. Virology. 275, 218-224.

Quiberoni, A., Stiefel, J.I., Reinheimer, J.A., 2000. Characterization of phage receptors in Streptococcus thermophilus using purified cell walls obtained by a simple protocol. J. Appl. Microbiol. 89, 1059-1065.

Quisel, J.D., Lin, D.C., Grossman, A.D., 1999. Control of development by altered localization of a transcription factor in B. subtilis. Mol. Cell 4, 665-672.

Raetz, C.R., Whitfield, C., 2002. Lipopolysaccharide endotoxins. Annu. Rev. Biochem. 71, 635-700.

Räisänen, L., Draing, C., Pfitzenmaier, M., Schubert, K., Jaakonsaari, T., von Aulock, S., Hartung, T., Alatossava, T., 2007. Molecular interaction between lipoteichoic acids and Lactobacillus delbrueckii phages depends on D-alanyl and alpha-glucose substitution of poly(glycerophosphate) backbones. J. Bacteriol. 189, 4135-4140.

Räisänen, L., Schubert, K., Jaakonsaari, T., Alatossava, T., 2004. Characterization of lipoteichoic acids as Lactobacillus delbrueckii phage receptor components. J. Bacteriol. 186, 5529-5532.

Raspaud, E., Forth, T., São-José, C., Tavares, P., de Frutos, M., 2007. A kinetic analysis of DNA ejection from tailed phages revealing the prerequisite activation energy. Biophys. J. 93, 3999-4005.

Ravantti, J.J., Gaidelyte, A., Bamford, D.H., Bamford, J.K., 2003. Comparative analysis of bacterial viruses Bam35, infecting a gram-positive host, and PRD1, infecting gram-negative hosts, demonstrates a viral lineage. Virology. 313, 401-414.

Riechmann, L., Holliger, P., 1997. The C-terminal domain of TolA is the coreceptor for filamentous phage infection of E. coli. Cell. 90, 351-360.

Riva, S., Polsinelli, M., Falaschi, A., 1968. A new phage of Bacillus subtilis with infectious DNA having separable strands. J. Mol. Biol. 35, 347-356.

Roessner, C.A., Ihler, G.M., 1984. Proteinase sensitivity of bacteriophage lambda tail proteins gpJ and pH in complexes with the lambda receptor. J. Bacteriol. 157, 165-170.

Rogers, H.J., Perkins, H.R., Ward, J.B., 1980. Microbial cell walls and membranes. Chapman and Hall, London.

Romantschuk, M., Bamford, D.H., 1985. Function of pili in bacteriophage phi 6 penetration. J. Gen. Virol. 66, 2461-2469.

Romantschuk, M., Olkkonen, V.M., Bamford, D.H., 1988. The nucleocapsid of bacteriophage phi 6 penetrates the host cytoplasmic membrane. EMBO J. 7, 1821-1829.

Rottenberg, H., 1989. Proton electrochemical potential gradient in vesicles, organelles, and prokaryotic cells. Meth. Enzymol. 172, 63-84.

Rowley, S.D., Brown, N.C., 1977. Bacillus subtilis DNA polymerase III is required for the replication of DNA of bacteriophages SPP-1 and Ø105. J. Virol. 21, 493-496.

Rydman, P.S., Bamford, D.H., 2000. Bacteriophage PRD1 DNA entry uses a viral membrane-associated transglycosylase activity. Mol. Microbiol. 37, 356-363.

Ryter, A., Shuman, H., Schwartz, M., 1975. Intergration of the receptor for bacteriophage lambda in the outer membrane of Escherichia coli: coupling with cell division. J. Bacteriol. 122, 295-301.

Salas, M., 2006. Phage ϕ29 and its relatives, in: Calendar, R. (Ed.), The Bacteriophages. Oxford University Press, New York, pp. 315-330.

Sambrook, J., Fritsch, E.F., Maniatis, T., 1989. Molecular Cloning: a laboratory manual, second ed. Cold Spring Harbor Press, Cold Spring Harbor, New York.

Sambrook, J., Russel, D.W., 2001. Molecular cloning: a laboratory manual, third ed. Cold Spring Harbor Laboratory Press, Cold Spring Harbor, New York.

Sankaran, K., Wu, H.C., 1994. Lipid modification of bacterial prolipoprotein. Transfer of diacylglyceryl moiety from phosphatidylglycerol. J. Biol. Chem. 269, 19701-19706.

Santos, M.A., de Lencastre, H., Archer, L.J., 1984. Homology between phages SPP1, 41c, 22a, ρ15 and SF6 of Bacillus subtilis. J. Gen. Virol. 65, 2067-2072.

São-José, C., Baptista, C., Santos, M.A., 2004. Bacillus subtilis operon encoding a membrane receptor for bacteriophage SPP1. J. Bacteriol. 186, 8337-8346.

São-José, C., de Frutos, M., Raspaud, E., Santos, M.A., Tavares, P., 2007. Pressure built by DNA packing inside virions: enough to drive DNA ejection in vitro, largely insufficient for delivery into the bacterial cytoplasm. J. Mol. Biol. 374, 346-355.

São-José, C., Lhuillier, S., Lurz, R., Melki, R., Lepault, J., Santos, M.A., Tavares, P., 2006. The ectodomain of the viral receptor YueB forms a fiber that triggers ejection of bacteriophage SPP1 DNA. J. Biol. Chem. 281, 11464-11470.

Scholl, D., Adhya, S., Merril, C., 2005. Escherichia coli K1's capsule is a barrier to bacteriophage T7. Appl. Environ. Microbiol. 71, 4872-4874.

Scholl, D., Rogers, S., Adhya, S., Merril, C.R., 2001. Bacteriophage K1-5 encodes two different tail fiber proteins, allowing it to infect and replicate on both K1 and K5 strains of Escherichia coli. J. Virol. 75, 2509-2515.

Schwarz, S., Hood, R.D., Mougous, J.D., 2010. What is type VI secretion doing in all those bugs? Trends Microbiol. 18, 531-537.

Sciara, G., Bebeacua, C., Bron, P., Tremblay, D., Ortiz-Lombardia, M., Lichière, J., van Heel, M., Campanacci, V., Moineau, S., Cambillau, C., 2010. Structure of lactococcal phage p2 baseplate and its mechanism of activation. Proc. Natl. Acad. Sci. U.S.A. 107, 6852-6857.

Seaman, P.F., Day, M.J., 2007. Isolation and characterization of a bacteriophage with an unusually large genome from the Great Salt Plains National Wildlife Refuge, Oklahoma, USA. FEMS Microbiol Ecol. 60, 1-13.

Serwer, P., Hayes, S.J., Thomas, J.A., Hardies, S.C., 2007. Propagating the missing bacteriophages: a large bacteriophage in a new class. Virol. J. 4:21.

Silhavy, T.J., Kahne, D., Walker, S., 2010. The bacterial cell envelope. Cold Spring Harb Perspect Biol. 2, a000414.

Silverman, J.A., Benson, S.A., 1987. Bacteriophage K20 requires both the OmpF porin and lipopolysaccharide for receptor function. J. Bacteriol. 169, 4830-4833.

Sonnenfeld, E.M., Beveridge, T.J., Doyle, R.J., 1985. Discontinuity of charge on cell wall poles of Bacillus subtilis. Can. J. Microbiol. 31, 875-877.

Spizizen, J., 1958. Transformation of biochemically deficient strains of Bacillus subtilis by deoxyribonucleate. Proc. Natl. Acad. Sci. U.S.A. 44, 1072-1078.

Steensma, H.Y., Blok, J., 1979. Effect of calcium ions on the infection of Bacillus subtilis by bacteriophage SF6. J. Gen. Virol. 42, 305-314.

Steinbacher, S., Baxa, U., Miller, S., Weintraub, A., Seckler, R., Huber, R., 1996. Crystal structure of phage P22 tailspike protein complexed with Salmonella sp. O-antigen receptors. Proc. Natl. Acad. Sci. U.S.A. 93, 10584-10588.

Stengele, I., Bross, P., Garcés, X., Giray, J., Rasched, I., 1990. Dissection of functional domains in phage fd adsorption protein. Discrimination between attachment and penetration sites. J. Mol. Biol. 212, 143-149.

Stent, G.S., 1963. Molecular biology of bacterial viruses. W.H. Freeman & Co, San Francisco and London, pp. 63 and 114.

Steven, A.C., Trus, B.L., Maizel, J.V., Unser, M., Parry, D.A., Wall, J.S., Hainfeld, J.F., Studier, F.W., 1988. Molecular substructure of a viral receptor-recognition protein. The gp17 tail-fiber of bacteriophage T7. J. Mol. Biol. 200, 351-365.

Suzuki, R., Inagaki, M., Karita, S., Kawaura, T., Kato, M., Nishikawa, S., Kashimura, N., Morita, J., 1999. Specific interaction of fused H protein of bacteriophage phiX174 with receptor lipopolysaccharides. Virus Res. 60, 95-99.

Szmelcman, S., Hofnung, M., 1975. Maltose transport in Escherichia coli K-12: involvement of the bacteriophage lambda receptor. J. Bacteriol. 124, 112-118.

Takác, M., Bläsi, U., 2005. Phage P68 virion-associated protein 17 displays activity against clinical isolates of Staphylococcus aureus. Antimicrob. Agents Chemother. 49, 2934-2940.

Tavares, P., Lurz, R., Stiege, A., Rückert, B., Trautner, T.A., 1996. Sequential headful packaging and fate of the cleaved DNA ends in bacteriophage SPP1. J. Mol. Biol. 264, 954-967.

Tavares, P., Santos, M.A., Lurz, R., Morelli, G., de Lencastre, H., Trautner, T.A., 1992. Identification of a gene in Bacillus subtilis bacteriophage SPP1 determining the amount of packaged DNA. J. Mol. Biol. 225, 81-92.

Tiyanont, K., Doan, T., Lazarus, M.B., Fang, X., Rudner, D.Z., Walker, S., 2006. Imaging peptidoglycan biosynthesis in Bacillus subtilis with fluorescent antibiotics. Proc. Natl. Acad. Sci. U.S.A. 103, 11033-11038.

Towbin, H., Staehelin, T., Gordon, J., 1979. Electrophoretic transfer of proteins from polyacrylamide gels to nitrocellulose sheets: procedure and some applications. Proc. Natl. Acad. Sci. U.S.A. 76, 4350-4354.

Traurig, M., Misra, R., 1999. Identification of bacteriophage K20 binding regions of OmpF and lipopolysaccharide in Escherichia coli K-12. FEMS Microbiol. Lett. 181, 101-108.

van Duin, J., 1988. The single-stranded RNA bacteriophages, in: Calendar, R. (Ed.), The Bacteriophages. Plenum, New York, pp. 117-167.

van Duin, J., Tsareva, N., 2006. Single-stranded RNA phages, in: Calendar, R. (Ed.), The Bacteriophages, second ed. Oxford University Press, New York, pp. 276-287.

van Houdt, R., Michiels, C.W., 2005. Role of bacterial cell surface structures in Escherichia coli biofilm formation. Res. Microbiol. 156, 626-633.

Veesler, D., Blangy, S., Spinelli, S., Tavares, P., Campanacci, V., Cambillau, C., 2010b. Crystal structure of Bacillus subtilis SPP1 phage gp22 shares fold similarity with a domain of lactococcal phage p2 RBP. Protein Sci. 19, 1439-1443.

Veesler, D., Robin, G., Lichière, J., Auzat, I., Tavares, P., Bron, P., Campanacci, V., Cambillau, C., 2010a. Crystal structure of bacteriophage SPP1 distal tail protein (gp

19.1): a baseplate hub paradigm in gram-positive infecting phages. J. Biol. Chem. 285, 36666-36673.

Villanueva, N., Salas, M., 1981. Adsorption of bacteriophage phi 29 to Bacillus subtilis through the neck appendages of the viral particle. J. Virol. 38, 15-19.

Vinga, I., Dröge, A., Stiege, A.C., Lurz, R., Santos, M.A., Daugelavicius, R., Tavares, P., 2006b. The minor capsid protein gp7 of bacteriophage SPP1 is required for efficient infection of Bacillus subtilis. Mol. Microbiol. 61, 1609-1621.

Vinga, I., São-José, C., Tavares, P., Santos, M.A., 2006a. Bacteriophage entry in the host cell, in: Wegrzyn, G. (Ed.), Modern Bacteriophage Biology and Biotechnology. Research Signpost, Kerala, India, pp. 165-203.

Vollmer, W., Blanot, D., de Pedro, M.A., 2008. Peptidoglycan structure and architecture. FEMS Microbiol. Rev. 32, 149-167.

Waldor, M.K., Friedman, D., Adhya, S., 2005. Phages: their role in bacterial pathogenesis and biotechnology. ASM Press, Washington.

Wang, J., Hofnung, M., Charbit, A., 2000. The C-terminal portion of the tail fiber protein of bacteriophage lambda is responsible for binding to LamB, its receptor at the surface of Escherichia coli K-12. J. Bacteriol. 182, 508-512.

Wang, J.D., Rokop, M.E., Barker, M.M., Hanson, N.R., Grossman, A.D., 2004. Multicopy plasmids affect replisome positioning in Bacillus subtilis. J. Bacteriol. 186, 7084-7090.

Webster, R.E., 1996. Biology of filamentous bacteriophage, in: Kay, B.K. (Ed.), Phage display of peptides and proteins. Academic, San Diego, pp. 281-304.

Weidel, W., 1958. Bacterial viruses; with particular reference to adsorption/penetration. Annu. Rev. Microbiol. 12, 27-48.

Weidenmaier, C., Peschel, A., 2008. Teichoic acids and related cell-wall glycopolymers in Gram-positive physiology and host interactions. Nat. Rev. Microbiol. 6, 276-287.

Weinbauer, M.G., 2004. Ecology of prokaryotic viruses. FEMS Microbiol. Rev. 28, 127-181.

Weiner, J.H., Rothery, R.A., 2007. Bacterial cytoplasmic membrane. Encyclopedia of life sciences. John Wiley & Sons, Ltd: Chichester.

Wendlinger, G., Loessner, M.J., Scherer, S., 1996. Bacteriophage receptors on Listeria monocytogenes cells are the N-acetylglucosamine and rhamnose substituents of teichoic acids or the peptidoglycan itself. Microbiology. 142, 985-992.

Whatmore, A.M., Reed, R.H., 1990. Determination of turgor pressure in Bacillus subtilis: a possible role for K+ in turgor regulation. J. Gen. Microbiol. 136, 2521-2526.

Wietzorrek, A., Schwarz, H., Herrmann, C., Braun, V., 2006. The genome of the novel phage Rtp, with a rosette-like tail tip, is homologous to the genome of phage T1. J. Bacteriol. 188, 1419-1436.

Winkler, H.H., Duckworth, D.H., 1971. Metabolism of T4 bacteriophage ghost-infected cells: effect of bacteriophage and ghosts on the uptake of carbohydrates in Escherichia coli B. J. Bacteriol. 107, 259-267.

Xiang, Y., Morais, M.C., Cohen, D.N., Bowman, V.D., Anderson, D.L., Rossmann, M.G., 2008. Crystal and cryoEM structural studies of a cell wall degrading enzyme in the bacteriophage phi29 tail. Proc. Natl. Acad. Sci. U.S.A. 105, 9552-9557.

Xu, J., 2001. A conserved frameshift strategy in dsDNA long tailed bacteriophages. Ph.D. thesis. University of Pittsburgh.

Yamamoto, H., Kurosawa, S., Sekiguchi, J., 2003. Localization of the vegetative cell wall hydrolases LytC, LytE, and LytF on the Bacillus subtilis cell surface and stability of these enzymes to cell wall-bound or extracellular proteases. J. Bacteriol. 185, 6666-6677.

Yasbin, R.E., Fields, P.I., Andersen, B.J., 1980. Properties of Bacillus subtilis 168 derivatives freed of their natural prophages. Gene. 12, 155-159.

Yasbin, R.E., Maino, V.C., Young, F.E., 1976. Bacteriophage resistance in Bacillus subtilis 168, W23, and interstrain transformants. J. Bacteriol. 125, 1120-1126.

Yasbin, R.E., Young, F.E., 1974. Transduction in Bacillus subtilis by bacteriophage SPP1. J. Virol. 14, 1343-1348.

Young, F.E., 1967. Requirement of glucosylated teichoic acid for adsorption of phage in Bacillus subtilis 168. Proc. Natl. Acad. Sci. U.S.A. 58, 2377-2384.

Young, K., 2010. Bacterial cell wall, in: Encyclopedia of Life Sciences. John Wiley & Sons, Ltd: Chichester.

Young, R., Wang, I.-N., 2006. Phage Lysis, in: Calendar, R. (Ed.), Bacteriophages. Oxford University Press, New York, pp. 104-125.

Yu, F., Mizushima, S., 1982. Roles of lipopolysaccharide and outer membrane protein OmpC of Escherichia coli K-12 in the receptor function for bacteriophage T4. J. Bacteriol. 151, 718-722.

Zaribnicky, V., 1969. Mechanism of T-even DNA ejection. J. Theor. Biol. 22, 33-42.

Zuber, B., Chami, M., Houssin, C., Dubochet, J., Griffiths, G., Daffé, M., 2008. Direct visualization of the outer membrane of mycobacteria and corynebacteria in their native state. J. Bacteriol. 190, 5672-5680.

JB JOURNAL OF BACTERIOLOGY SEPTEMBER 2011, VOLUME 193, NUMBER 18, PAGES 4571–5057

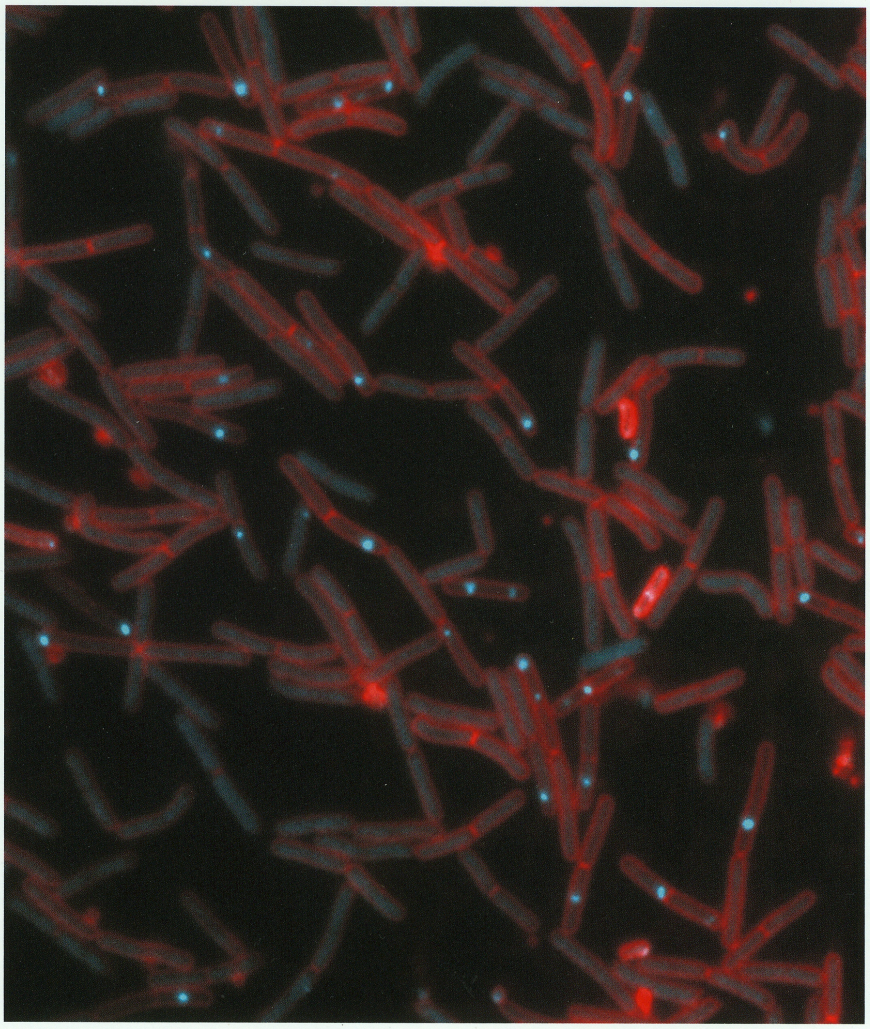

September 2011
Volume 193
Number 18
Published Twice Monthly

AMERICAN SOCIETY FOR MICROBIOLOGY

JB
Journal of Bacteriology

Dans ce travail de thèse on a utilisé le bactériophage SPP1 qui infecte la bactérie Gram-positive *Bacillus subtilis* comme modèle d'étude pour disséquer ces différentes étapes clés pour le démarrage de l'infection virale.

In this study we used bacteriophage SPP1 that infects the Gram-positive bacterium *Bacillus subtilis* as a model system to dissect the different steps leading to transfer of the phage genome from the viral capsid to the host cell cytoplasm.

Mots-clés: bactériophage SPP1, entrée du virus; ions Ca^{2+}; potentiel de membrane; bactérie Gram-positif; YueB.

Key-words: bacteriophage SPP1, virus entry; Ca^{2+} ions; membrane voltage; Gram-positive bacterium; YueB.

Unité de Virologie Moléculaire et Structurale,
CNRS UPR3296 et IFR 115,
Bâtiment 14B, Avenue de la Terrasse,
91198 GIF SUR YVETTE Cedex

PÔLE : INGENIERIE DES PROTEINES ET CIBLES THERAPEUTIQUES

UNIVERSITÉ PARIS-SUD 11
UFR «FACULTÉ DE PHARMACIE DE CHATENAY-MALABRY »
5, rue Jean Baptiste Clément
92296 CHÂTENAY-MALABRY Cedex